Groundwater Flow Systems of North-eastern Eyre Peninsula (G-FLOWS Stage-2): Hydrogeology, geophysics and environmental tracers

Taylor AR, Pichler MM, Olifent V, Thompson J, Bestland E, Davies PJ, Lamontagne S, Suckow A, Robinson N, Love A, and Munday T

Goyder Institute for Water Research

Technical Report Series No. 15/37

www.goyderinstitute.org

Goyder Institute for Water Research Technical Report Series ISSN: 1839-2725

The Goyder Institute for Water Research is a partnership between the South Australian Government through the Department of Environment, Water and Natural Resources, CSIRO, Flinders University, the University of Adelaide and the University of South Australia. The Institute will enhance the South Australian Government's capacity to develop and deliver science-based policy solutions in water management. It brings together the best scientists and researchers across Australia to provide expert and independent scientific advice to inform good government water policy and identify future threats and opportunities to water security.

Enquires should be addressed to: Goyder Institute for Water Research
Level 1, Torrens Building
220 Victoria Square, Adelaide, SA, 5000
tel: 08-8303 8952
e-mail: enquiries@goyderinstitute.org

Citation

Taylor AR, Pichler MM, Olifent V, Thompson J, Bestland E, Davies PJ, Lamontagne S, Suckow A, Robinson N, Love A and Munday T. 2015. Groundwater Flow Systems of North-eastern Eyre Peninsula (G-FLOWS Stage-2): Hydrogeology, geophysics and environmental tracers. Goyder Institute for Water Research Technical Report Series No. 15/37, Adelaide, South Australia

Contents

Acknowledgements viii
Executive summary ix
1 Introduction 1
1.1 Study design 2
2 Study Area 4
2.1 Site selection 4
2.2 Climate 4
2.3 Vegetation and land use 5
2.4 Surface water hydrology 7
2.5 Geology, geomorphology and soils 8
2.6 Groundwater 9
3 Methods 12
3.1 Hydrogeology 12
3.2 Environmental tracers 13
3.3 Airborne electromagnetics 17
3.4 Hydrogeological modelling 18
4 Hydrogeology 20
4.1 Surface geology 20
4.2 Groundwater yield 21
4.3 Hydrostratigraphy 22
4.4 Regional potentiometric surface 31
4.5 Regional terrain analysis 34
5 Environmental tracers 36
5.1 Groundwater salinity 36
5.2 Major ions 37
5.3 Strontium isotopes 44
5.4 Stable isotopes 46
5.5 Anthropogenic gas tracers (CFCs and SF_6) 48
5.6 Radiocarbon 51
5.7 Chemistry transects 53
5.8 Discussion 57
6 Airborne electromagnetics 58
6.1 Cleve Hills AEM 59
6.2 Coastal Plain AEM 64
6.3 Discussion 64
7 Conclusions and Recommendations 66
7.1 Conclusions 66
7.2 Recommendations 67

References 68
Appendix A Groundwater flow systems 73
Appendix B Field sampling data..........89

Figures

Figure 1.1 Location map of the study area for G-FLOWS-2 Task 2 (black extent) including the location of geophysical EM surveys 2

Figure 1.2 Flow chart of project approach 3

Figure 2.1 Annual rainfall (blue bars) and annual evaporation (red line) for (a) Cleve and (b) Whyalla 5

Figure 2.2 Current land use map for the study area 6

Figure 2.3 Location of major surface water streams and catchments within the study area 7

Figure 2.4 An example of groundwater discharge to the Driver River approximately 20 km west of Arno Bay 8

Figure 2.5 Conceptual geology and hydrogeological diagram for the Cleve Hills..........8

Figure 2.6 Hydrogeological conceptual model of the Coastal Plain south west of Whyalla, red labels – groundwater salinity, blue labels – aquifer pressure (metres Australian Height Datum freshwater equivalent) dashed red line – extent of mineralisation. Figure 9, in Jeuken (2011) 9

Figure 2.7 Existing simplified hydrostratigraphic representation of the north eastern Eyre Peninsula. Figure 3, in Berens et al. (2011) 11

Figure 3.1 Collection of a dissolved noble gas sample using the copper tube method of Weiss (1968)..........14

Figure 3.2 Collection of an SF_6 sample following the protocol set out by CSIRO IAS..........15

Figure 3.3 Conceptual diagram of the AEM setup..........17

Figure 3.4 Broader map of the Eyre Peninsula, showing available airborne electromagnetic (AEM) surveys across the Northern Eyre Peninsula..........18

Figure 4.1 Simplified surface geology map for the study region..........21

Figure 4.2 Groundwater yields for the study region 22

Figure 4.3 Conceptual understanding of the hydrostratigraphy of the Cleve Hills region 24

Figure 4.4 Western hydrogeological transect, orange dots represent wells with lithology, red dash is the standing water level and error bars represent the screened or open interval, location of transect shown in Figure 4.9 25

Figure 4.5 Southern hydrogeological transect, orange dots represent wells with lithology, red dash is the standing water level and error bars represent the screened or open interval, location of transect shown in Figure 4.9 26

Figure 4.6 South-eastern hydrogeological transect, orange dots represent wells with lithology, red dash is the standing water level and error bars represent the screened or open interval, location of transect shown in Figure 4.9..........27

Figure 4.7 Simplified hydrostratigraphy for the Coastal Plain region..........28

Figure 4.8 Hydrogeological transect for the Coastal Plain, blue lines represent the location of groundwater wells 30

Figure 4.9 Potentiometric surface for the study area, blue dots represent the groundwater wells (data points) used to generate the surface, purple lines represent the location of the four hydrostratigraphic and piezometric transects....32

Figure 4.10 The relationship between hydraulic head and changes in land surface elevation along four piezometric transects: (a) Western, (b) Southern, (c) South-eastern and (d) Coastal Plain....33

Figure 4.11 Groundwater seeps observed at (a) Carappee Hill and (b) Secret Rocks....34

Figure 4.12 Regional terrain map using the MrVBF index to indicate areas of erosional and depositional terrain, also includes the location of candidate wells selected for potential sampling in this study....35

Figure 5.1 TDS of groundwater in the study area....36

Figure 5.2 Illustrative diagram of screened intervals of sampled wells with lithology type, against salinity..37

Figure 5.3 Piper diagram illustrating major ion composition of groundwater analysed in this study and groundwater samples from previous work in the study region by Risby and Harrington (2014)....38

Figure 5.4 Groundwater wells in the study region sampled for hydrochemistry and environmental tracers, including wells recently sampled by Risby and Harrington (2014)....39

Figure 5.5 Major dissolved ions versus chloride....41

Figure 5.6 Chloride deposition for the study area; source Davies and Crosbie (2014)....43

Figure 5.7 Strontium isotope ratio vs 1/Sr (L/mg) of groundwater, geology, seawater and rainfall....45

Figure 5.8 Isotopic composition of groundwater samples relative to (a) the Adelaide LMWL and rainfall from the Eyre Peninsula and (b) relative to the Adelaide amount weighted means for different monthly rainfall amounts....47

Figure 5.9 Plot (a) $\delta^{18}O$ versus elevation of the land surface and plot (b) $\delta^{2}H$ excess versus chloride....48

Figure 5.10 Concentrations of CFC-11 versus CFC-12 for groundwater in the study area....49

Figure 5.11 CFC-12 concentrations in groundwater versus depth below the watertable....50

Figure 5.12 Concentrations of SF_6 in groundwater versus depth below the watertable; shaded areas represent the expected range in SF_6 concentration at air-water equilibrium under normal conditions (yellow) and with a large amount of excess air and a low recharge temperature (blue)....51

Figure 5.13 Concentrations of CFC-12 versus ^{14}C in groundwater including interpretation using a lumped parameter models....52

Figure 5.14 Concentrations of ^{14}C in groundwater versus depth below the watertable; including an interpretation of vertical infiltration velocities for two different aquifer depths (a) 40 m and (b) 80 m using lumped parameter models....53

Figure 5.15 Chloride concentrations against distance along the three transects....54

Figure 5.16 Deuterium composition versus distance along the three transects....54

Figure 5.17 Radiocarbon concentration versus distance along the three transects....55

Figure 5.18 Chloride concentration with distance along the coastal transect....55

Figure 5.19 $^{87}Sr/^{86}Sr$ composition with distance along coastal transect....56

Figure 5.20 Trends in ^{14}C with distance along coastal transect....57

Figure 6.1 Depth slice (at 20m below ground surface) of areas of inverted AEM in the Cleve Hills case study area (approximately the same area as Figure 6.6 and Figure 6.9) overlying the land surface topography....58

Figure 6.2 Using MrVBF analysis of surface topography to highlight contiguous surface drainage lines in the south-eastern part of the case study area (Cleve Hills) of the northern Eyre Peninsula. The paler areas are the low/flat parts of the landscape....59

Figure 6.3 Pseudo-coloured Interval conductivity (8-12 m) below the ground surface from a layered earth inversion of TEMPEST AEM data, acquired over the Cleve Hills in Eastern Eyre Peninsula. The image is overlain on 1stVD magnetics (grayscale image) highlighting the complex folded metasediments of the region. Flight lines 60690 and 60750 are also shown. 60

Figure 6.4 Pseudo-coloured Interval conductivity (17-23 m) below the ground surface from a layered earth inversion of TEMPEST AEM data, acquired over the Cleve Hills in Eastern Eyre Peninsula. The image is overlain on 1stVD magnetics (grayscale image) highlighting the complex folded metasediments of the region. Flight lines 60690 and 60750 are also shown. 61

Figure 6.5 Pseudo-coloured Interval conductivity (17–23 m) draped on a perspective view of the Cleve Hills region Red and green colours indicate a more conductive part of the landscape. Blues are resistive areas often associated with fresh rock or sub-crop. 61

Figure 6.6 Conductivity-depth section (1D Layered Earth Inversion (top) for flight line 60790. The flight line is overlain on a Landsat true colour composite image (bottom panel). See Figure 6.3 and 6.4 for flight line locations. 62

Figure 6.7 Conductivity-depth section (1D Layered Earth Inversion (top) for flight line 60690. The flight line is overlain on a Landsat true colour composite image (bottom panel). See Figure 6.3 and 6.4 for flight line locations. 63

Figure 6.8 Pseudo-coloured Interval conductivity (17–23 m) below the ground surface from a layered earth inversion of TEMPEST AEM data, acquired over the Cleve Hills in Eastern Eyre Peninsula. The image is overlain on 1stVD magnetics (grayscale image) highlighting the complex folded metasediments of the region. Also overlain on the image are well water quality data indicative of groundwater salinities. Higher salinities are more commonly associated with lower more conductive parts of the landscape. 63

Figure 6.9 AEM inversion for the Coastal Plain transect 65

Figure 7.1 Hydrogeological conceptual model for the Cleve Hills (same area as figures in Chapter 6.1)....66

Apx Figure A 1 Original and mapped transects 76

Apx Figure A 2 Western transect. Surface and well data, smoothed and average....77

Apx Figure A 3 South-eastern transect. Surface and well data, smoothed and averaged....78

Apx Figure A 4 Southern transect. Surface and well data, smoothed and average 78

Apx Figure A 5 Western transect topography flow contours 79

Apx Figure A 6 Western transect topography surface stream function, Ψ 79

Apx Figure A 7 Western transect well flow contours 80

Apx Figure A 8 Western transect well surface stream function, Ψ 80

Apx Figure A 9 Western transect average flow contours 81

Apx Figure A 10 Western transect average surface stream function, ...81

Apx Figure A 11 South-eastern transect topography flow contours 82

Apx Figure A 12 South-eastern transect topography surface stream function, Ψ 82

Apx Figure A 13 South-eastern transect well flow contours 83

Apx Figure A 14 South-eastern transect well surface stream function, Ψ 83

Apx Figure A 15 South-eastern transect average flow contours 84

Apx Figure A 16 South-eastern transect average surface stream function, Ψ 84

Apx Figure A 17 Southern transect topography contours 85

Apx Figure A 18 Southern transect topography surface stream function, Ψ 85
Apx Figure A 19 Southern transect well flow contours 86
Apx Figure A 20 Southern transect well surface stream function, Ψ 86
Apx Figure 21 Southern transect average flow contours 87
Apx Figure A 22 Southern transect average surface stream function, Ψ 87
Apx Figure A 23 Western transect. Z_0 = 100 m. Baseline gradients, dΦ/dX. Curves for surface topography, wells and their average 88
Apx Figure A 24 Western transect. Z_0 = 5000 m. Baseline gradients, dΦ/dX. Curves for surface topography, wells and their average....88

Tables

Table 5.1 Recharge estimates for the Cleve Hills samples and unconfined Coastal Plain sample....44
Table 5.2 Relative proportions of strontium contributed by rainfall and rock to the strontium isotope composition of groundwater for the Coastal Plain 46

Apx Table B.1: Sampled well details....89
Apx Table B.2: General chemistry and major ions 90

Acknowledgements

The Goyder Facilitating Long-Term Water Solutions (G-FLOWS Stage-2) project team extend warm thanks and give acknowledgement to the landholders of the Cleve Hills and Kimba communities on Eyre Peninsula. In particular those who offered their time and local knowledge to help locate wells. This project would be much lighter in data collected were it not for this help. Of note for regional geological information, as well as local individual and industry contacts, was Barry Schubert of 'Minerals on Eyre' who gave much of his own time and efforts to see our sampling completed with as much detail as possible. Other locals of note were Francis Beinke, Nigel Girdham, Barry Smith and the Turnbull Boys. All contacts were helpful and a more amiable community could not be asked for.

Uranium SA and Archer Exploration also stand out as great industry support, offering access to sites for sampling and making information freely available, this has proved to be a great help to the project and is very much appreciated.

Recent research on groundwater in the region has led to an increase in the data used and this report is better for it. For this we acknowledge the efforts of Lyz Risby and the report generated by Lyz and Glenn Harrington.

The quality and accuracy of this report was greatly improved thanks to thorough reviews provided by Stan Smith and Matthias Raiber of CSIRO and Adrian Werner of Flinders University.

Executive summary

This project assessed the groundwater resources contained in the very complex hydrogeological setting of the north-eastern Eyre Peninsula, where access to groundwater may become a deciding factor for the economic development of the region. The landscape across this setting contains the geologically old Cleve Hills and the more recent sedimentary systems of the Coastal Plain adjacent to Spencer Gulf. Aquifers in this area generally have low yields and high salinities, with some wells exhibiting salinity higher than seawater. Fresh groundwater is rare and is a limiting factor in paddock stocking densities and the prospect of mining development in the area is of concern for landholders seeking to ensure their access to groundwater remains unaffected.

The aims for Task 2 of the Goyder Facilitating Long-Term Water Solutions (G-FLOWS Stage-2) project were to:

- identify potential groundwater resources (fresh or saline) in north-eastern Eyre Peninsula
- describe potential aquifers, their connectivity to one another, and the potential for the occurrence of regional flow systems
- provide an initial evaluation of key system properties, such as recharge rates and the sources for groundwater salinity.

Assessing groundwater resources in this region is difficult because the infrastructure (groundwater monitoring wells, etc.) is limited. In this study, a multidisciplinary approach was used combining desktop and field techniques, including:

- a review of the existing lithological, well monitoring and airborne geophysical data to evaluate potential aquifers (that is, to define the hydrostratigraphic units in the region) and to derive a regional potentiometric surface (that is, an estimation of the regional watertable)
- a field campaign to collect groundwater chemistry (major ions, salinity) and environmental tracer data (mainly chlorofluorocarbons, sulfur hexafluoride, stable isotopes of the water molecule, radiocarbon and strontium isotope ratios) to characterise properties such as recharge rates
- a conceptual modelling evaluation of the potential for regional flow systems.

KEY FINDINGS

Hydrostratigraphy

The Cleve Hills region is geologically very complex, with a geological history spanning at least 2700 million years. The landscape consists of a succession of small hills interspersed with narrow valleys. Climate is temperate to semi-arid with rainfall ranging between 300–500 mm/year, typically highest at higher elevations. There is no well-defined surface water drainage. From a hydrogeological point of view, the Cleve Hills include fractured bedrock, saprolite (weathered bedrock), and various more recent surface deposits including colluviums, aeolian sands and valley alluvial deposits of up to several tens of meters thick in some areas. The most extensive valley fill deposits occur in palaeovalleys west of the Cleve Hills. Aside from occasional clay lenses potentially developing confining conditions locally, all hydrostratigraphic units appear connected. However, whether the more extensive saprolite and fractured bedrock units are well connected and laterally form a regional flow system remains unclear.

The Coastal Plain hydrogeological system is simpler, consisting of Tertiary or younger age sediments overlying bedrock. This system includes two confined aquifers: the Melton Limestone and the Kanaka Beds (hereafter referred to as the Tertiary Limestone and Sand Aquifer, respectively) and an unconfined Quaternary aquifer.

Potentiometric surface

The regional watertable (here approximated using potentiometric surfaces) can provide clues for the relative significance of regional and local groundwater flow systems, with an undulating watertable usually indicating the presence of local flow systems. The watertable in the Cleve Hills region was generally close to the ground surface and followed the regional topography, with a pronounced regional mound at higher elevations. The shape of the watertable was evaluated in more detail along three transects spreading away from the Cleve Hills. In general, because the watertable was at or very close to the surface there, valleys appeared as a focus for groundwater discharge. This is consistent with high groundwater salinities in the valleys. In the Coastal Plain, the potentiometric surfaces sloped downward towards Spencer Gulf and there was an upward hydraulic gradient between the confined and unconfined aquifers.

Environmental tracers

A wide range in groundwater salinity was found in the Cleve Hills, from <1500 mg/L (as Total Dissolved Solids (TDS)) to >14,000 mg/L. In general, the ionic composition of groundwater was similar to rainfall, suggesting that the origin of the saline groundwater was primarily through cyclic salts (that is, the concentration of salts in rainfall by evaporation and plant transpiration). The stable isotope composition for groundwater (deuterium and oxygen-18) was variable but tended to decrease with elevation. This is consistent with the tendency for rainfall to also become depleted along orographic gradients. However, stable isotopes in groundwater did not match meteoric water for Adelaide (the closest location for which this was available), suggesting a different origin for the rainfall. Groundwater from the Coastal Plain aquifers tended to have a stronger evaporation signal in stable isotopes relative to the Cleve Hills, indicating a different recharge mechanism there (that is, a greater potential for evaporation prior to recharge). Strontium isotope ratios also suggested that a greater proportion of the salt content (up to 30%) could originate from weathering in Coastal Plain groundwater.

Infiltration velocities were evaluated using age-dating environmental tracers (chlorofluorocarbons, sulfur hexafluoride and radiocarbon) sampled from 27 wells across the Cleve Hills. Sulfur hexafluoride concentrations ranged from background (0.2 fmol/kg of water) to twice the concentrations expected from equilibrium with modern air (~14 fmol/kg). Such high sulfur hexafluoride concentrations have been noted elsewhere in inland Australian groundwater and may represent a geological source of SF_6 or the presence of similar compounds that currently cannot be analytically separated from SF_6. Vertical infiltration velocities estimated using chlorofluorocarbons ranged between 50–1500 mm/year and the ones derived from radiocarbon between 10–300 mm/year. It is not possible to estimate recharge rates from the vertical infiltration velocities because aquifer porosity is not known but suspected to vary greatly. For example, porosity in valley fills could be ~30% but in fractured bedrock it could be <1%. Assuming a 1% porosity, a 50 mm/year infiltration velocity would result in a very low recharge rate of 0.5 mm/year. Recharge rates estimated using chloride mass-balances were also low, generally ranging between 0–2 mm/year.

The trends in the environmental tracers suggested the presence of local flow systems in the Cleve Hills region. For example, groundwater ^{14}C activity above background was found across the study area, whereas a trend from young to older groundwater would have been expected between high and low elevations if a regional system had been present. In the Coastal Plain, ^{14}C suggested leakage between the unconfined and confined aquifer. However, as more than one source of water may be present – including seawater intrusion – inter-aquifer leakage requires further evaluation in the Coastal Plain.

Airborne electromagnetic (AEM) surveys

A number of previous geophysical surveys were re-interpreted to provide a consistent evaluation of the geological systems in the Cleve Hills and Coastal Plain. In the Cleve Hills, AEM identified significant areas of unconsolidated valley fills and saprolite, which may form significant aquifers. The regolith is quite extensive, consistent with the geological age of the bedrock, and may extend to 100 m into the bedrock in some areas. Modelled groundwater conductivities did not match very well with field measurements but suggested most of the groundwater in surficial deposits is saline. The poor match between modelled and measured salinities was due, in part, to the very simple geological model used to interpret the geophysical data when compared to the complexity of the geological environment in the Cleve Hills. However, AEM appeared successful at mapping large-scale lithological zones in both the Cleve Hills and Coastal Plain.

Regional groundwater modelling

The likelihood for the presence of regional and local flow systems in the Cleve Hills was evaluated using analytical models of groundwater flow. A key assumption in these models was to assume that the regolith and fractured bedrock systems in the Cleve Hills form one laterally connected aquifer. As expected from the undulating topography, this modelling revealed that local flow systems should be significant in the Cleve Hills. This tendency would be further reinforced if there is not one continuous aquifer system in the region. Local flow systems are less likely in the Coastal Plain because of the flat topography.

Synthesis and Recommendations

Potential aquifers exist in the Cleve Hills and consist of a mixture of valley fill deposits, saprolite and fractured bedrock. Typical valley fills would be up to several tens of meters thick and a few km wide, so these do not represent major potential groundwater reserves. Most of this groundwater will also be saline. However, palaeovalleys west of the Cleve Hills could host a larger volume of (probably saline) groundwater. Saprolite and weathered bedrock could also form more extensive aquifers, but the evidence to date suggests that they do not because they are not well connected. The highest likelihood to find fresh groundwater reserves will be in recharge areas (such as on bedrock outcrops at higher elevations) because a shallow watertable combined with a semi-arid climate will result in groundwater salinisation in discharge areas (valleys). Irrespective of the limited size of the aquifers, recharge rates are probably low in the region and this would significantly limit sustainable extraction rates.

This assessment was greatly complicated by the scarcity of groundwater monitoring infrastructure in north-eastern Eyre Peninsula, in particular the absence of a nested piezometer network in easily accessible areas. There was also very limited infrastructure on the parts of the landscape (bedrock outcrops and palaeovalleys) most likely to offer suitable groundwater resources in terms of volume or low salinity. Piezometer nests would also be much better tools (relative to the single wells with long screens presently available) to evaluate recharge rates using environmental tracers, especially if efforts are made to also characterise aquifer porosity for the geological formation they are located in. Thus, the recommendations from this study are to:

- Focus further evaluation of the region’s groundwater resources on those landscape units most likely to fill a water resource need, such as palaeovalleys (for volume) or bedrock outcrops (for low salinity).
- Install a piezometer nest network in the key hydrostratigraphic units identified during the study to better characterise and, eventually, manage the resource. This would be especially useful to help calibrate remote sensing information obtained by airborne electromagnetics or other techniques.
- Initiate rainfall sampling across the region’s elevation gradient to determine the local meteoric water line for the stable isotopes of water. Stable isotopes are a relatively inexpensive tracer and provide useful information about recharge mechanisms along elevation gradients.
- Proceed cautiously with the exploitation of groundwater resources in north-eastern Eyre Peninsula because the aquifers are small and the recharge rates probably low.

1 Introduction

The Eyre Peninsula is rich in natural resources and contributes in excess of two and half a billion dollars per year towards the South Australian economy (Eyre Peninsula Natural Resources Management Board, 2009). Water is a limiting factor for economic growth, with the region currently relying on surface water imported from the River Murray and on groundwater extracted from local aquifers. Groundwater in the region is primarily extracted from the Southern Basins Prescribed Wells Area (SBPWA) located in the southern Eyre Peninsula between the townships of Port Lincoln and Coffin Bay. The SBPWA contributes approximately 40% of the total potable and non-potable water resource (Department for Water, 2011). Groundwater resources in non-prescribed areas across the region are not well characterised but may offer an opportunity for further economic development and population growth. Recently, the Resources and Energy Sector Infrastructure Council (RESIC) conducted a study into the potential future demand for infrastructure by the resources and energy sectors in South Australia (Parsons Brinckerhoff, 2011), Eyre Peninsula was identified as a priority region for industrial development. However, a key limitation for future development is that, for most of the region, groundwater resources have not been characterised.

The G-FLOWS Stage-2 project aims to increase the knowledge about the character of groundwater resources in the Eyre Peninsula. In this report (G-FLOWS Stage-2 Task 2), particular attention is given to the north-eastern part of the Eyre Peninsula. This region was selected because of its potential for future economic development and for the availability of some existing information, such as geophysical mapping. North-eastern Eyre Peninsula resides between the townships of Kimba in the north, Whyalla in the east, Port Neill in the south and Kilroo in the west. The study area has two distinct components – the elevated Cleve Hills region inland and the Coastal Plain (Figure 1.1).

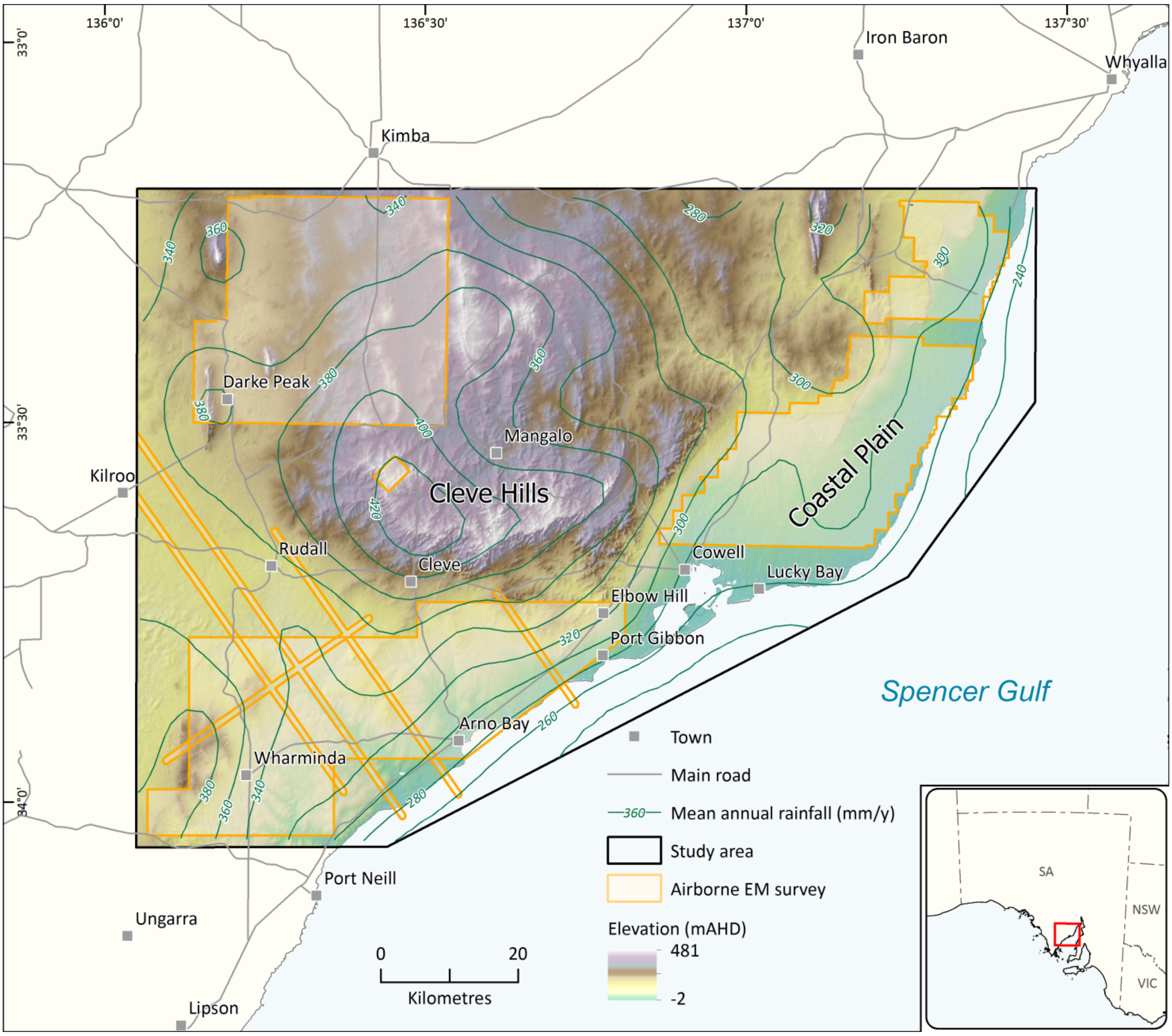

Figure 1.1 Location map of the study area for G-FLOWS-2 Task 2 (black extent) including the location of geophysical EM surveys

1.1 Study design

G-FLOWS Stage-2 (hereafter referred to as G-FLOWS 2) builds on the approaches to conceptualise the hydrogeology of remote regions used in the G-FLOWS Stage-1 project (Gilfedder and Munday, 2013; Leaney et al., 2013; Ley-Cooper and Munday, 2013; Munday et al., 2013) and aims to complement activities being undertaken in the South Australian Government by the Department of Environment, Water and Natural Resources (DEWNR) Facilitating Long Term Outback Water Solutions (FLOWS) Initiative and the Department of State Development (DSD) Plan for Accelerating Exploration (PACE) 2020 Program. Key objectives for G-FLOWS 2 Task 2 were to:

- Identify potential groundwater resources (fresh or saline) in north-east Eyre Peninsula;
- Describe potential aquifers, their connectivity to one another, and the potential for the occurrence of regional flow systems;
- Provide an initial evaluation of key system properties, such as recharge rates and the sources for groundwater salinity.

These objectives were achieved through a combination of (Figure 1.2):

- A review of the existing lithological and well monitoring data to evaluate potential aquifers (that is, define the hydrostratigraphic units in the region) and to derive a regional potentiometric surface (that is, a regional watertable map);
- A re-evaluation of existing airborne geophysical data;
- A field campaign to collect groundwater chemistry (major ions, salinity) and environmental tracer data (mainly chlorofluorocarbons, sulfur hexafluoride, stable isotopes of the water molecule, radiocarbon and strontium isotope ratios);
- Conceptual modelling of the potential for regional groundwater flow systems.

The wells sampled for the field campaign add value to part of a previous survey in the region by Risby and Harrington (2014). Two additional tracers (noble gases and tritium) were also collected but the results for these tracers arrived very late at the time of writing the report. Therefore no interpretation of the results is provided but results for these tracers can be found in Appendix B .

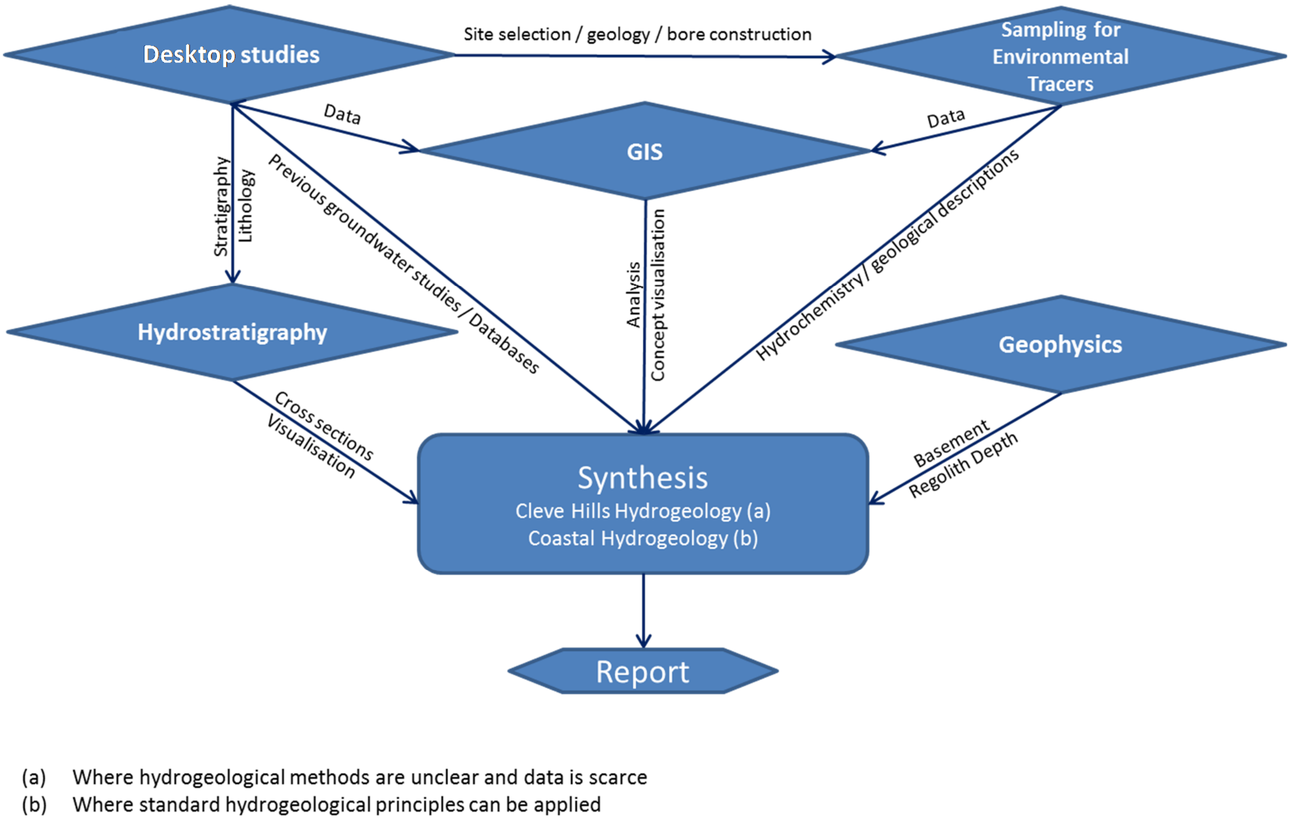

Figure 1.2 Flow chart of project approach

2 Study Area

2.1 Site selection

The study site was determined by the objectives of the G-FLOWS 2 project. The Kimba-Cleve region was selected as a suitable study site for the north-eastern Eyre Peninsula due to sufficient well coverage and existing geophysical Airborne Electromagnetic (AEM) data in the region (Figure 1.1). Wells to be sampled within this region were selected using the following criteria:

1. Geographic location, particularly the presence of topographic gradients and inferred valleys, identified using a digital elevation model (DEM) a regional potentiometric surface for the area and a terrain map (described in Chapter 3).
2. Location within two survey areas of high-resolution AEM data, one covering a 900 km^2 region to the southwest of Kimba, and another covering a similar extent northeast of Cowell along the Coastal Plain (Figure 1.1).
3. The depth of wells, and hence geologic unit intercepted at the screened depth. Priority was allocated to the fractured rock zone.
4. The suitability of well construction for hydrochemical and tracer sampling.

Candidate wells were initially identified using The National Groundwater Information System (NGIS) available through the Bureau of Meteorology (BOM) (BOM, 2013). These data were then validated by cross referencing with the South Australian state groundwater database WaterConnect, available through DEWNR (DEWNR, 2014). Geographic location of wells and lithology data was validated using the South Australian Resources Information Geoserver (SARIG) available through DSD (DSD, 2014). The regional potentiometric surface map (Figure 4.9) and terrain map (Figure 4.12) were used to assist with selecting wells that most likely intercepted potential areas of groundwater flow. Well locations were plotted over the potentiometric surface and terrain maps and wells that were situated along inferred flow lines and within valleys were highlighted for further investigation.

The suitability of the wells for environmental tracer sampling was then assessed using construction and screen interval data available on WaterConnect. Many wells listed on the government database had incomplete construction or lithological details, and hence were discarded from the analysis. Only wells with lithological logs were included, as hydrochemical data obtained can only yield meaningful interpretations if accompanied by some knowledge of the hydrogeological unit that the screened interval intercepts. Out of approximately 5000 total wells in the region, a final shortlist of 25 suitable wells was produced. Two distinct field areas of very different geology, geomorphology and hydrogeology were chosen for this study namely; 1) the Cleve Hills fractured rock province and 2) sedimentary aquifers of the Coastal Plain.

2.2 Climate

The study region is categorised as temperate and semi-arid, experiencing hot, persistently dry summers and cool, wet winters (BOM, 2014) with localised and intense rains occurring sporadically in the summer months. The mean annual rainfall for the greater part of the eastern Eyre Peninsula study area is between 300–400 mm/year. There is a marked difference between the hills and the coast, as seen in Figure 2.1, with a mean annual rainfall of 405 mm at Cleve and 254 mm at Whyalla. This further emphasises the orographic nature of rainfall in the Cleve Hills. Long-term annual averages for other nearby localities include 321 mm at Arno Bay and 346 mm at Kimba (BOM, 2014).

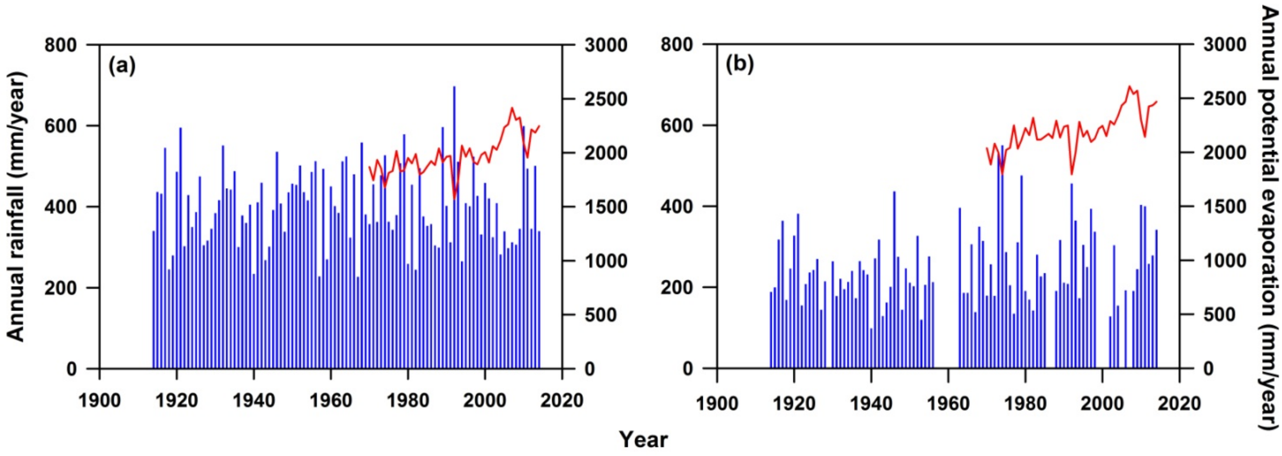

Figure 2.1 Annual rainfall (blue bars) and annual evaporation (red line) for (a) Cleve and (b) Whyalla

Rainfall occurs over an average of 73 days per year with June, July and August being the wetter months in this semi-arid climate zone. Total annual rainfall at Cleve was 501 mm in 2013 and 340 mm in 2014 (BOM, 2014). Mean maximum annual temperature is 22.1 °C and the mean minimum annual temperature is 11.4 °C. In summer the temperature ranges between 15 to 31 °C and in winter, averages range between 5 to 18 °C.

Potential annual evaporation rates are in the order of 2000 mm/year. Despite wide fluctuations, Figure 2.1 clearly shows an increasing trend in evaporation over the record for both stations. The mean annual potential evaporation is ~1977 mm at Cleve and ~2202 mm at Whyalla. Actual evaporation is linked to available water and climate factors so is much less than the potential evaporation. Actual evaporation rates across Eyre Peninsula are generally between 200–600 mm/year (Golder Associates, 2014).

Observed changes in climate include a decrease in rainfall on Eyre Peninsula over the last 20 years and, simultaneously, an increase in average annual temperature (Berens et al., 2011). This is consistent with a projected future drier climate for the region (Charles and Fu, 2015). The implication for groundwater recharge rates (that is, a likely decrease) is significant for water resources management, especially in areas where the groundwater is younger (i.e. where groundwater recharge is an ongoing process).

2.3 Vegetation and land use

Land use in the study area is dominated by dryland cropping, pasture grazing and native vegetation, and to a lesser extent a number of mining tenements (Figure 2.2). Extensive land clearing on the flat and gently sloping areas of the Cleve Hills has occurred from the 1870s until as recently as the early 1980s (Harding et al., 2002). Twenty eight percent of the Eastern Cleve Hills region is estimated to still be covered by remnant vegetation, predominantly native scrubland (Harding et al., 2002). These small zones of native scrub coincide with peaks, rocky outcrops and areas of steeper terrain, with cropping and pasture restricted to flatter regions. Larger areas of vegetation comprise conservation parks. The Coastal Plain is predominantly used for dryland cropping and grazing, with smaller areas used for conservation of native vegetation including saltbush, hummock grass and chenopod shrubland.

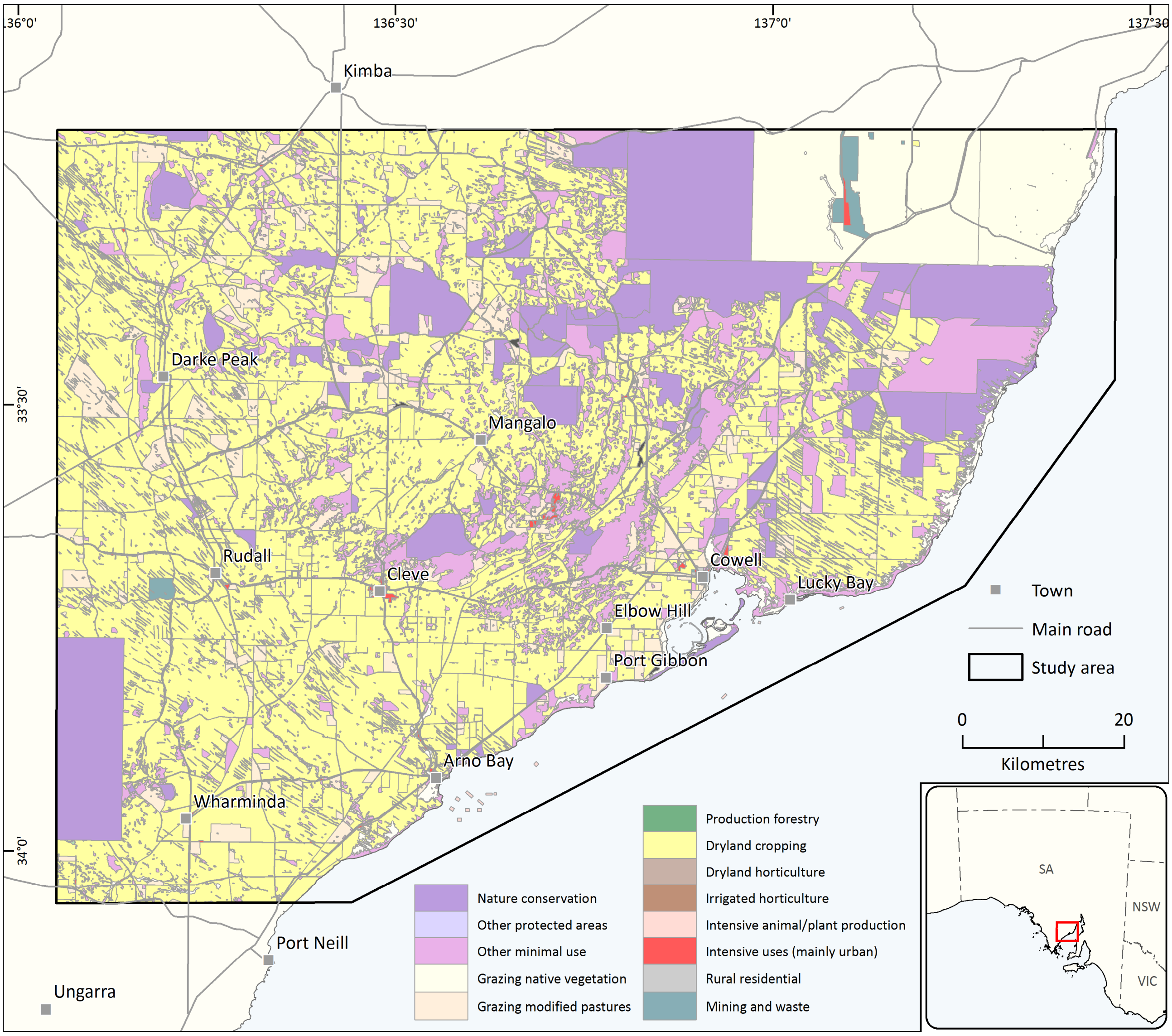

Figure 2.2 Current land use map for the study area

2.4 Surface water hydrology

There is almost no permanent surface water on the north-eastern Eyre Peninsula. High evaporation potential along with high infiltration capacity in sandy soils across much of the area results in little opportunity for the persistence of standing surface water. Surface water in the study area is ephemeral and occurs only during short periods after significant rainfall (Berens et al., 2011). Groundwater discharge supports ephemeral surface water flows in some zones and is noted after heavier rainfall periods as hillside 'soaks' and in ephemeral stream flows. The major ephemeral streams occurring in the study area include Salt Creek in the eastern Cleve Hills and the Driver River to the south and east of Darke Peak (Figure 2.3). These streams typically flow only intermittently during periods of high rainfall and are not utilised for water supply. Very little connection to the ocean exists via surface water flows.

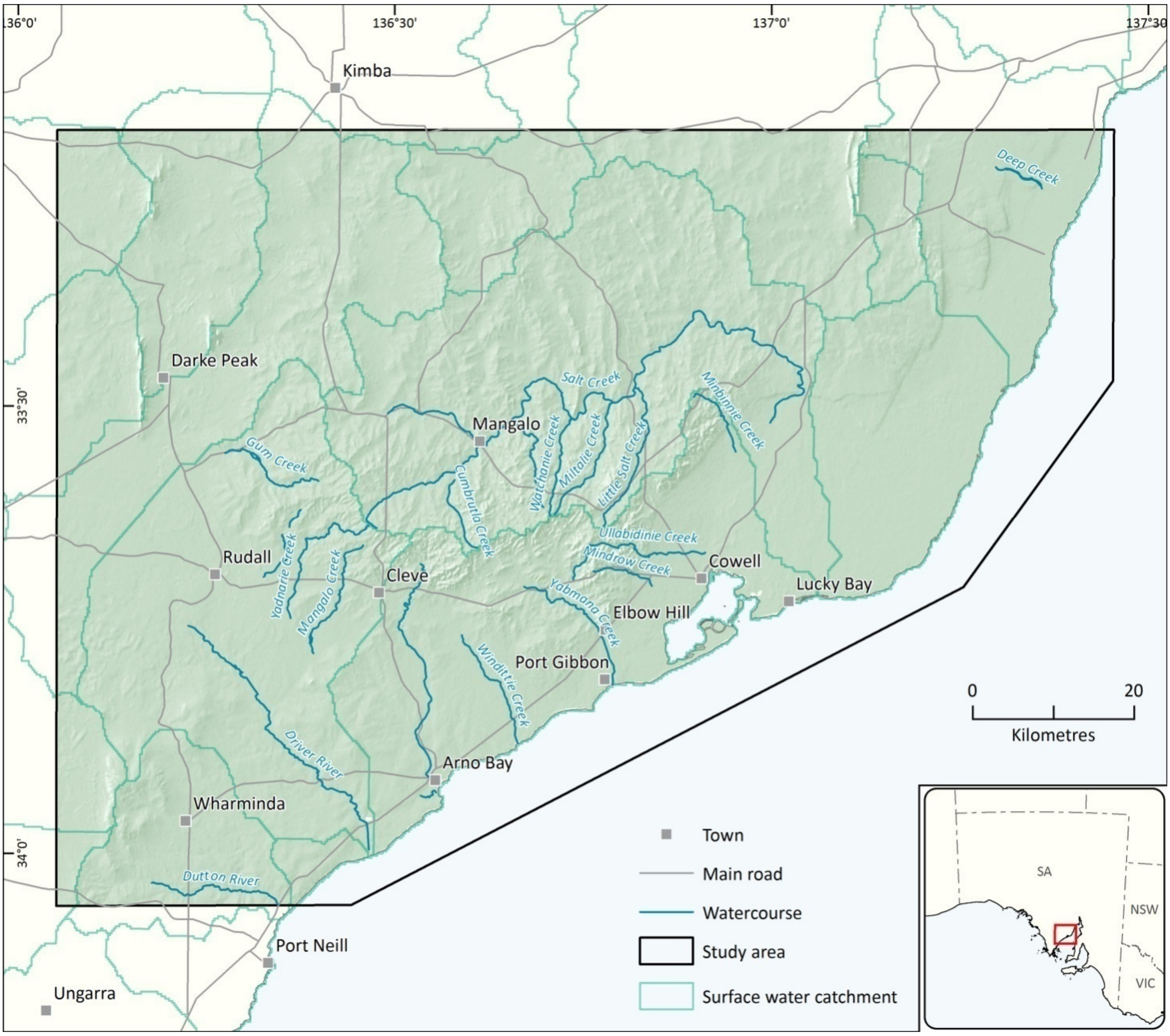

Figure 2.3 Location of major surface water streams and catchments within the study area

The subdued upland topography provides low relief across much of the area and streams draining the region flow to the east and south towards Spencer Gulf (Harding et al., 2002). Despite the lack of permanent water bodies, seasonal flooding and water logging of soils occurs, especially in low-lying areas during wet years. Dryland salinity issues are of concern and reflect the shallow depths to watertable in the low lying topographical regions across this study area, as well as high evaporation rates.

Figure 2.4 An example of groundwater discharge to the Driver River approximately 20 km west of Arno Bay

2.5 Geology, geomorphology and soils

2.5.1 CLEVE HILLS

The Eyre Peninsula is a geologically complex and heterogeneous region. The Cleve Hills area has a geologic history spanning 2700 million years (Twidale et al., 1985). Much of this history involves the formation of the Gawler Craton (Drexel and Preiss, 1995; Drexel et al., 1993). The area is dominated by fractured rock basement consisting of Precambrian metamorphosed sedimentary (metasedimentary) units with granitic intrusions (Figure 2.5). This basement is exposed in weathered outcrops such as Darke Peak (Early Proterozoic Hutchison Group Warrow Quartzite) and Carappee Hill (Early Proterozoic Lincoln Complex Granite). Within the Hutchison Group metasedimentary units are minor amounts of biochemical (dolostones) and chemical (ironstone) sediments.

Overlying the basement is a thick clayey weathered profile that is present in most of the area (Parker et al., 1984; Sheard and Primary Industries and Resources SA CSIRO Division of Exploration and Mining and CRC LEME Australia, 2008). In low lying areas as well as low gradient slopes, colluvium, aeolian sands, regolith, saprolite and valley alluvial deposits occur to depths of tens of metres.

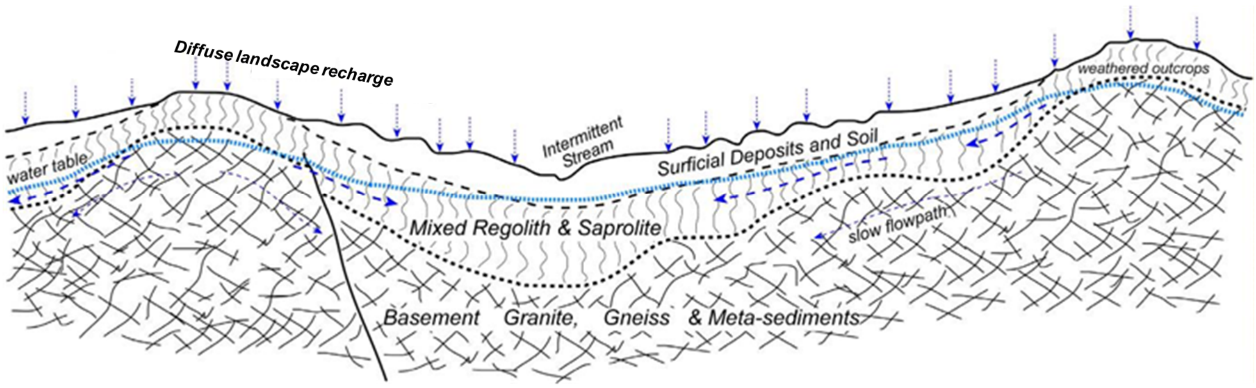

Figure 2.5 Conceptual geology and hydrogeological diagram for the Cleve Hills

Darke Peak is a prominent landscape feature in the study area and is representative of the Cleve Hills area geology and geomorphology. The variable nature of geology across the region results in a wide variety of soil textures. Generally, soils are sandy with high infiltration capacity and colours ranging from cream white to orange-brown. The flat, arable regions of the study area have sandy loam topsoil with clayey horizons. Other widely occurring soils are siliceous sands over clays as well as shallow stony soils with calcareous horizons occurring on the ridgelines of the hills (Twidale et al., 1985). Longitudinal aeolian sand dunes are a dominant feature of the topography, these tend to be orientated in a northwest-southeast direction from Arno Bay to Darke Peak.

2.5.2 COASTAL PLAIN

Bordering the Cleve Hills on the east is a sequence of Tertiary sedimentary strata of up to 100 m thick. The sequence both on-laps the basement rocks and is in fault contact with the basement (Figure 2.6). The sedimentary sequence consists of non-marine carbonaceous alluvial strata (Eocene-Oligocene Kanaka Beds), marine limestone and marl (Oligocene-Miocene Melton Limestone), non-marine sandy clay (Pliocene Gibbon Beds), and Quaternary marine and aeolian deposits (Jeuken, 2011). Similar to the Cleve Hills, a thick weathered profile is present between the basement rocks and the Tertiary sedimentary sequence (Drexel and Preiss, 1995).

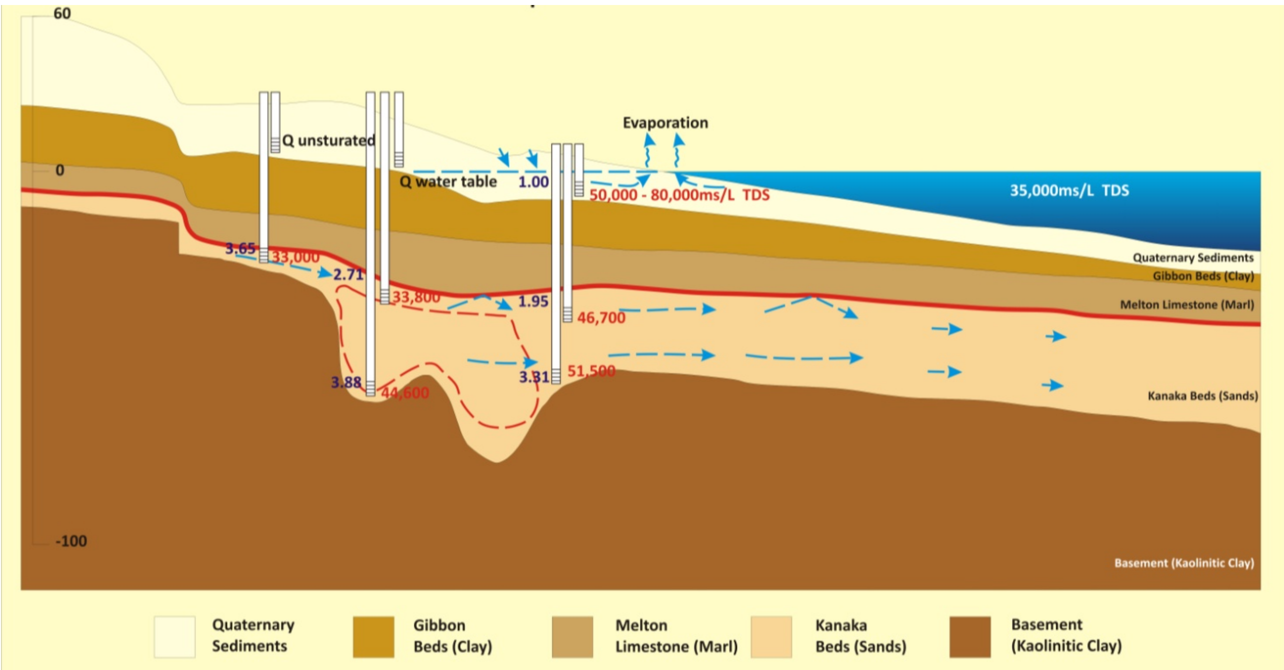

Figure 2.6 Hydrogeological conceptual model of the Coastal Plain south west of Whyalla, red labels – groundwater salinity, blue labels – aquifer pressure (metres Australian Height Datum freshwater equivalent) dashed red line – extent of mineralisation. Figure 9, in Jeuken (2011)

2.6 Groundwater

2.6.1 EYRE PENINSULA

Groundwater resources in Eyre Peninsula are sparse and generally of poor quality. Hence, any available resources are invaluable for a variety of purposes including town water supply, agriculture, stock, industry and mining. The majority of potable groundwater occurs in the groundwater lenses that reside within the Quaternary limestone sediments of the Bridgewater Formation. The lenses are defined by groundwater with a salinity of less than 1500 mg/L (Love et al., 1994). The lenses have good quality potable water because of a high infiltration capacity through sink holes and the karstic nature of the aquifer. Surrounding these lenses is saline groundwater within various Tertiary sand units. The other major unit that contains groundwater are the fractured rock aquifers of the Gawler Craton. Here, groundwater is characterised by high salinity and low yields.

Previous research by Love et al. (1994) in the groundwater lenses of the County Musgrave Prescribed Wells Area (CMPWA) in the western Eyre Peninsula near the township of Elliston and Bramfield, has shown that it takes in excess of 65 mm of rainfall per event to result in groundwater recharge. Love et al. (1994) used CFCs to calculate that the long term average recharge in the region was in the order of 30 mm/year. This was consistent with a compartmental mixing model using tritium that gave a long term recharge rate of 30 mm/year. Based on mapping a reduction of the size of these groundwater lenses, Love and co-workers inferred a reduction of recharge in County Musgrave from 1973 to 1993. To the best of our knowledge no similar mapping has occurred since Love et al. (1994). Recent researchers have focused on developing conceptual models and estimation of recharge rates in the southern groundwater lenses of Eyre Peninsula (Bresciani et al., 2014; Ordens et al., 2011). Unfortunately, outside of the potable groundwater lenses, little groundwater investigation has occurred.

2.6.2 CURRENT GROUNDWATER USE

The limited understanding of the regional-scale hydrogeology in the study area is a legacy of the limited groundwater use and development. Aquifers of the region have previously not been fully utilised except for occasional domestic and livestock consumption. Primarily, this would appear to be because most wells have low yields and access only saline waters. Salinity in most instances is well beyond that which is suitable for livestock. The drilling of water wells for domestic and stock use across much of the area has decreased because of the distribution of mains water via Whyalla from the Murray River at Morgan.

2.6.3 INFRASTRUCTURE

Unused, abandoned and decommissioned groundwater wells are typical across the study area. Many wells drilled during post-World War II boom times found low water quality and yield. Well construction was also difficult because of sandy surficial material or very hard regolith at shallow depths. Documented location for many wells is also inaccurate. Difficulty in locating wells was very common during field work, in some cases infrastructure had been obliterated entirely, with no sign of a well at all. In some cases, the well was fitted with a functioning windmill, which tends to hinder sampling due to permanent fittings in the well casing preventing the deployment of submersible sampling pumps. Wells drilled during the early and mid-20th century were steel-cased and, because most groundwater is saline, are corroded or collapsed. The field sampling team went to great lengths to ascertain the sampling feasibility of wells, as the well condition often did not reflect the well status identified in WaterConnect. Well selection and spatial coverage provided one of the most significant challenges to the desktop selection of suitable sites and the field collection of samples.

2.6.4 HYDROGEOLOGY

As mentioned above, the hydrogeology of the study area has received limited attention (Berens et al., 2011). Exceptions to this are Henschke et al. (1994), Henschke et al. (2001) and Harding et al. (2002) whose primary focus was in regard to dryland salinity management. Recent work by Risby and Harrington (2014) for DEWNR encompasses much of the Eyre Peninsula including a number of wells sampled for environmental tracers within our study area. All of the aforementioned studies used a simplified overview of the hydrostratigraphic sequence (Figure 2.7). This describes the area as one of young deposits lying over much older basement.

The preceding geological description has highlighted the complex nature of the basement geology and this also applies when considering the hydrogeology of the region. Extended periods of exposure of the basement surface have resulted in various amounts of weathering and are likely to have complicated the hydrogeological setting. Additionally, variably weathered and fractured upper basement surfaces are likely to offer a variety of surficial sedimentary, fractured rock and combined aquifer types. Jurassic aquifers exist only in a small section of the south-central part of the study area, and are not considered in this report because of a lack of sampling opportunity, although they do warrant further investigation. Tertiary deposits remain poorly described except where they are clearly defined in the Coastal Plain area. Unconsolidated Quaternary deposits hosting groundwater represent the major component of basement cover at all locations; these exist as fluvial, alluvial, colluvial and aeolian deposits.

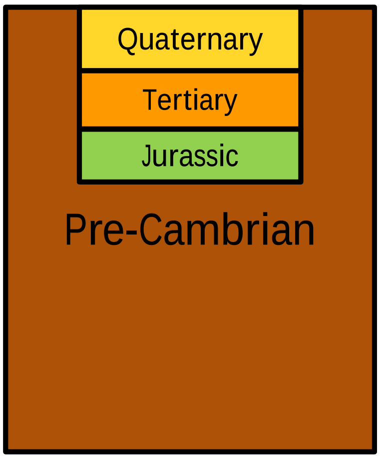

Figure 2.7 Existing simplified hydrostratigraphic representation of the north eastern Eyre Peninsula. Figure 3, in Berens et al. (2011)

Henschke et al. (1994) conducted an investigation of groundwater flow and hydrochemistry for a small catchment in the vicinity of Darke Peak, and Harding et al. (2002) conducted a study on salinity in the Eastern Cleve Hills region. Henschke et al. (2001) provide good insight into groundwater systems through their study of dryland salinity in the lower Driver River catchment. The Henschke et al. (2001) study within the Driver River catchment describes groundwater flow directions for some areas as being very localised and not necessarily corresponding with surface catchments.

Despite the lack of broad-scale knowledge of groundwater in the region, previous studies support the concepts of localised aquifer systems. Harding et al. (2002) conceptualised that localised flow systems of less than 3 km are presumed to be present in the most steeply sloping regions within the Cleve Hills, while intermediate groundwater flow systems of greater than 5 km are thought to occur in less steep regions. However, this conclusion was inferred from topographic gradients without characterising the nature of the regional watertable.

3 Methods

3.1 Hydrogeology

3.1.1 DATA AQUISITION

Data related to groundwater wells associated with the study area were extracted from NGIS (BOM, 2013) and cross-referenced with WaterConnect (DEWNR, 2014). Geographic location of wells and lithology were validated using SARIG (DSD, 2014). Additional datasets pertaining to local hydrogeological investigations by industry include data packages supplied by Uranium SA and Archer Exploration. Previously published environmental tracer data was sourced from studies by Risby and Harrington (2014) and Swaffer et al. (2014). Rainfall and climate data was also sourced from the BOM Climate Data Online (CDO) portal (BOM, 2014). All of the data collated from BOM, DEWNR and SARIG is available under a creative commons license in Australia.

3.1.2 SURFACE GEOLOGY

A simplified map of the surface geology was produced using the 1:2 million (2M) surface geology layer from SARIG (DSD, 2014). The different geological units were grouped into three categories: surficial sediments, metasedimentary basement rock and granitic basement rock. Tertiary and Quaternary unconsolidated sediments were classified as surficial sediments. Thick Jurassic-age sedimentary deposits of the Polda Basin are included as a separate unit, although they are only minor components of the study area. Members of the Lincoln Complex granites collectively form the granitic component of the basement. Metasedimentary units of the Sleaford Complex, Hutchison Group and other schists and dolomite units were grouped as metasedimentary basement rock.

3.1.3 HYDROSTRATIGRAPHY

Simplified hydrostratigraphic cross-sections were constructed along four transects in the study area, with the aim to highlight key hydrogeological processes or structures Transects were selected on the basis of the density of sampled wells, including those sampled in this project and by Risby and Harrington (2014). Most of the available lithological and stratigraphic data utilised were within a 2 km radius of a given transect. However, in some regions a paucity of data meant deviations of as much as 6 km were necessary. These data points were then projected at right angles onto the transect line.

3.1.4 REGIONAL POTENTIOMETRIC SURFACE

Given the complex geology of the study region in combination with a general paucity of both hydraulic head data and aquifer information, careful consideration was given to the method and data used for constructing a regional water level map. Following collation of well data for the study area, hydraulic head data was plotted and interpolated using the Topo-to-raster tool in ArcGIS to produce a hydrologically correct potentiometric surface from point data. The surface was presented overlying the high resolution one second Shuttle Radar Topography Mission (SRTM) DEM and includes contours from which the potential direction of groundwater flow can be inferred.

Hydraulic head data from fractured rock aquifers is most difficult to interpret because we do not know how well connected the fault and fracture systems are. Therefore, the regional potentiometric surface map represents groundwater residing in various hydrogeological units, including unconsolidated sediments, karstic limestone, sandstones as well as igneous and metasedimentary units and only represents 'potential' directions for groundwater flow. The main purpose of the map was to provide a preliminary composite overview of groundwater levels and hydraulic gradients for the entire region to facilitate with the selection of candidate wells for environmental tracer sampling.

3.1.5 REGIONAL TERRAIN ANALYSIS

In addition to the DEM and regional potentiometric surface, valleys and the Coastal Plain in the Eyre Peninsula have the potential to host local-scale and intermediate-scale groundwater flow systems. This was explored by determining the Multi-resolution Valley Bottom Flatness (MrVBF) index across the study area. Essentially, this index can identify where erosion and sediment deposition occurs in the landscape (Gallant and Dowling, 2003), which can in turn be used to identify valley and Coastal Plain aquifers. Candidate wells suitable for environmental tracer sampling were then identified and plotted to look at their alignment within these valley systems. Suitable wells were included in the field sampling campaign.

3.2 Environmental tracers

In this study, a select suite of environmental tracers were sampled to characterise and understand hydrological processes including precipitation patterns, recharge rates, recharge conditions and the scale of the groundwater flow systems. Environmental tracers are defined following Cook and Böhlke (2000) as 'natural or anthropogenic compounds or isotopes that are widely distributed in the near sub surface environment of the earth such that variations in their abundances can be used to determine pathways and time scales of environmental processes'. Tracers used in this study and their application include, the stable isotopes of water (deuterium ($\delta^{2}H$) and oxygen-18 ($\delta^{18}O$)) to identify water sources to aquifers and the extent of evaporation during recharge in the study area. The strontium isotope ratio, (strontium-87 (^{87}Sr) to strontium-86 (^{86}Sr)) was used for determining water-rock interaction as well as mixing between water sources with different dissolved constituents. The anthropogenic gas tracers, chlorofluorocarbons (CFC-11 and CFC-12) and sulfur hexafluoride (SF_6), tritium (^{3}H), radiocarbon (^{14}C) and dissolved noble gases were used for determining the mean residence time (MRT) of groundwater.

3.2.1 PURGING AND SAMPLING

At each well, the standing water level was measured using a Solinst 107 Temperature, Level, and Conductivity (TLC) Meter. In addition, the casing height, casing inside diameter (ID) and total depth of the well were measured. The cross-sectional area of the casing and the difference between the total depth of the well and the standing water level were subsequently used to calculate a purge volume for three standing water columns within a given well.

Purging and sampling at each well were carefully conducted by monitoring discharge rates from and water level in the well to ensure that the water level was not reduced to the level of the screened interval. In the case of an open hole, care was taken not to reduce the water level to the open section or if the water level was within the open section, not to draw the water level down to within metres of the pump below the watertable. This methodology of carefully purging the well was to ensure that groundwater samples were collected without contact with the atmosphere.

Purging and sampling of all wells was conducted using a variety of submersible pumps (Grundfos MP1 and a Super Twister 12V) that were specially modified for sampling environmental tracers. These pumps have either a stainless steel pump head (MP1) or a combination of Polyvinyl chloride (PVC) and stainless steel (Super Twister) and high pressure nylon discharge hose. These modifications are most important to prevent sample contamination with the atmosphere, as well as any plastic components that possibly contain CFCs.

3.2.2 FIELD MEASUREMENTS

General chemical and physical parameters measured included, electrical conductivity (EC), temperature, pH, dissolved oxygen (DO) and oxidation reduction potential (ORP). Each parameter was measured in the field under gently flowing conditions within a flow cell using a YSI Multi-Probe System (MPS). Parameters were recorded at the initial purging stage, at regular intervals during purging, as well as post sampling. Alkalinity was also determined in the field using a Hach Digital Titration kit.

3.2.3 COLLECTION OF GROUNDWATER SAMPLES

Groundwater samples were collected for general chemistry (including for pH, EC and alkalinity), major and minor ions. Duplicate samples for general chemistry and major ions were collected, filtered with a 0.45 µm Acrodisc syringe filter and placed in well rinsed 125 mL PET plastic bottles. Samples for cation analysis were acidified with nitric acid (HNO_3) to pH <2. For δ^2H and $\delta^{18}O$, duplicate samples were collected, filtered as above, and placed in a 28 mL gas-tight glass bottle (McCartney Bottle) to prevent evaporation. Strontium isotope samples were collected in 500 mL PET bottles under gently flowing conditions. Tritium (^3H) samples were collected in duplicate in 500 mL PET plastic under gently flowing conditions to avoid excessive air and capped without a headspace to avoid contact with the atmosphere. Duplicate samples for dissolved noble gases were collected in copper tubes following Weiss (1968). Briefly, this involved creating a gas tight connection between the copper tube and the discharge hose, gently flushing the tube and applying a back pressure using a flow regulator before clamping the copper tube at each end without trapping any air (Figure 3.1).

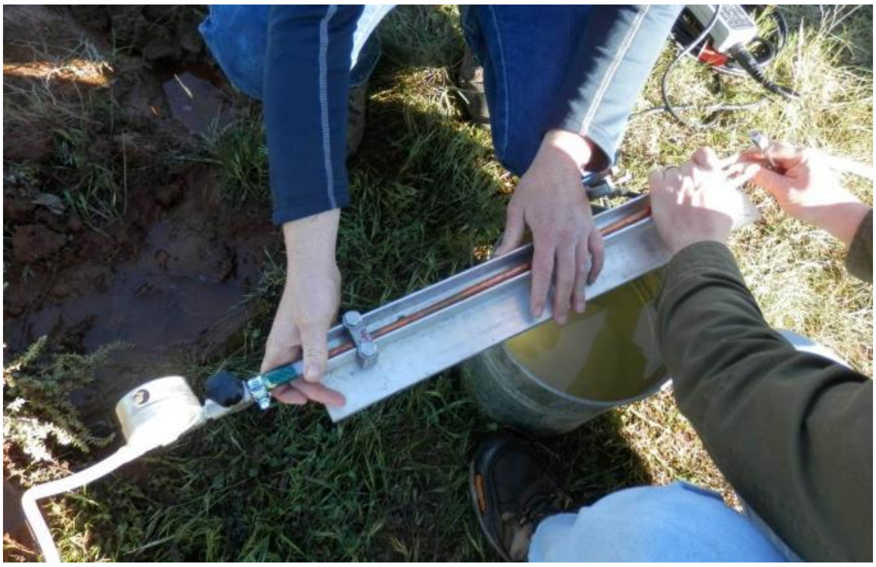

Figure 3.1 Collection of a dissolved noble gas sample using the copper tube method of Weiss (1968)

Samples for ^{14}C were collected in 5 L PET plastic jerry cans. Samples for CFCs were collected following the sampling protocols of CSIRO Isotope Analysis Service (IAS). Briefly, this involved placing the nylon discharge hose into the bottom of a 125 mL glass bottle that is placed inside a 10 L steel bucket. Samples were collected using a gentle pumping rate and bottles were bottom-filled until the 10 L bucket overflowed. Samples were collected in triplicates and capped under water to prevent exposure to the atmosphere. Samples for SF_6 were collected following a procedure similar to the CFC collection procedure, but using a single 1 L glass bottle placed inside the 10 L bucket (Figure 3.2).

Figure 3.2 Collection of an SF_6 sample following the protocol set out by CSIRO IAS

3.2.4 ANALYTICAL METHODS

General chemistry and major and minor ion concentrations in groundwater were determined at CSIRO Analytical Services Unit (ASU), Waite Campus, Adelaide. Cations were analysed by inductively coupled plasma optical emission spectrometry (ICP-OES) and anions by ion chromatography. Samples for δ^2H and $\delta^{18}O$ were analysed by GNS Science (Te Pü Ao, New Zealand) where measurements were made using an Isoprime mass spectrometer following, for δ^2H, reduction at 1100 °C using a Eurovector Chrome HD elemental analyser and for $\delta^{18}O$, by water equilibration at 25 °C using an Aquaprep device. Strontium isotope ratios ($^{87}Sr/^{86}Sr$) for all groundwater samples were analysed at the University of Adelaide School of Earth and Environmental Sciences with a Finnigan MAT262 Thermal Ionisation Mass Spectrometer.

Samples for radiocarbon analysis were measured by single stage accelerator mass spectrometry (AMS) at The Australian National University, Canberra. Samples were prepared by first precipitating the dissolved inorganic carbon from 5 L of groundwater as strontium carbonate ($SrCO_3$) under alkaline conditions (pH >11). The $SrCO_3$ precipitate was then acidified and purified cryogenically into aliquots of carbon dioxide (CO_2) for measurement by AMS (Fallon et al., 2010). SF_6 and CFC samples were measured at CSIRO Isotope Analysis Service (IAS), Waite Campus, Adelaide. SF_6 samples were measured using a specific gas chromatograph with an electron capture detector as an aliquot of high purity nitrogen that had been equilibrated with 300 mL of groundwater at 25 °C. CFC samples (CFC-11 and CFC-12) were also measured by gas chromatography after stripping from the water samples under a stream of high purity nitrogen following Busenberg and Plummer (1992).

3.2.5 CHLORIDE MASS BALANCE

The chloride mass balance (CMB) method is a common approach used to estimate groundwater recharge in semi-arid areas. The basis of the method implies that all chloride in groundwater is derived from rainfall and that an increase in chloride concentration in groundwater relative to rainfall is the result of evapotranspiration prior to recharge. The key assumptions are that the hydrologic system is at steady state and that there is no additional source of chloride in the subsurface, such as halite dissolution. Here, the following equation from Erickkson and Khunakasem (1969) provides estimates of the recharge rate to an aquifer under steady-state conditions:

$$R = PC_P./.C_R \tag{3.1}$$

Where R is the recharge rate (mm/year), P is annual precipitation (mm/year), C_p is the chloride concentration of precipitation (mg/L) and C_R is the chloride concentration of groundwater (mg/L).

3.2.6 STRONTIUM ISOTOPES

Strontium isotope ratio ($^{87}Sr/^{86}Sr$) analysis of groundwater systems is a well-established method of identifying water sources, degree of water-rock interactions, and in many cases mixing relationships between the sources of dissolved constituents in water (Bullen and Kendall, 1998; Shand et al., 2009). The most common mixing is between dissolved constituents in rainfall (usually dominated by sea spray) and those arising from aquifer mineral weathering. As part of this study, all groundwater samples and one sea water sample from the study area were analysed for strontium isotope ratios. In addition, strontium ratio values for rainfall, soil and geological formations were sourced from the following: rainfall values were from Raiber et al. (2009), values for soil carbonates from Dart et al. (2005), values for the Melton Limestone from Elderfield (1986) and values for the Precambrian basement rocks from Webb et al. (1982). These values and the data measured from the field sampling campaign were utilised in a mixing equation.

Assuming mixing between two end-members, the proportion of each end-member contributing to the observed strontium ratio of the groundwater can be identified using the following equation from Capo et al. (1998) presented in Green et al. (2004):

$$\frac{M_1^{\mathrm{Sr}}}{M_1^{\mathrm{Sr}}+M_2^{\mathrm{Sr}}} = \frac{(^{87}\mathrm{Sr}/^{86}\mathrm{Sr})_{mix} - (^{87}\mathrm{Sr}\ /\ ^{86}\mathrm{Sr})_2}{(^{87}\mathrm{Sr}\ /\ ^{86}\mathrm{Sr})_1 - (^{87}\mathrm{Sr}\ /\ ^{86}\mathrm{Sr})_2} \tag{3.2}$$

3.2.7 LUMPED PARAMETER MODELLING

Environmental tracers can be used to estimate MRT for a groundwater sample providing that:

1. the input function for a particular tracer to the aquifer is known,
2. tracer concentrations are corrected for environmental factors (temperature, pressure, salinity and excess air),
3. a representation of the flow system is provided.

A complete evaluation of the environmental tracer data is beyond the scope for this report. However, a preliminary analysis was made using lumped parameter models (LPM) where idealised aquifer systems (piston flow and exponential model) are used to evaluate the behaviour of groundwater flow and mixing in the subsurface. This evaluation was made with the software LUMPY (Suckow, 2013) which provides the capacity to adjust input concentrations for a given tracer to account for different environmental factors. For example, in the simplest cases of the Piston Flow Model (PM) and the Exponential Model (EM), the groundwater sample is assumed to have one source of water and a unique age (PM) or an exponential age distribution (EM) respectively (Małoszewski and Zuber, 1996). In the plots for the PM and EM models the numbers on the plots represent the MRT. In more complex cases, the groundwater sample may have any age distribution and can include water from a range of sources (rainfall, river, other aquifers, etc.) each with its own age. In the Binary Mixture Model (BM), the sample is a mixture of groundwater, one of which is young and one which is old. The numbers presented on each tracer plot for the BM model represent the mixing fraction of the old component of water. The main advantages of lumped parameter models are that they are zero-dimensional and require few parameters. However, lumped parameter models assume that groundwater flow is constant and that the underlying age-distribution of groundwater is constant and has been previously characterised.

3.3 Airborne electromagnetics

A component of the G-FLOWS 2 investigation was to assess the suitability of using AEM as a tool to aid in characterising hydrogeological properties of large regions, especially to identify water salinity and basement lithology. AEM works by flying an airborne platform slowly and close to the earth's surface. The AEM transmitter induces a current into the earth by generating an electromagnetic field. The underlying ground exposed to this primary field, in turn will generate what is known as a secondary field response that is recorded at the receiver (Figure 3.3).

Some underlying materials such as sulfides, graphite, saprolite, clay-rich sediments and saline groundwater can be good conductors and when in the presence of an induced primary field, generate their own EM secondary field. In very resistive areas, no electric response from the ground is measured but when the system is flown over a conductive body a response can be measured, so EM local anomalies can be detected when there is enough contrast with the surrounding host geology. Geophysical methods of exploration, in particular AEM, have proven useful for delineating palaeodrainage systems (Jessel et al., 2015) and for characterising large regional aquifers (Ley-Cooper and Munday, 2013) and allow extensive spatial coverage to be obtained quickly.

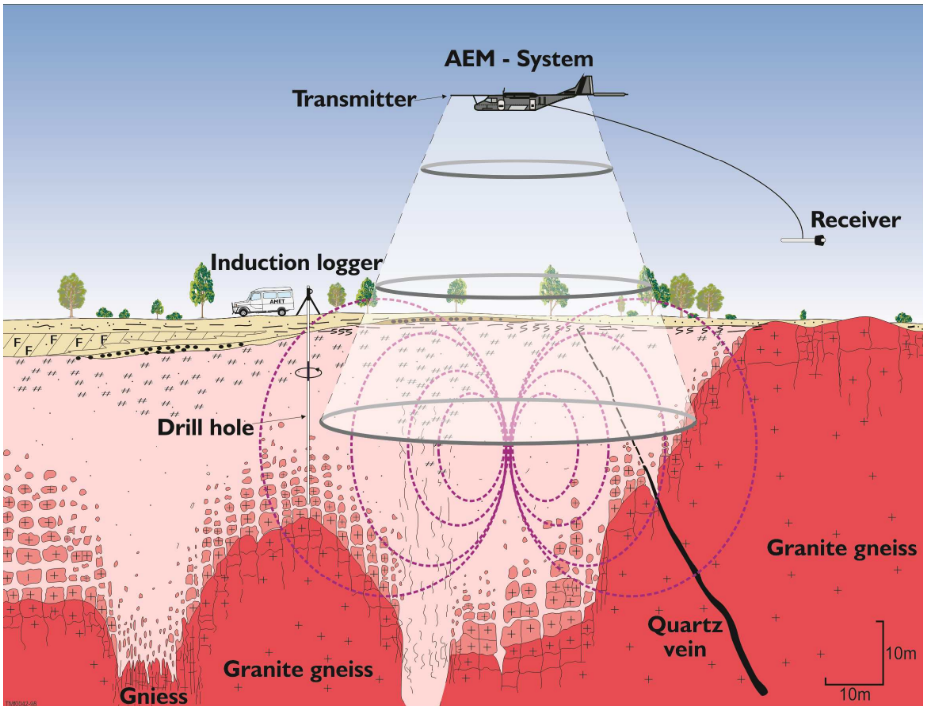

Figure 3.3 Conceptual diagram of the AEM setup

The spatial coverage of AEM data over the northern Eyre Peninsula and southern Gawler Ranges is shown in Figure 3.4. G-FLOWS 2 compiled these data from DSD (DSD, 2014) as well as through direct contact with exploration companies throughout the region. An additional small dataset north-west of Kimba (shown in blue; Figure 3.4) was acquired by DSD in support of G-FLOWS 2. Figure 3.4 shows the discontinuous and scattered nature of the AEM coverage in this prospective setting. This pattern is characteristic of the acquisition of AEM in mineral exploration, which tend to be highly focused small areas of interest at tenement-scale within the broader landscape. The different colours of the AEM areas in Figure 3.4 indicate the different EM acquisition systems (including both fixed wing and helicopter systems) that are used. The type of system that is used has implications for the way their data is processed and interpreted, which is important in trying to deal with multiple areas in a spatially consistent manner. AEM data for the Kimba-Darke Peak region was obtained using TEMPEST systems, a fixed-wing aircraft mounted setup, and data for the Coastal Plain area was obtained from REPTEM, a helicopter-mounted setup. Further technical specifications related to these and other EM acquisition systems used in the Eyre Peninsula can be found in Ley-Cooper et al. (2015).

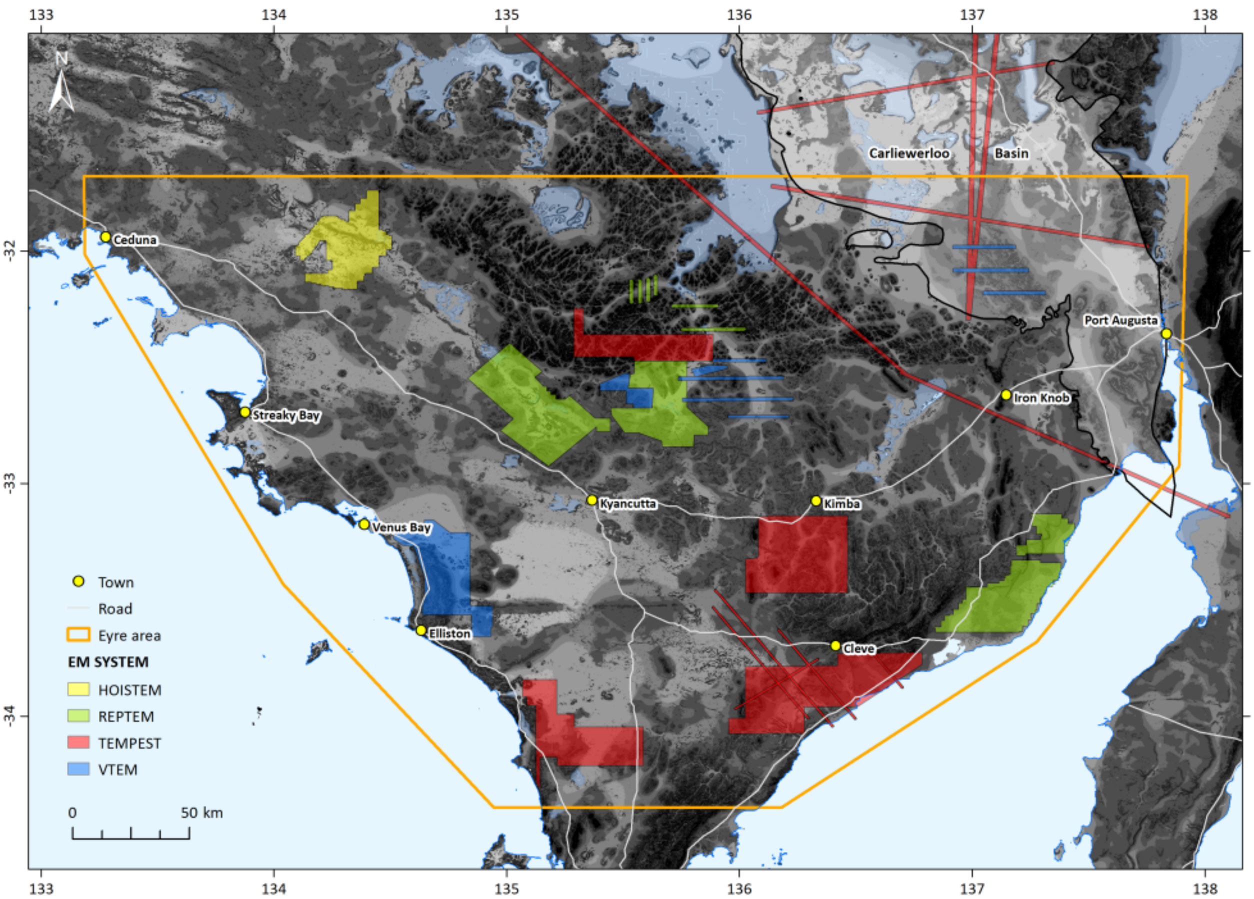

Figure 3.4 Broader map of the Eyre Peninsula, showing available airborne electromagnetic (AEM) surveys across the Northern Eyre Peninsula

AEM data were inverted (modelled) using a one-dimensional layered earth inversion (LEI), under the assumption that conductors are flat lying and represent variations in aquifers and/or groundwater quality. The aim for employing this method was to attain spatially consistent models of ground conductivity from different AEM systems, taking account of their specific characteristics. To assist in the process, the project team also reviewed and examined the availability and applicability of different algorithms for inverting data from these systems. In the context of inverting AEM data from a hydrogeological perspective, two commonly used methods were considered – Geoscience Australia's Layered Earth Inversion (GA-LEI) see Brodie and Richardson (2015) and Aarhus University's AarhusInv LEI (Auken et al., 2014).

The final choice of algorithm used to invert all AEM datasets in the study area was largely defined by its availability in the public domain, specifically the Geoscience Australia LEI. The code is capable of inverting data from all of the commercial time-domain systems available in Australia today, including dual moment systems, and has been demonstrated through the G-FLOWS Stage-1 project (Ley-Cooper and Munday, 2013) which dealt with historical AEM data from systems that have since been superseded. An added benefit of using open source code is that with the advent of new AEM datasets in the study area, their information content could be readily incorporated into this existing knowledge base. The GA-LEI algorithm is a deterministic regularized inversion that inverts each AEM sample/sounding independently (i.e. in sample-by-sample fashion) via a gradient-based down-hill search (Brodie and Richardson, 2015).

3.4 Hydrogeological modelling

In order to further investigate the presence or absence of regional groundwater flow, a hydrogeological model based on Tóth (1963; 2009) was applied to three transects in the Cleve Hills. The major question investigated was whether or not groundwater flow can move over distances of 30–40 km, based on the hydrogeological information available. The framework for the model is based on the available hydraulic head data and lithology collated for the study area. In order to make an assessment, a model is proposed based on gravity driven basin models (Tóth, 1963; 2009). The main assumptions are that watertables are static, working in the two dimensions of a cross-section for a given transect is adequate, and that the aquifer has constant and uniform porous properties. Based on these assumptions, the calculations specific to the modelling and the results of the modelling can be found in Appendix A .

4 Hydrogeology

The primary objective of this project was to obtain a greater understanding of groundwater flow, and as a precursor to this, an improved hydrogeological understanding of the region needed to be developed. It is apparent that the hydrogeology of the region is extremely complex as it contains a number of different aquifer types within both the Cleve Hills and Coastal Plain. Field observations, lithological logs from WaterConnect and SARIG, as well as existing geological maps and geological notes were combined to produce a simplified surface geology map highlighting the predominant hydrogeological units. In addition, an improved understanding of the hydrostratigraphy of the region was developed and presented in four hydrostratigraphic cross-sections (three in the Cleve Hills, one in the Coastal Plain). In order to determine the presence of local-scale and or regional-scale groundwater flow systems, a regional potentiometric surface is presented and discussed. In addition, more intimate analysis of hydraulic head data is presented and discussed for four piezometric cross-sections.

4.1 Surface geology

Topographically, the Cleve Hills are a reflection of the structure of the underlying basement rock (Twidale et al., 1985). The current landscape is a result of the erosion of less resistant rocks, with the more resistant rock units remaining as plateaus and ridges with valleys formed in-between. Hills and ridgelines are comprised of quartzite, granite and gneiss while softer schists have been eroded to form the valleys. Faulting has also played a role in the present elevation of the Cleve Hills (Drexel et al., 1993). Infilling by aeolian and colluvial/alluvial sediments that are predominantly of Quaternary age has also occurred in the valleys.

Regionally, several faults exist, and can act as groundwater flow boundaries. However, the nature of these boundaries is undetermined. A number of mylonite zones (not on map) occur throughout the region. These zones are considered similar to faults, and as such also have the potential to either increase or decrease the hydraulic conductivity of these zones. To the east of the Cleve Hills is a major fault, separating the coastal sedimentary Cowell Basin from the hills (Figure 4.1). Coastal settings in the north-eastern parts of the study area are low lying with almost no undulation. The Coastal Plain extends inland up to 6 km to the west of the coast towards a somewhat obscured fault escarpment which provides approximately 50 m of relief from the uplifted fault to the coast.

The ancient landscape displays little relief except for the areas immediately adjacent to the prominent outcrops of granitic and metamorphic rocks. The extensive geological period over which the landscape has developed infers a number of erosional periods resulting in a complex upper basement surface. Intrusions, faulting and folding have altered relief over vast geological time periods and sub-surface channels are likely to have had directional changes, been in-filled, over cut by erosion and had newer landscapes develop over the top. The degree of weathering and fracturing of these rocks is irregular and can occur up to 100 m below the surface (Berens et al., 2011). Elevation of the area ranges from approximately 250–400 m above sea level, with localised highs in excess of 450 m (Figure 4.2).

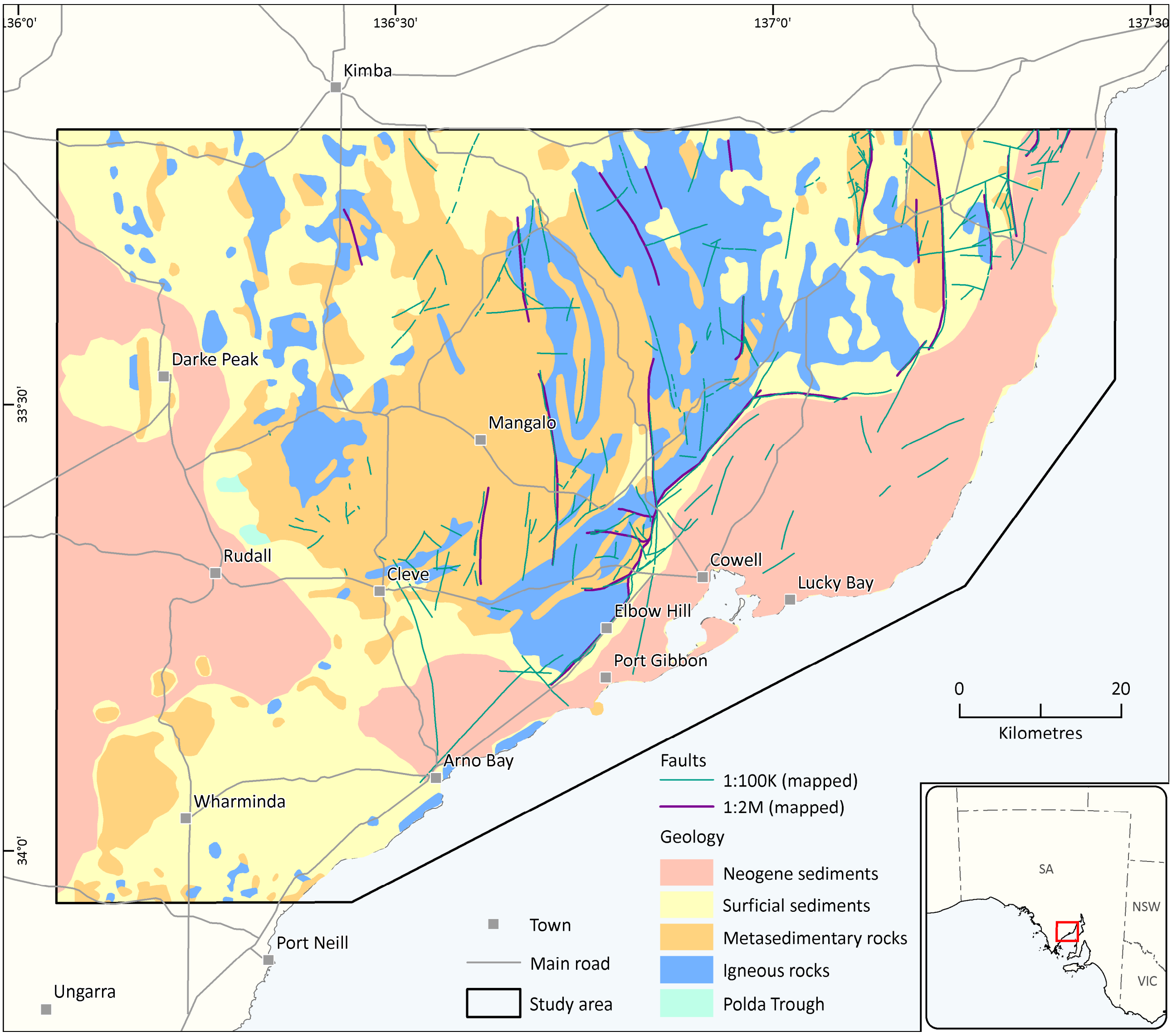

Figure 4.1 Simplified surface geology map for the study region

4.2 Groundwater yield

Groundwater yield data collated for the study area indicate that in general the aquifers present have very low yields (Figure 4.2). The majority of wells have yields of less than 0.5 L/s with occasional wells with yields greater than 10 L/s. There is no obvious relationship with elevation or hydrogeological unit. Many wells have yields that vary considerably over a small spatial area which is consistent with other fractured rock aquifers in South Australia (Green et al., 2007; Leaney et al., 2013; Love et al., 2002).

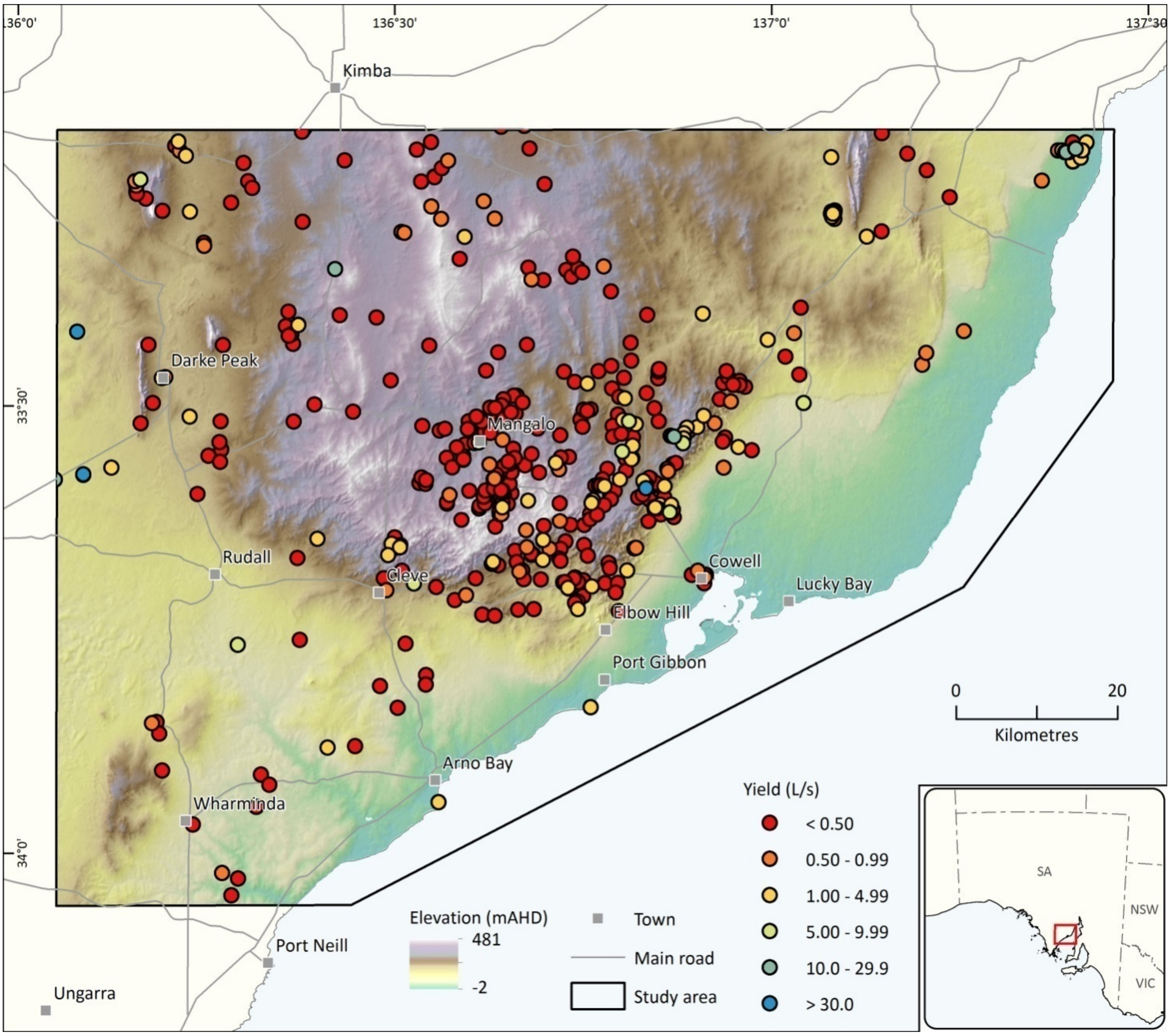

Figure 4.2 Groundwater yields for the study region

4.3 Hydrostratigraphy

In the Cleve Hills study region, aquifers occur in Pre-Cambrian fractured rocks as well as in Tertiary and Quaternary deposits laying unconformably over bedrock. Jurassic sediments occur in the lower parts of some wells in the study area, but are not within the list of sampled wells for this study. Deeper, Jurassic sedimentary aquifer systems are likely to occur within the Polda Basin, which extends into the south-western part of the study area (Berens et al., 2011). In the larger upland valley settings, sedimentary and fractured rock systems may have both confined and unconfined components, but the lack of piezometer nests and spatially appropriate measurement opportunities means aquifer separation and confining layers for pressured systems cannot be defined at any location. Likewise, the deeper sedimentary systems of the far eastern Polda Basin deposits are poorly described.

The hydrostratigraphy for the Coastal Plain has been previously characterised to a greater extent than the Cleve Hills. An unconfined and unconsolidated Quaternary system lies over confining beds of the Gibbon Beds and Melton Limestone. These clays and limestones behave as the upper confining layer for the Tertiary confined aquifer system. The Tertiary aquifer system extends from the polymict sand deposits downwards through to the upper part of the basement. In-situ weathered granite basement (saprolite) is noted at the base of some drill holes. The extents of fractures within the granite, which may be hydraulically active, are unknown. Groundwater levels within the coastal setting reflect a low upward vertical flow potential from the confined Tertiary aquifer into the unconfined aquifer. Unconfined Quaternary sediments are unsaturated in the west and the lateral hydraulic gradient indicates flow towards the coast. Standing water level data used to define flow and vertical potential have been density corrected (Post et al., 2007).

4.3.1 HYDROSTRATIGRAPHIC CROSS-SECTIONS

Four transects following the hydraulic gradient and down possible 'flow lines' were inferred from the potentiometric surface (Figure 4.9). Simplified hydrostratigraphic cross-sections were constructed for these four transects using a combination of lithological and stratigraphic logs (Figure 4.4, Figure 4.5, Figure 4.6 and Figure 4.8). These transects should provide a fair representation of the hydrogeological systems of the region. The location of these transects is shown in Figure 4.9.

The lithological information was grouped into five broad hydrostratigraphical categories: surficial sediments, saprolite, clay horizons, metasedimentary rock, and igneous rock. Surficial sediments include topsoil, sands and unconsolidated sediments containing only minor components of clay. These unconsolidated surficial sediments are likely to be conducive to recharge, especially where they occur at elevation. Saprolite was classified as any material that was indicated to have undergone in situ weathering and have a clayey composition. These are likely to act as semi-confining layers, or possess a lower conductivity than unconsolidated surficial deposits, and where they occur at the surface are unlikely to be representative of recharge areas. Clay horizons include any significant clay layers recorded in lithological logs and are interpreted as a potential confining layer, or as a layer of very low conductivity. Basement rocks are separated into metasedimentary and igneous. Despite being likely to have similar behaviour in terms of hydraulics, they may be differently weathered. Much variation exists in the degree of metamorphism experienced in the area. Metamorphism of igneous rock as well as sedimentary rock is common, especially in the vicinity of the mylonite shear zones.

Cleve Hills

Surficial sediments

Surficial sediments are widespread but generally thin. These sediments are also generally thin or absent at high elevation on steep topography, but typically thicker and with a greater lateral extent towards the valley bottoms. Sediments in the valleys and channels of the Western and Southern transects, for example, are in the order of 30–50 m thick (Figure 4.4).

Clay and saprolite

The cross-sections highlight the lack of a regionally continuous clay aquitard and so the presence of an extensive confined system can be ruled out. Clay and saprolite layers appear thicker and have a greater lateral extent in valleys and channels than in the hills. Around the higher topographic features, clay and saprolite occur as isolated and localised thin lenses. Thus locally, confined systems may be found in valleys. Recharge is also likely to be lower in some valleys due to the presence of clays immediately at the land surface, as observed in parts of the Western and Southern transects (Figure 4.4 and Figure 4.5). In other areas where thin layers of surficial unconsolidated sediment overlies clay or saprolite, depth of infiltration of recharge waters and the extent of vertical downward flow is likely to be limited. These settings can be expected to support only shallow groundwater systems with limited depth of circulation. Thicker channel sediments observed in valleys on the Western transect (Figure 4.4) may form sedimentary aquifers, however the maximum depth of these is still only 50 m, so they are unlikely to host significant hydrogeological systems.

Basement Rocks

Basement geology is extremely heterogeneous, as observed in the Western and South-eastern transects particularly. Several localised igneous intrusions are observed in the Western and South-eastern transects. Depth to basement is typically shallow and the basement is exposed on most slopes and upland settings.

Where this is the case, no sedimentary aquifer is likely to exist. Weathering profiles in basement rocks may be an important hydrogeological factor but their characterisation requires more lithological information than currently exists.

In many places, the exposed basement rocks show zones (as lenses) of clay and saprolite derived from the weathering. The co-existence of clays and fracture zones introduces further complexity into the potential groundwater flow behaviour because the aquifers then have a combination of sedimentary and fractured rock system properties. The lack of piezometer nests at sufficient depth prevented a closer investigation of confining layers, inter-aquifer groundwater exchange, or even the location of pressured systems.

Weathering

Drill logs show that in many places the basement is intensely weathered, with the products of weathering making for extremely difficult interpretations of hydrostratigraphy. Across the study area, many drill logs have weathered zone descriptions which use colloquial or lay terms. Based on examination of over 100 lithological logs, the weathering zone is approximately 100 ± 50 m thick. However, there seems to be very little sedimentary or weathered zone geological descriptions that can be related over distances beyond a few kilometres. In other words, Quaternary, Tertiary, Jurassic and Precambrian deposits can sometimes be identified, but their hydrogeological properties are much less definable due to variable weathering on differing basement geologies and unclear vertical/horizontal boundary layers. The profile of the weathered regolith is presumed to follow the topography of the basement (Harding et al., 2002).

Summary

Interpretations of the available lithological information for the Cleve Hills area reasonably points to a hydrogeological system comprising unconsolidated surficial sediments overlying weathered basement (Figure 4.3). Together, the surficial sediments and weathered basement appear to act as one unconfined hydrogeological system, with localised confining conditions possible. Overall, the simplified cross-sections and surface geology map defined here are useful as a guide to the regional hydrogeology. They highlight the heterogeneous nature of the subsurface geology in the region.

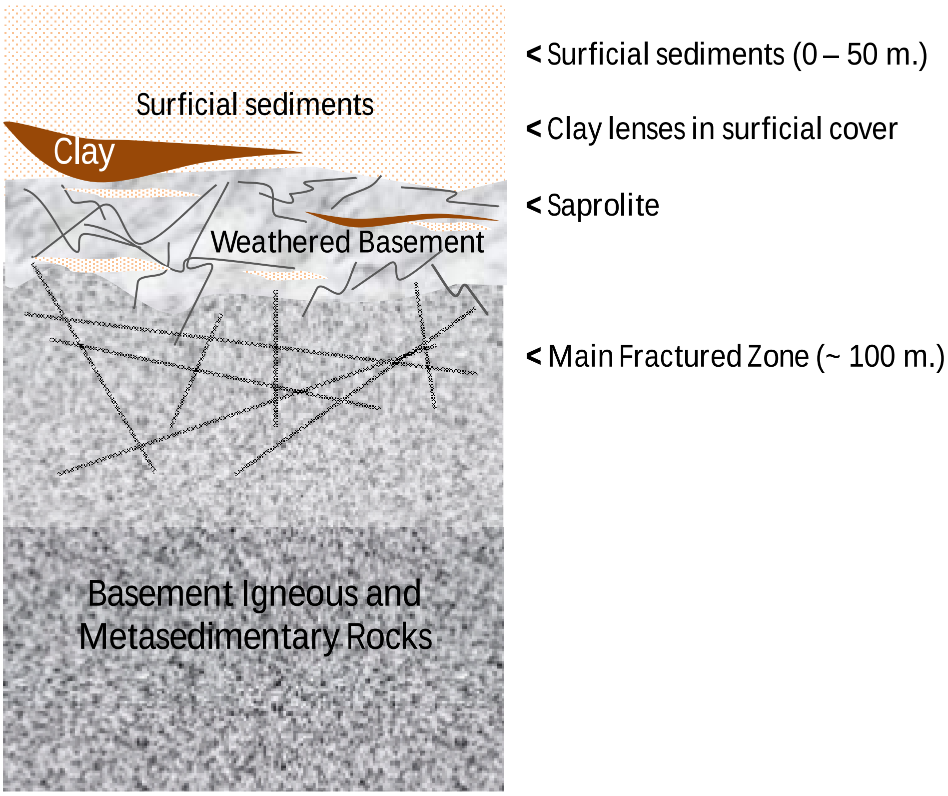

Figure 4.3 Conceptual understanding of the hydrostratigraphy of the Cleve Hills region

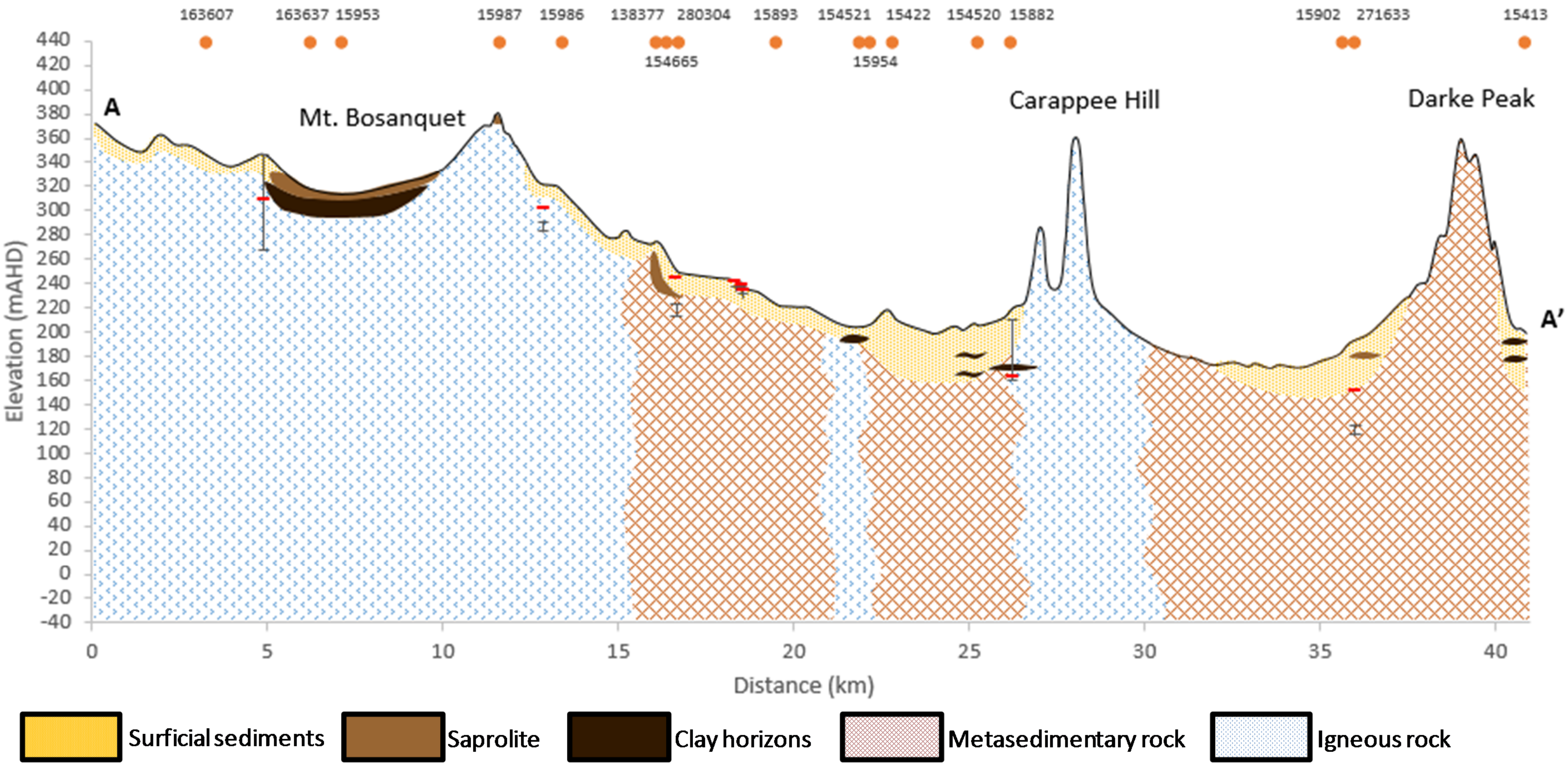

Figure 4.4 Western hydrogeological transect, orange dots represent wells with lithology, red dash is the standing water level and error bars represent the screened or open interval, location of transect shown in Figure 4.9

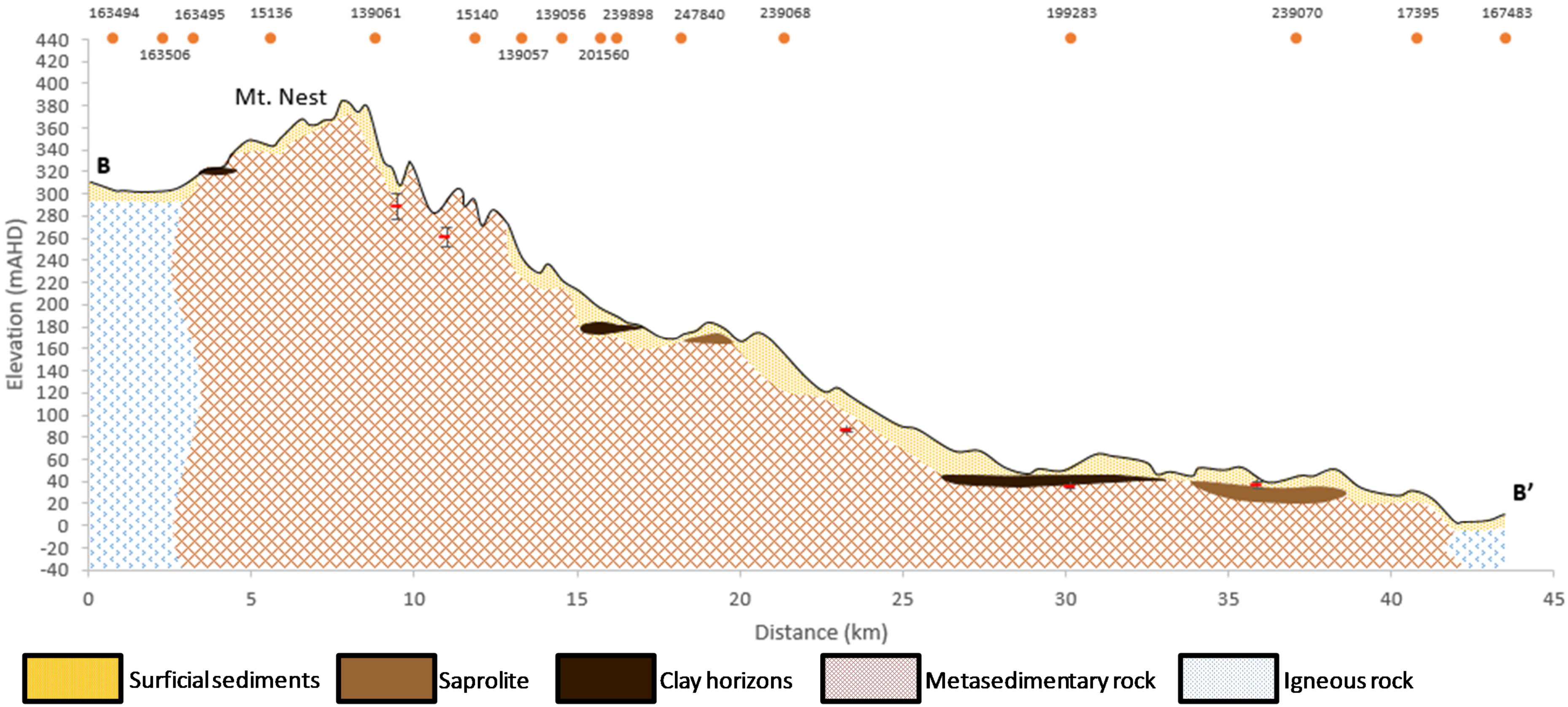

Figure 4.5 Southern hydrogeological transect, orange dots represent wells with lithology, red dash is the standing water level and error bars represent the screened or open interval, location of transect shown in Figure 4.9

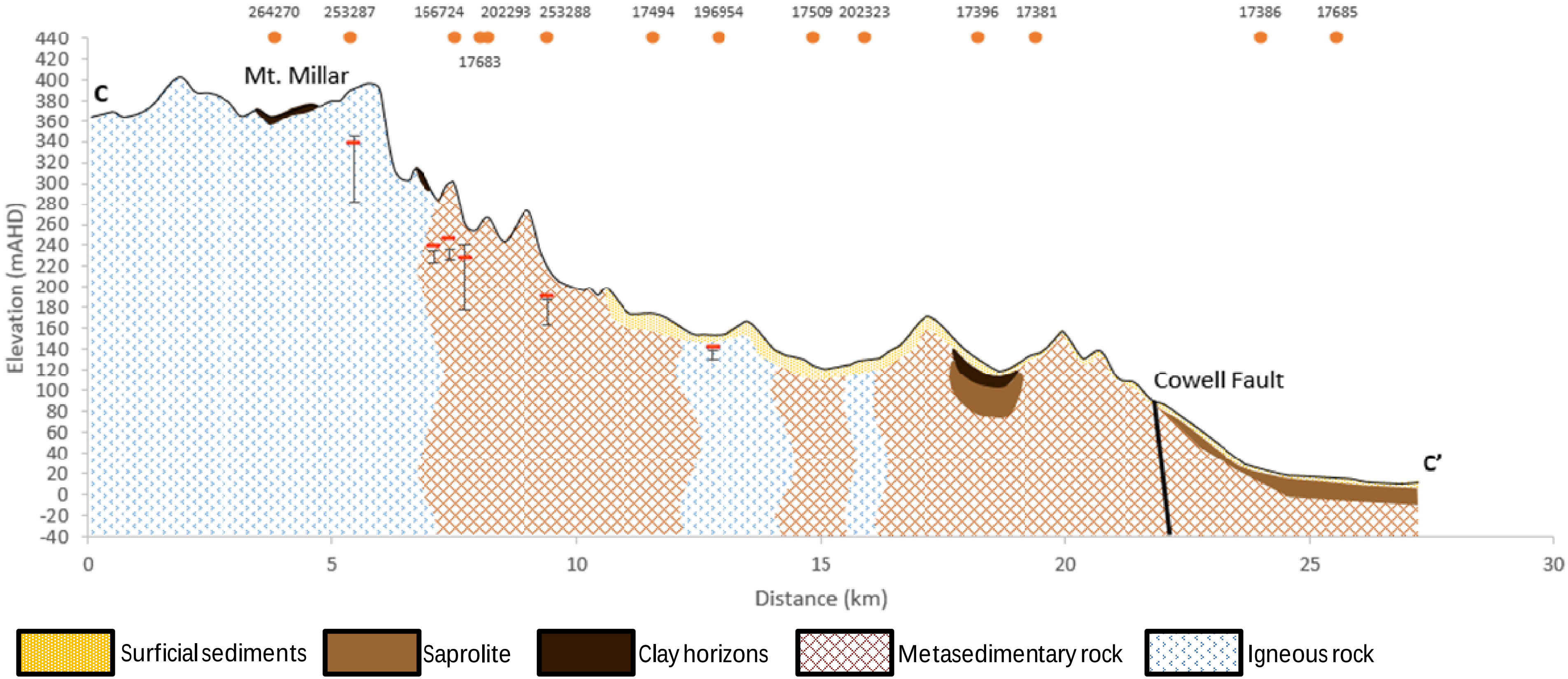

Figure 4.6 South-eastern hydrogeological transect, orange dots represent wells with lithology, red dash is the standing water level and error bars represent the screened or open interval, location of transect shown in Figure 4.9

Coastal Plain

Coastal aquifers exist on the east of the study region under the Coastal Plain sloping down towards Spencer Gulf (Figure 4.8). The land surface consists of clay pans with quartz sand, shelly sands and minor salt deposits. Water features, such as creeks, rivers or lakes, in the north-east coastal area are virtually absent in this area of low relief. As previously mentioned, a fault escarpment west of the Coastal Plain marks the transition between the elevated hills setting to the west and exposes siliceous sandy alluvium, colluvium and aeolian deposits. This escarpment has a north-south orientation (Figure 4.1) and an elevation of 50 metres Australian Height Datum (mAHD). Holocene deposits including shelly white beach sands obscure the escarpment.

Both fractured basement rock and sedimentary rock deposits are present near the coast, forming a multi-component hydrogeological system. Confining layers are regional and therefore more clearly identifiable with previous hydrogeological characterisations undertaken by Jueken (2011) and Thompson (2014). A simplified hydrostratigraphy for the Coastal Plain is presented in Figure 4.7.

Basement rocks of the Gawler Craton are overlain by Tertiary and Quaternary deposits. The Kanaka Beds form the oldest Tertiary (Eocene) unit to unconformably overlie the Gawler Craton basement. The Kanaka Beds are composed of calcareous sand and shale with no matrix. There are traces of white clay and grey to black lignite interlaid into parts of the calcareous sands. The Kanaka Beds have a thickness of up to 40 m and are overlain intermittently by fluvial derived polymict sands of mid-Tertiary age. The sands are fossiliferous, unconsolidated, and also contain gravel and quartzite. The thin fossiliferous sand and gravely sheet varies from 1–6 m in thickness. Unconformably overlying the polymict sand sheets is the Melton Limestone.

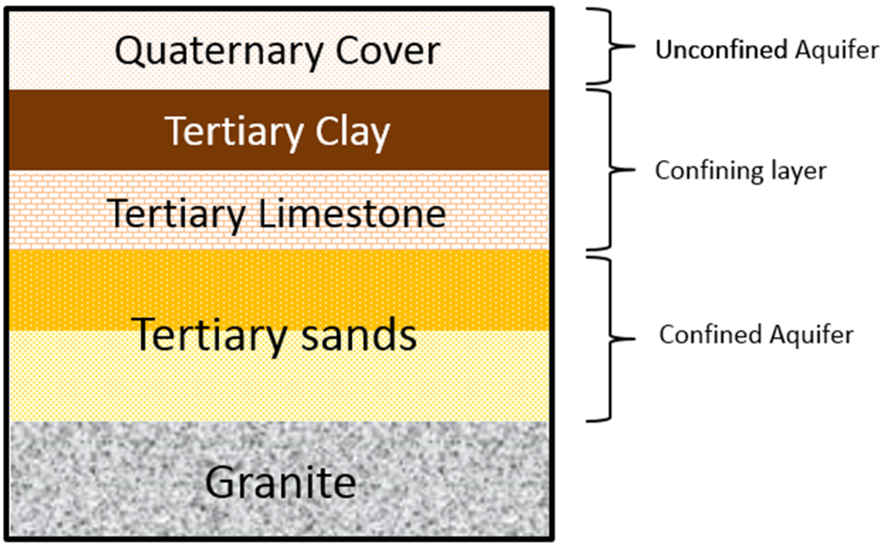

Figure 4.7 Simplified hydrostratigraphy for the Coastal Plain region

The mid to upper Tertiary Melton Limestone is in intermittent contact with the Kanaka Bed between polymict sand sheets. This bio-clastic limestone is a fossiliferous deposit with a quartzite sand component with occurrences of calcareous clay and glauconite. The Melton Limestone ranges from 16–20 m thick in the study area.

The Gibbon Beds conformably overlie the Melton Limestone. This is a fluvial deposit from the late Tertiary (Pliocene-Pleistocene). The non-fossiliferous and non-marine Gibbon Beds are 16-18 m thick in the study area and contain mottled grey, red and yellow clayey sand, gravel and silt. To the west of the low relief coastal setting, the Gibbon Beds and Melton Limestone pinch-out and make contact with the sloping Gawler Craton basement. Where the Gibbon Beds pinch out to the west, the Quaternary sediments continue. Quaternary units overlie the Gawler Craton basement rock throughout many areas of the Eyre Peninsula.

At the coast there have been two sedimentary aquifers identified. Quartzite sand and gravel units host the Tertiary and Quaternary aquifers. The flow path for both aquifers is west to east towards the coast (Jeuken, 2011). The Tertiary aquifer has a higher hydraulic head than the Quaternary aquifer. Both Tertiary and Quaternary aquifers are hydraulically separated by the confining Melton Limestone and Gibbon Beds. The Quaternary aquifer is saturated only to the east of the region and appears to be perched on the low permeability Gibbon Beds. Both aquifers are hyper-saline and are not suitable for domestic or livestock water supply (Jeuken, 2011).

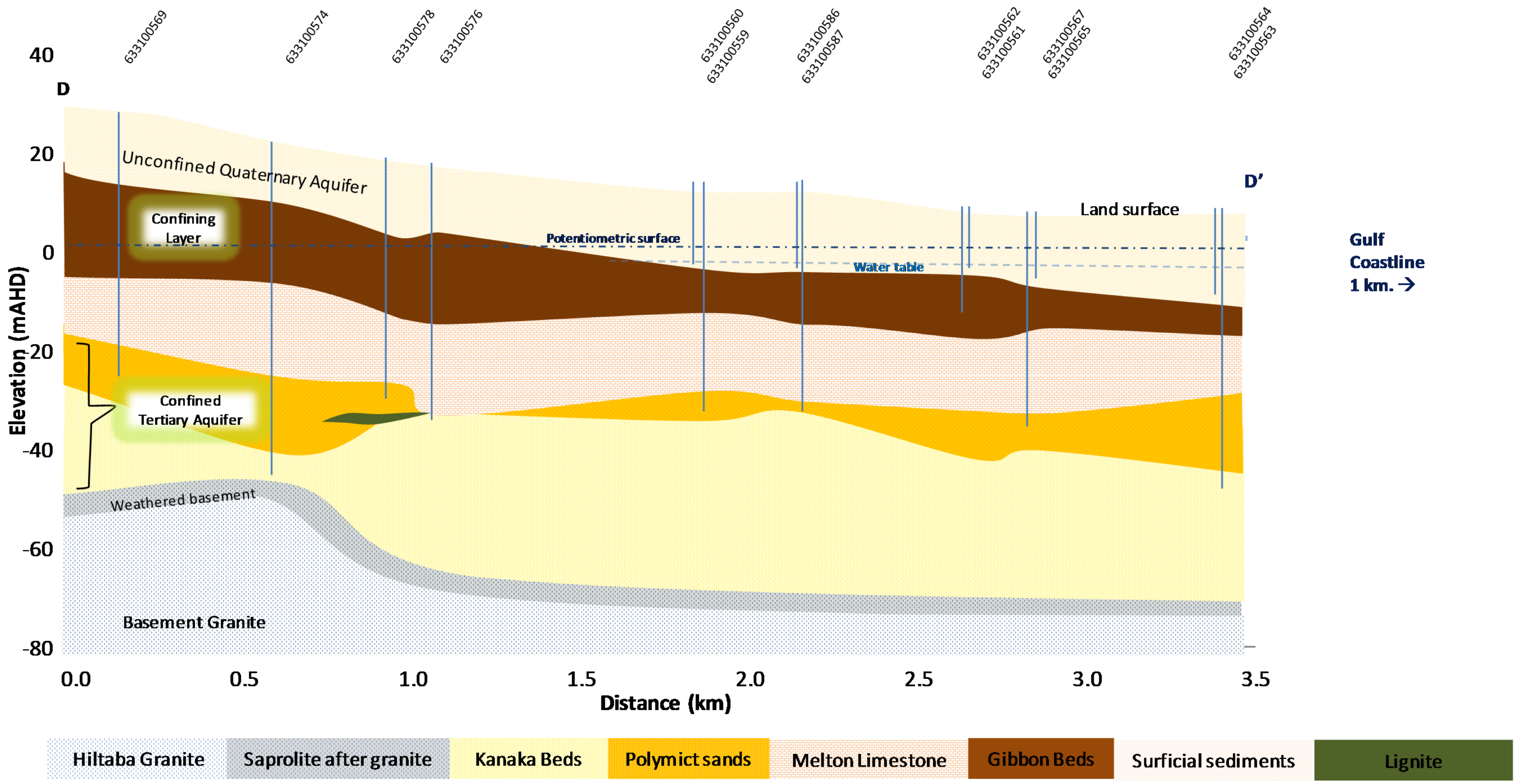

Figure 4.8 Hydrogeological transect for the Coastal Plain, blue lines represent the location of groundwater wells

4.4 Regional potentiometric surface

Because of the paucity of hydrogeological information currently available in the study area, an aquifer-specific potentiometric surface evaluation is not possible. Therefore, a regional potentiometric surface was constructed by assuming connectivity between all aquifers in the region. It is important to note that this is in contrast to the interpretation provided by Risby and Harrington (2014) that was focussed towards prescribed water resource areas to the west. In addition, as previously mentioned, the potential for extreme anisotropy in fractured bedrock aquifers can result in a poor correlation between hydraulic gradients and actual flow direction. Therefore, the regional groundwater potentiometric surfaces was primarily used as a guide for selecting the areas targeted for further investigation using environmental tracers and geophysics.

The potentiometric surface map for the study area is shown in Figure 4.9. Hydraulic head values are expressed in 20 m contours as well as a colour ramp on the map, with the highest values being in excess of 300 m and the lowest values of 0 m at sea level. It is apparent that undulations in the potentiometric surface are present and that the surface closely follows the broad-scale topography of the region. Therefore, the topography can be used as a proxy for the shape of the watertable to infer approximate and broad-scale potential flow directions and systems, due to the absence of sufficiently dense hydraulic head data for the region to achieve this. For example, very few wells are drilled at the tops of the hills due to the limited usefulness for stock use, so there is limited data on the watertable depth at these locations. These factors make a true understanding of the potentiometric surface across the entire landscape difficult to obtain.

There is a large groundwater mound present which coincides with the regions of highest elevation (Figure 4.9). This is in contrast to a much lower potentiometric surface near the coast and in the valley systems to the west of the hills near Darke Peak, Rudall and Arno Bay. In addition, the steepest gradient in the potentiometric surface occurs to the southeast of the hills near Cowell and Cleve, which coincides with abrupt changes in topography. If regional-scale groundwater flow is occurring, as inferred from the hydraulic gradients presented here, the potential directions of this flow would be from the hills to the west, south and southeast.

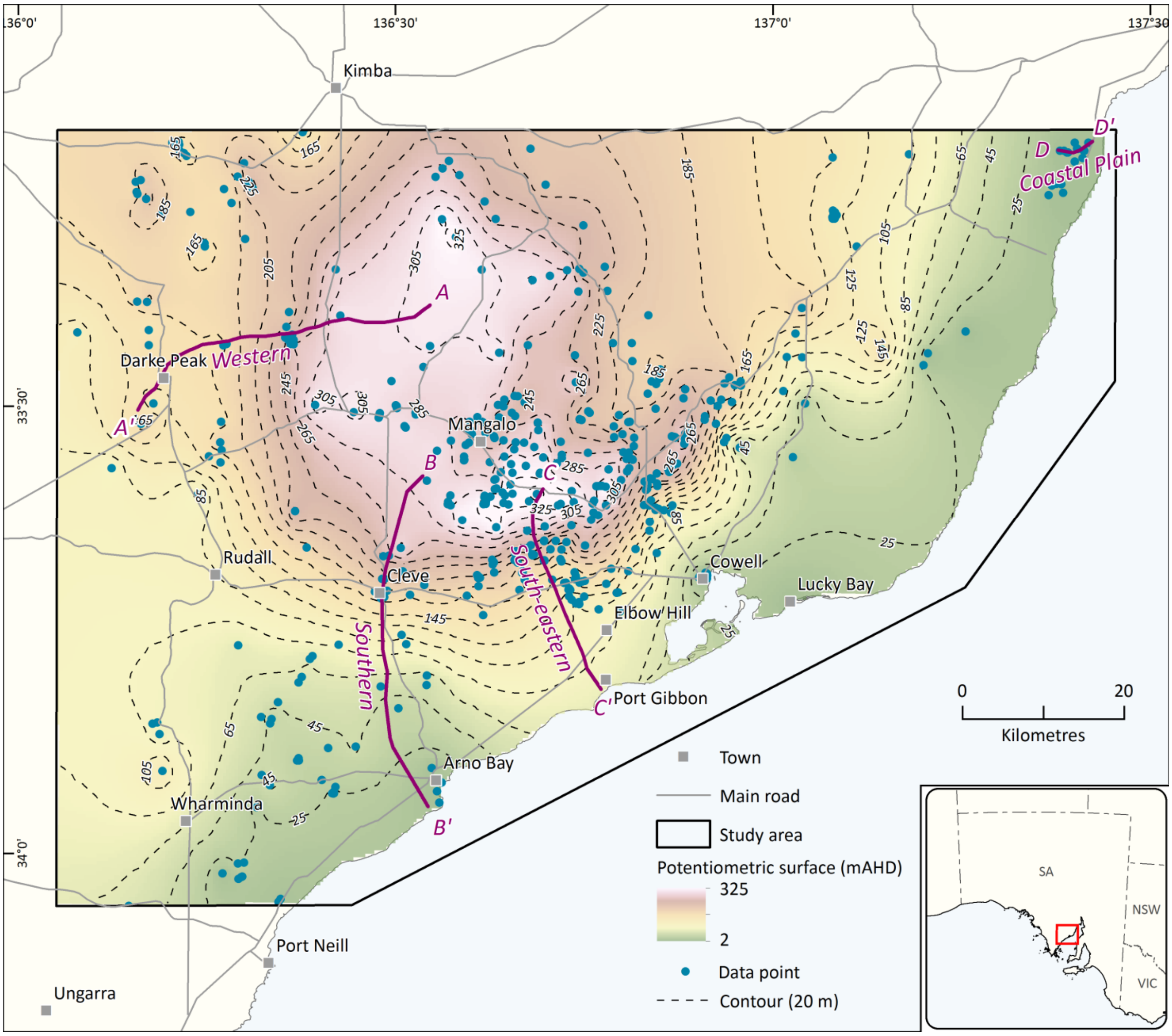

Figure 4.9 Potentiometric surface for the study area, blue dots represent the groundwater wells (data points) used to generate the surface, purple lines represent the location of the four hydrostratigraphic and piezometric transects

4.4.1 PIEZOMETRIC TRANSECTS

To provide further supporting evidence that the regional potentiometric surface follows the topography, trends in hydraulic head variation were evaluated in more detail at each transect (Figure 4.10). Based on this approach, highly localized flow systems are likely in the Cleve Hills as undulations in topography are apparent and show discharge and recharge occurring at various points along a given transect. The Coastal Plain however, follows the typical characterisation of the aquifers elsewhere in the Eyre Peninsula, and they have been divided into Quaternary and Tertiary sedimentary units underlain by basement granite. The hydraulic head data here shows a potential for downward flow.

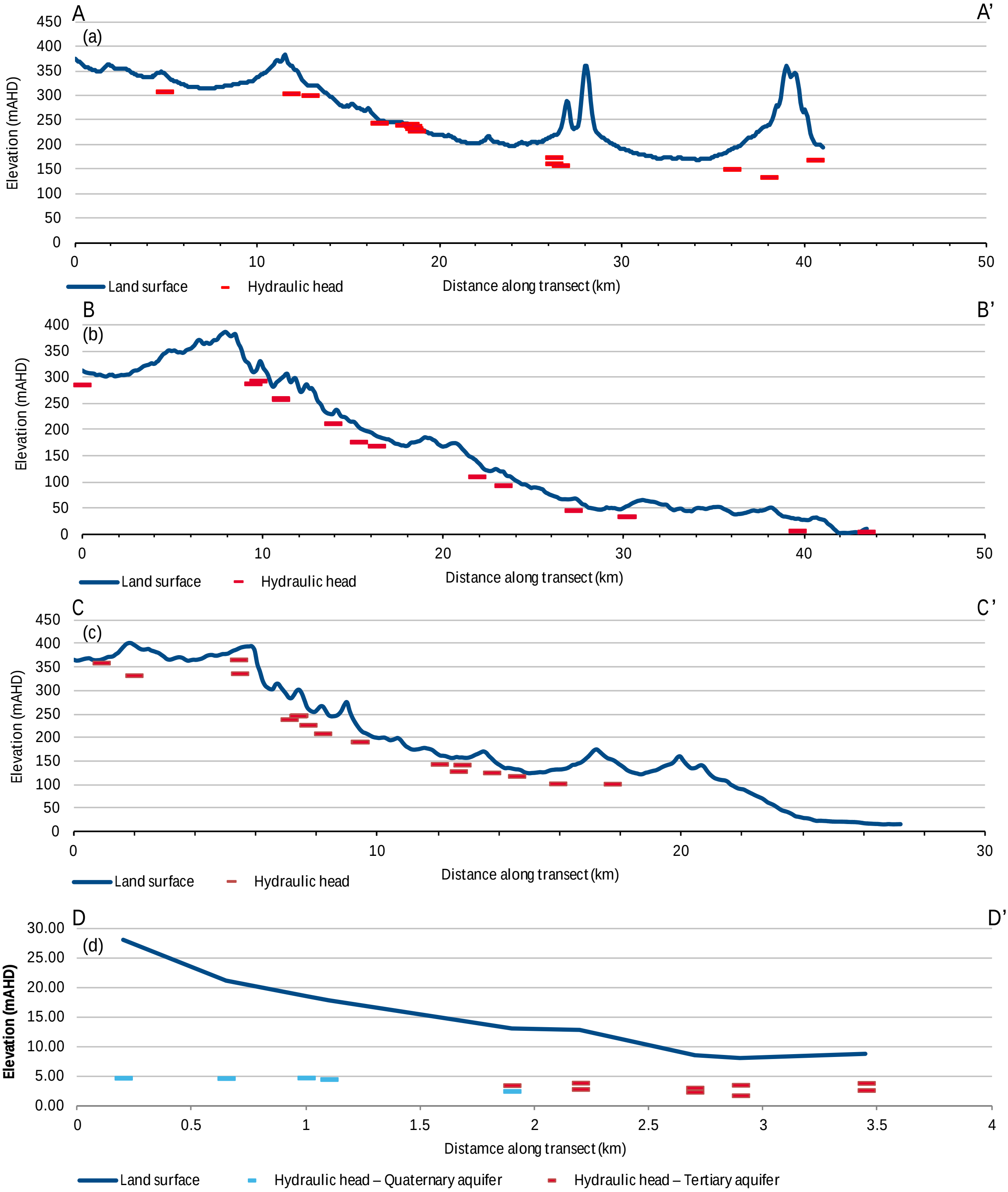

Figure 4.10 The relationship between hydraulic head and changes in land surface elevation along four piezometric transects: (a) Western, (b) Southern, (c) South-eastern and (d) Coastal Plain

Anecdotal evidence from landholders in the region and personal observations during the field sampling campaign indicate that a number of groundwater seeps (groundwater discharge zones) occur in the elevated regions of metamorphic and granitic rock outcrops, such as Carappee Hill. At an elevation of approximately 340 mAHD a groundwater seep is evident (Figure 4.11a).

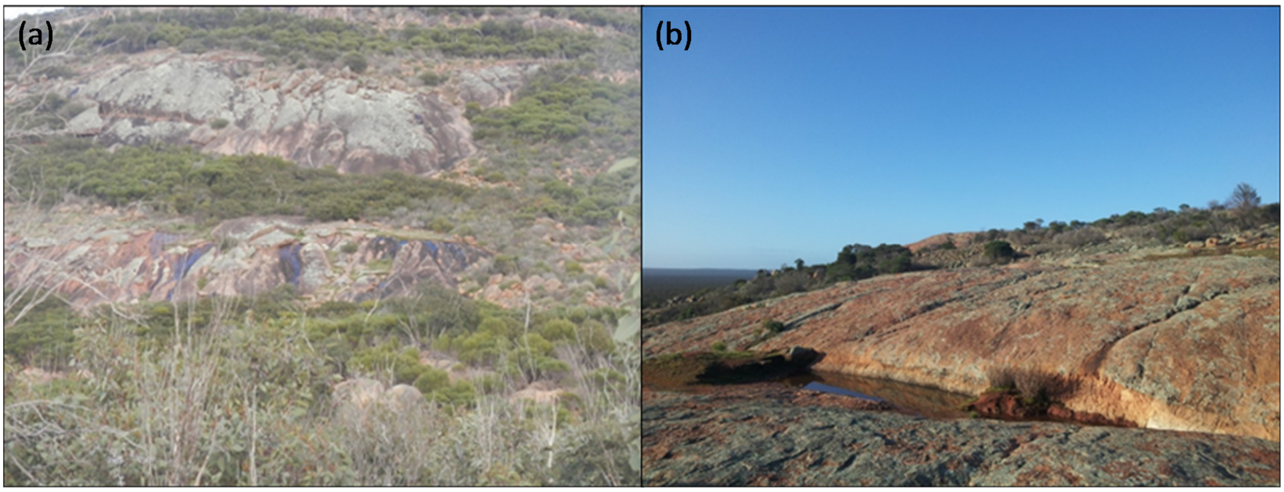

Figure 4.11 Groundwater seeps observed at (a) Carappee Hill and (b) Secret Rocks

4.5 Regional terrain analysis

The existence of palaeovalley networks across the region is likely to have a significant effect on aquifer extent and groundwater flowpaths. Long periods of erosion, weathering, tectonic extension, faulting and folding allow for the development of many channel or valley forms. Followed by late stage sedimentation, channel formations have become obscured by modern deposits. These valley sediments are known to occur over much of arid and semi-arid South Australia (Magee, 2009), and can be high-yielding aquifers, albeit with varying water quality.

As previously described, a terrain map was developed using MrVBF to identify the most likely litho-structurally controlled drainage lines within the study region (Figure 4.12). The most significant potential palaeodrainage system identified by the MrVBF analysis begins south of Kimba and extends south past Darke Peak to outflow at the coast in the vicinity of Arno Bay (Figure 4.12). Another extensive flat low topographic region is present southwest of Kimba near Mangalo, but there is no obvious connection to other systems or outflow apparent.

While indications of palaeovalleys from MrVBF can be used as a general guide to infer the presence of palaeovalleys or valley systems, implicit knowledge of palaeovalley sediments can only be verified from lithology. The Cleve Hills appear to be an appropriate geological setting for the formation of palaeovalley aquifers. However, because the well infrastructure is now largely defunct in the area, only limited sampling of groundwater in potential palaeovalley aquifers was possible here. Nevertheless, the MrVBF analysis combined with the available lithology has identified areas that could be further investigated through a targeted drilling program.

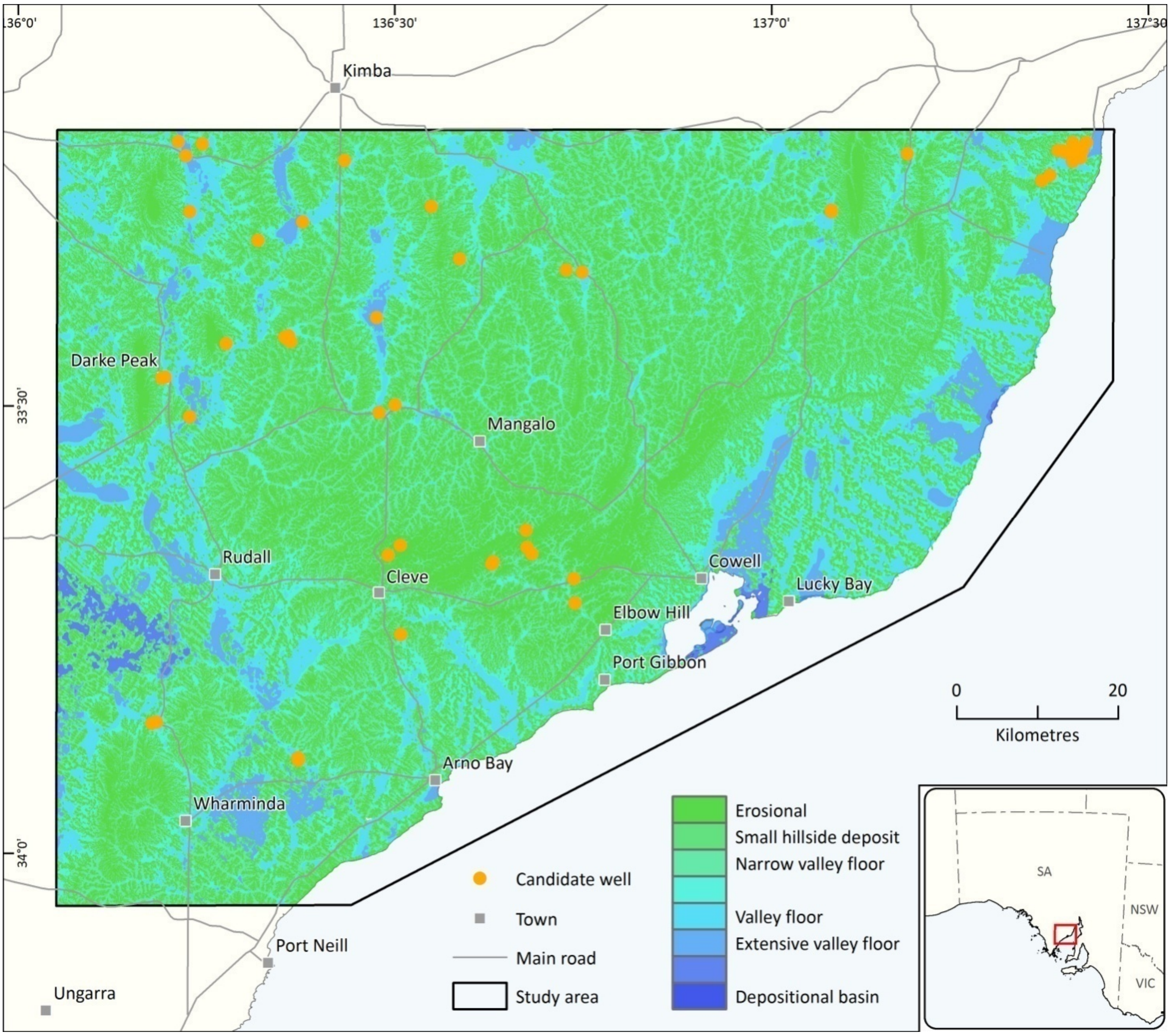

Figure 4.12 Regional terrain map using the MrVBF index to indicate areas of erosional and depositional terrain, also includes the location of candidate wells selected for potential sampling in this study

5 Environmental tracers

5.1 Groundwater salinity

Groundwater salinity presented as total dissolved solids (TDS) in mg/L for all available wells in the study area are superimposed on the one second DEM of the study region (Figure 5.1). Salinity varies from fresh to 1.5-times seawater, with no clear spatial pattern. In the Cleve Hills, groundwater salinity varies considerably between adjacent wells, typical of what is found in many fractured rock aquifer systems in semi-arid environments. In contrast, there is less variability in the Coastal Plain, where the majority of groundwater has salinity greater than 14,000 mg/L.

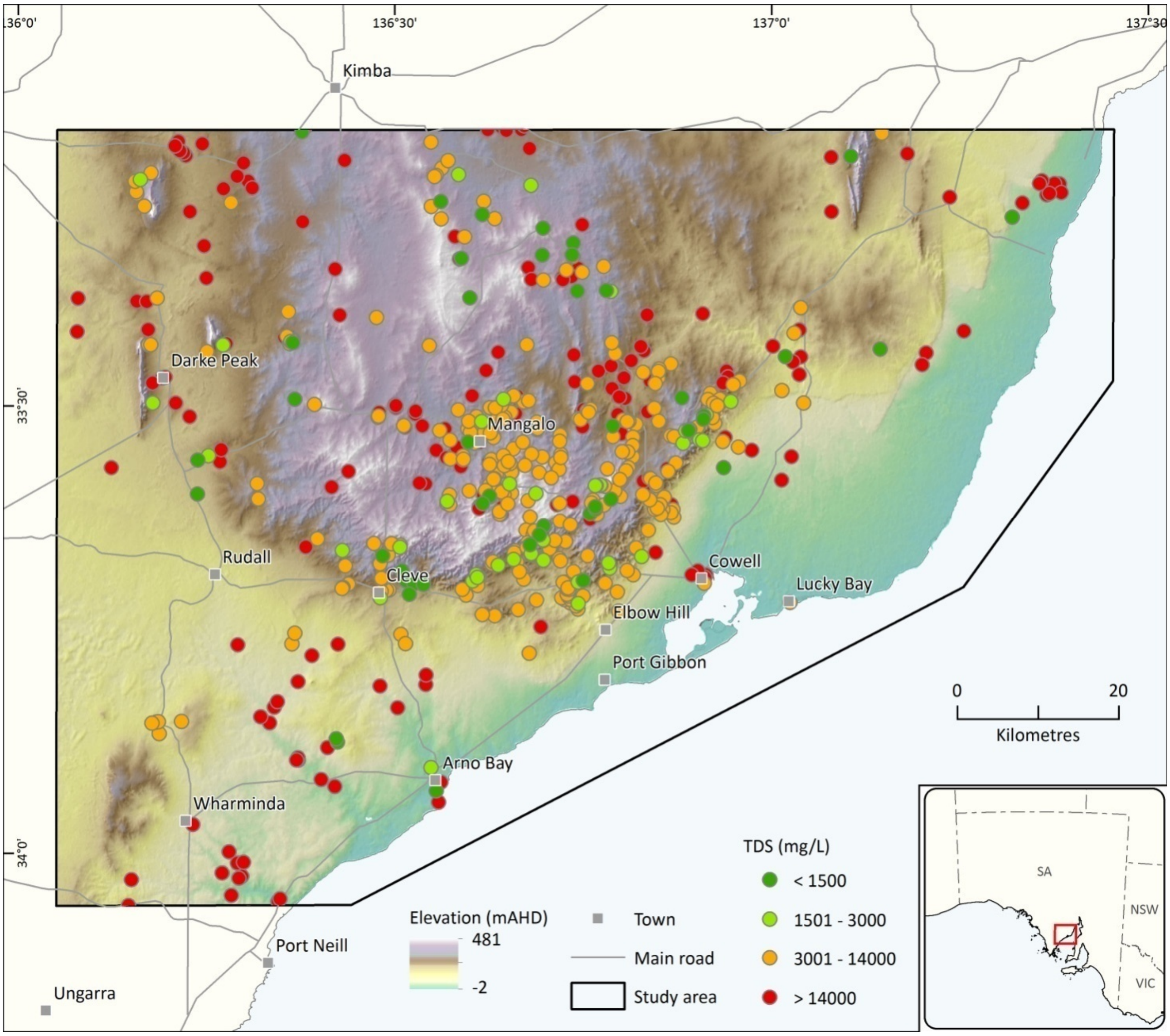

Figure 5.1 TDS of groundwater in the study area

Figure 5.2 is a comparison between lithology and groundwater salinity presented as electrical conductivity (EC). Overall, the data shows a wide scatter with no apparent correlation between salinity, lithology and depth. Wells intercepting the igneous and metamorphic rock formations have large open sections as they were completed as open holes, presumably due to the low yield in these settings. Such large well completions are undesirable for analysis of environmental tracers in fractured rock systems. The best approach for sampling environmental tracers in fractured rock environments is to use short screens and nested piezometers (Love et al., 2002). In contrast, the majority of observation wells in the Coastal Plain are piezometers (i.e. have short screens) and are thus more optimally designed for environmental tracer sampling.

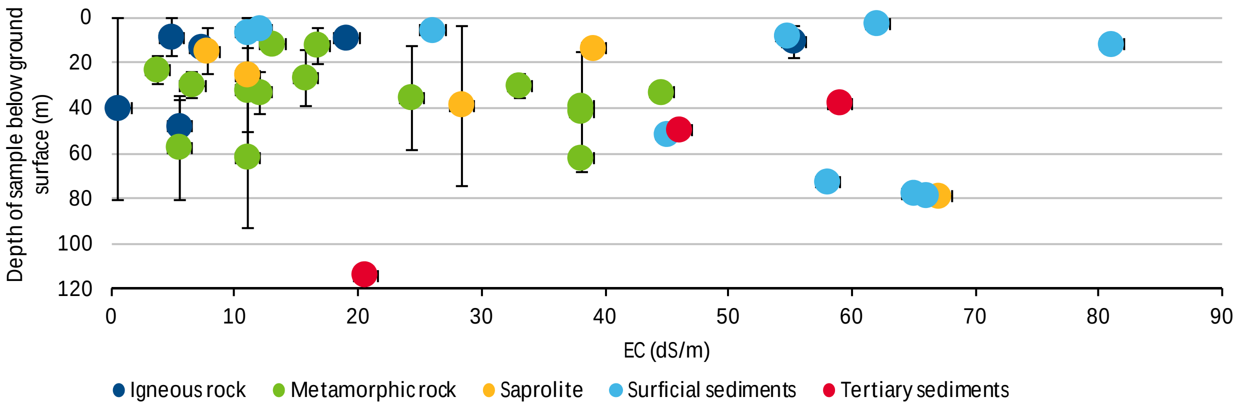

Figure 5.2 Illustrative diagram of screened intervals of sampled wells with lithology type, against salinity

5.2 Major ions

Analysis of the major ion composition can be used to determine the origin of dissolved solutes in groundwater. In particular, it can be determined whether the salinity can be attributed to cyclic salts from marine aerosols and precipitation, or from interaction with weathering processes of the aquifer material. Major ion compositions for all groundwater samples and seawater from the Spencer Gulf are presented as a Piper Diagram (Figure 5.3). The sampling locations for the major ion and tracers data are shown in Figure 5.4. All samples plot in a close group with a strong sodium-chloride type composition, with the exception of two fresher samples that possess a slightly greater calcium-magnesium-bicarbonate water type. This may suggest a common source for groundwater in this region. The samples also have a similar composition to the Spencer Gulf seawater, suggesting a marine aerosol and cyclic origin of salts.

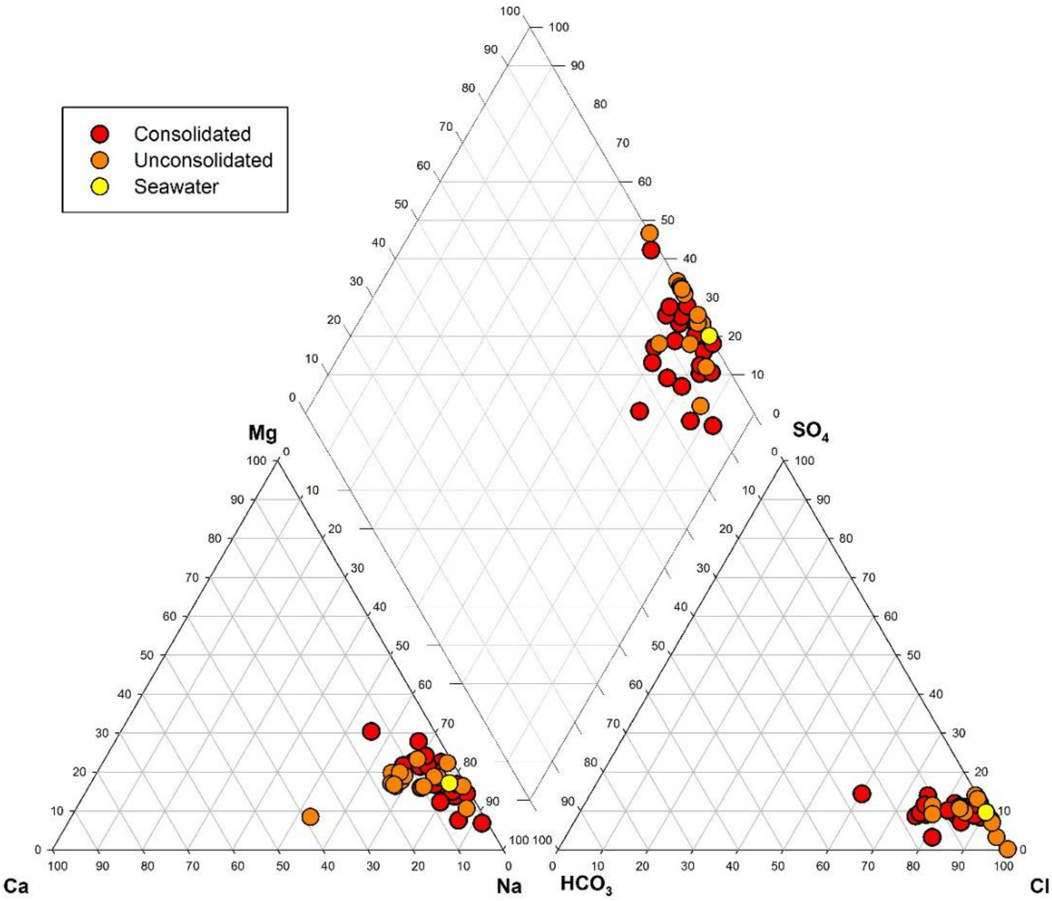

Figure 5.3 Piper diagram illustrating major ion composition of groundwater analysed in this study and groundwater samples from previous work in the study region by Risby and Harrington (2014)

Ion concentrations have been plotted against chloride and compared to a seawater – rainfall dilution line (Figure 5.5). Chloride behaves conservatively in a groundwater system and is only affected by evaporative processes. Chloride is not added or removed by mineral precipitation or water-rock reactions, aside from the dissolution of halite. In this system chloride is assumed to behave conservatively as there are no known halite deposits or chloride-bearing minerals in the study area. A body of water undergoing evapotranspiration that contains salts purely from marine origin in precipitation and dry deposition will plot consistently along the seawater – rainfall line. The presence of water-rock or water – soil interactions can be identified by any deviation from the seawater – rainfall line. An ion – chloride ratio higher than that of seawater indicates the addition of elements to the groundwater from dissolution and desorption of minerals in the aquifer parent material, whereas a ratio below the seawater line indicates ion removal from groundwater by precipitation of minerals or adsorption to aquifer substrate.

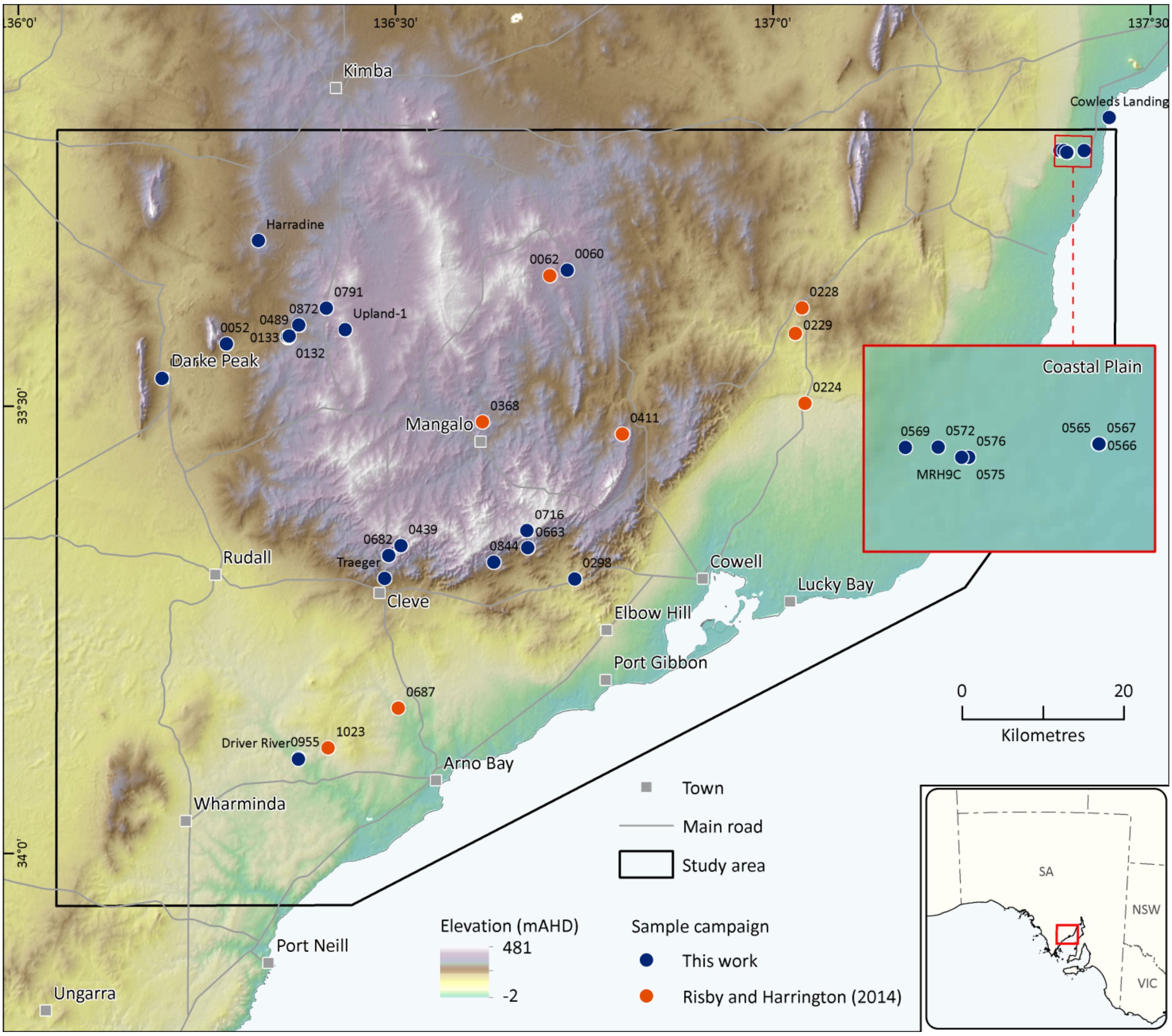

Figure 5.4 Groundwater wells in the study region sampled for hydrochemistry and environmental tracers, including wells recently sampled by Risby and Harrington (2014)

Cleve Hills

Salinity across the region ranges from very fresh to hypersaline, with chloride concentrations ranging from 145–26,000 mg/L. There is no spatial or geologic trend in groundwater salinity within the study area, except for a general spatial trend of hypersalinity at lower elevation and in valleys, and less saline to brackish waters at the higher elevation. Groundwater around Cleve typically had a lower salinity than around Kimba and Darke Peak, consistent with higher rainfall at Cleve. Wells situated in surficial cover and saprolite also had a slightly higher average salinity, and also a larger range in salinity, than those in basement rock. This could be indicative of discharge and evaporation from the shallow watertable. The major ions can thus be interpreted as comprising of two groups: one of fresher samples originating from higher elevation and hence higher rainfall and recharge rates, and one of high salinity samples originating from regions of lower rainfall and higher evapotranspiration (i.e. discharge areas). Most major ions plot closely to the seawater-rainfall dilution line, in particular at higher salinities, consistent with a cyclic origin for groundwater salinity. Sodium correlates very closely with chloride (Figure 5.5a) indicating that sodium chloride is the dominant type of salt, in agreement with the Piper Diagram. A good linear relationship also exists between chloride and TDS, (R^2=0.99), indicating that chloride is behaving conservatively in this system. This is important for supporting the validity of using the chloride mass balance method to estimate recharge rates Bromide/chloride ratios are used to analyse the relative contributions of chloride to the groundwater system from wet and dry deposition (Figure 5.5f) versus the dissolution of halite. Molar bromide/chloride ratios are close to the expected range for marine aerosols, and do not show any deviation from this at high salinities. This further suggests there is no halite in the profile that could be dissolving and contributing to the high salinity of the waters.

The freshest waters (<7000 mg/L chloride concentrations) have concentrations of ions such as calcium, strontium, magnesium as well as total alkalinity above that of the seawater-rainfall dilution line (Figure 5.5). These fresher samples also have the highest calcium-bicarbonate composition on the Piper Diagram (Figure 5.3). This is most likely due to the weathering of soil and regolith carbonates. The calcium-bicarbonate ratios were mostly consistent with calcium carbonate dissolution with a proportion of contributing magnesium carbonate dissolution.

The composition then becomes increasingly homogeneous with increasing salinity and is very close to the seawater-rainfall dilution line. One explanation for this trend is that the ions that are added relative to rainfall at low salinities are being re-precipitated at high salinity when saturation of different minerals is reached, and thus removed from the water (Hem, 1989).

Anomalously low sodium and potassium to chloride ratios below the seawater-rainfall dilution line indicates probable cation exchange reactions with clay surfaces (Hem, 1989) reflective of the known presence of clay lenses within the soil profile in some areas. Overall, the composition of major elements are consistently similar to that of marine aerosols and rainfall, indicating that the dominant source of elevated groundwater salinity in this region is from the evapoconcentration of cyclic salts, with minor input from water-rock interactions.

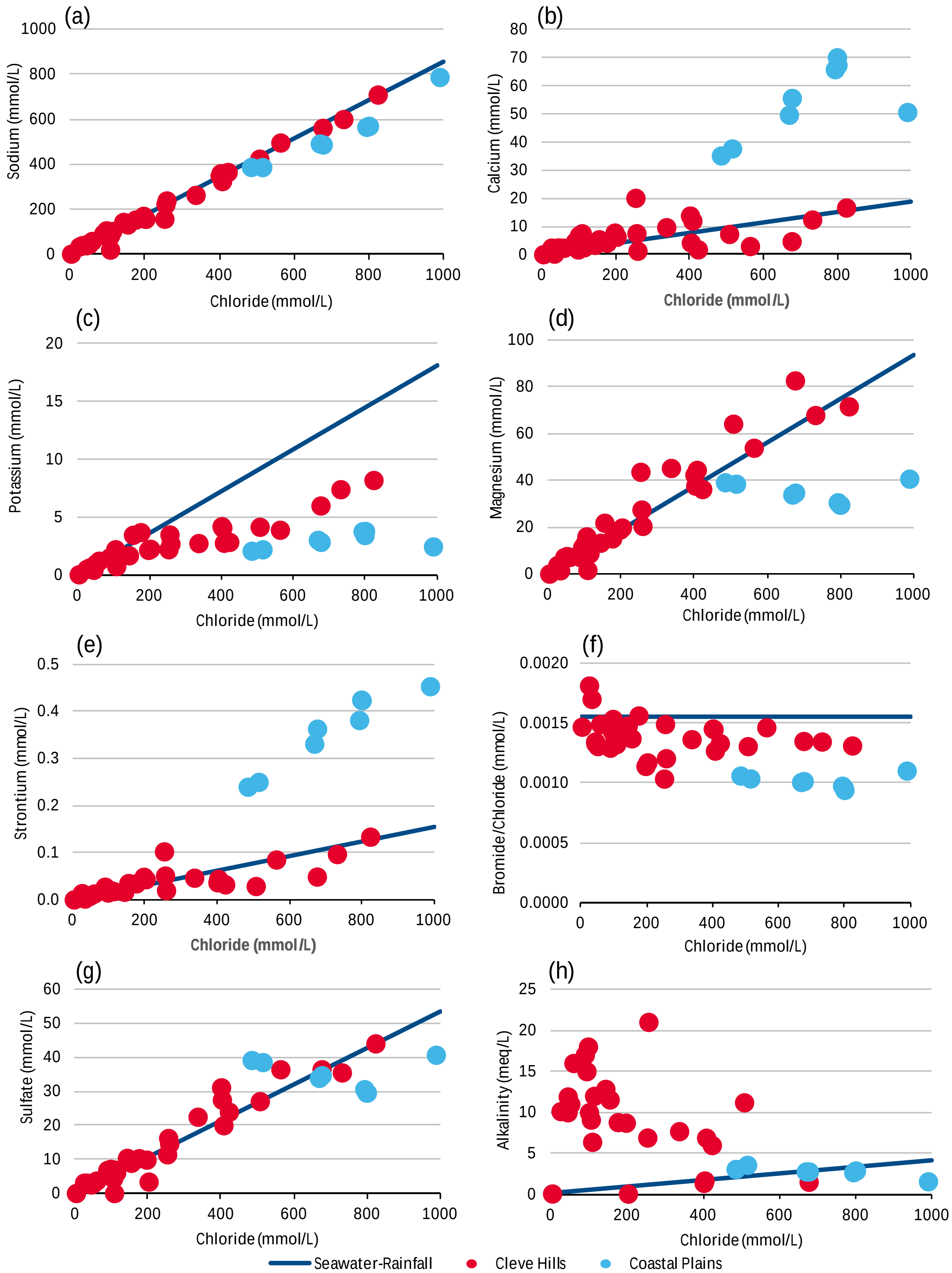

Figure 5.5 Major dissolved ions versus chloride

Coastal Plain

Chloride concentration in the Coastal Plain region range from 17,000–35,000 mg/L. The freshest samples occurred in the confined Tertiary aquifer with the highest salinity originating from the unconfined surficial sediments. Overall, major ion to chloride plots for the Coastal Plain setting do not show a close relationship with the seawater-rainfall dilution line as observed in the Cleve Hills region. This may indicate that water-rock interaction over long residence times is a more significant contributor to salinity than it is in the Cleve Hills region where shorter residence times are apparent.

Bromide-chloride ratios were consistently below that of seawater, indicating that halite deposits may be present and dissolution of these may be contributing to the salinity. Sodium and potassium concentrations also fall below the seawater-rainfall dilution line, likely due to interactions with clays. The calcium-sulfate ratio for two samples from the Tertiary aquifer was indicative of gypsum dissolution, but this is not apparent with the remainder of the samples.

Strontium to chloride and calcium to chloride compositions plot significantly above the seawater-rainfall dilution line, and show an increasing trend with increasing salinity. This indicates that the addition of these elements to the groundwater from the weathering of parent rock or dissolution of calcium and strontium-bearing minerals in the aquifer is a likely contributor to the high salinity, in addition to cyclic marine aerosol-originated salts. This increase also suggests progressive addition of elements over time along a flow path. Possible reactions include calcium carbonate dissolution, most likely originating from the Melton Limestone, and gypsum dissolution from the Tertiary sands.

5.2.1 CHLORIDE MASS BALANCE

The chloride concentration for groundwater samples (C_R) was used to estimate recharge rates in the study area using the chloride mass-balance (Eq. 3.1). Rainfall values for each location were obtained from the interpolated data set for the study area shown in Figure 1.1 (BOM, 2014). As there is no known halite in the soil profile in the study area, it can be assumed that chloride remains dissolved, and as such the assumptions for the CMB to be applicable are met. Chloride deposition for each location was obtained from the dataset displayed in Figure 5.6 after Davies and Crosbie (2014).

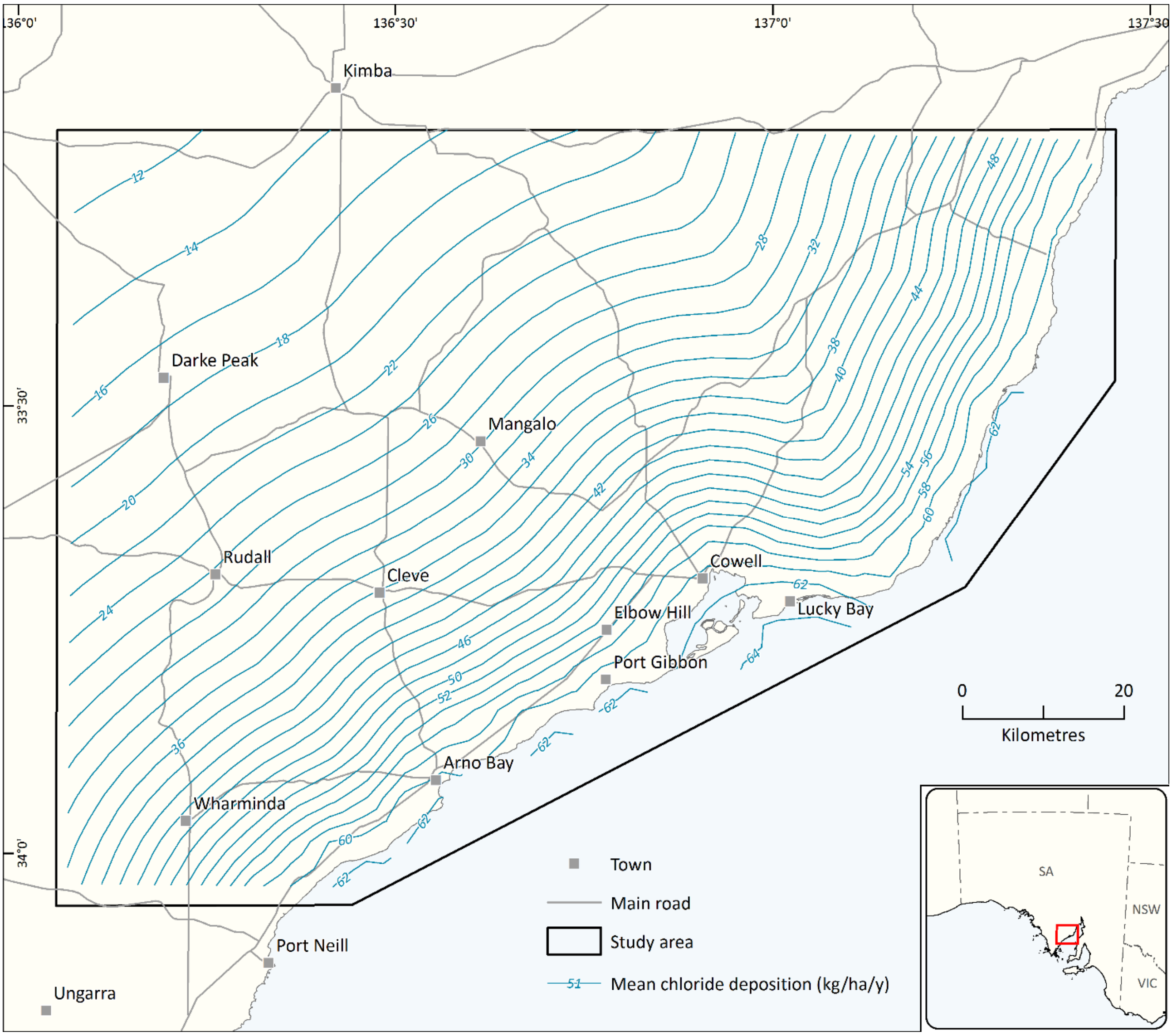

Figure 5.6 Chloride deposition for the study area; source Davies and Crosbie (2014)

Table 5.1 shows estimated recharge rates from point locations in the study area. These are generally low, ranging between 0–2 mm/year for most samples barring the anomalously fresh sample Upland-1 with an estimate of 13.1 mm/year. The one sample from the unconsolidated aquifer of the Coastal Plain region has a very low recharge rate estimate of 0.13 mm/year, reflective of the low rainfall in this region. This indicates that modern recharge into this aquifer is very low to minimal. These ranges in recharge are similar to those estimated by Risby and Harrington (2014) for wells in the Cleve Hills.

Table 5.1 Recharge estimates for the Cleve Hills samples and unconfined Coastal Plain sample

UNIT NO.	CHLORIDE DEPOSITION (kg ha/y)	RECHARGE (mm/y)
623000439	33	2.09
623000663	41	2.23
623100060	24	1.13
HARRADINE	15	0.47
623000844	41	1.23
613100133	18	0.52
623000716	39	1.04
623000682	33	0.85
623000298	48	1.19
613100489	18	0.29
613100132	18	0.20
613100863	17	0.12
613000955	46	0.18
613100052	17	0.44
UPLAND-1	19	13.10
613100872	18	0.15
TRAEGER	35	0.98
613100791	18	0.12
633100565	59	0.17

Despite the fact the groundwater chloride mass balance method assumes steady state, in reality this is unlikely to be the case for the study region due to recent and ongoing land use change, as well as climate variability over time. Steady-state conditions for chloride in fractured rock aquifers are known to take a significant amount of time to re-establish after land use changes, especially if the fractures are widely spaced (Cook, 2003). For example, in the Clare Valley, South Australia equilibrium conditions are not thought to have been re-established after land clearing 100 years ago (Love et al., 2002).

Since widespread land clearing in the Eyre Peninsula has occurred for approximately 100 years and continued until as recently as the early 1980s (Harding et al., 2002) it is possible that the system has not yet reached steady-state, especially in areas where the most recent land clearing has occurred. As such, these estimates should be treated as estimates of the absolute minimum recharge rate.

Recharge estimates from this method apply to the particular point in the landscape where recharge occurred, which may not coincide with the sampled well locations. Hence, differences in chloride concentration between the recharge point and the well location can produce erroneous estimates. A more detailed understanding of likely recharge and discharge locations could aid in determining the most accurate sample locations for recharge estimation.

5.3 Strontium isotopes

Strontium isotope ratios ($^{87}Sr/^{86}Sr$) for groundwater samples range from 0.7127 to 0.7386 with rainfall assumed to be 0.711 and seawater 0.7092. The groundwater values are within the range expected for mixing of rainfall-derived solutes and solute sourced from weathering of high-ratio Precambrian basement rock minerals. This dataset largely lacks discreet mixing lines between high and low ratio sources. There is no widespread obvious relationship between salinity and a high ratio strontium isotope source. Thus, given this data, the dominant source of the widespread high salinity groundwater in this area is evaporation and transpiration of rainfall and not rock weathering.

This approach has been successfully applied in the Murray Basin to determine inter-aquifer leakage (Dogramaci and Herczeg, 2002) and has been applied here. Mobilisation of accumulated salts in the soil zone concentrated by evaporation and transpiration can increase the salt concentration of the recharging water (Shand et al., 2009) and hence become a higher-concentration end-member than pure rainfall. Here values for varying degrees of evapo-concentrated rainfall have been used as end-member 1, and an average value of the ratios of silicate rocks pertinent to the study region obtained from Webb et al. (1982) as end-member 2. Proportions of strontium derived from rainfall for the Cleve Hills samples range from 0.65–0.98, and the Coastal Plain samples are presented below in Table 5.2.

The Quaternary aquifer groundwater $^{87}Sr/^{86}Sr$ ratios are not on this mixing line, due to its lower strontium isotope value of 0.7184, which is closer to that of carbonate minerals. Carbonate minerals in the study area include the underlain Melton Limestone and overlaid shelly, quartzite sands (soil carbonate) within the surficial cover. The Quaternary sample has the closest composition to the samples from the upper Tertiary, indicating that diffusive mixing through the limestone confining layer is a possible source of the isotopic signature of this sample.

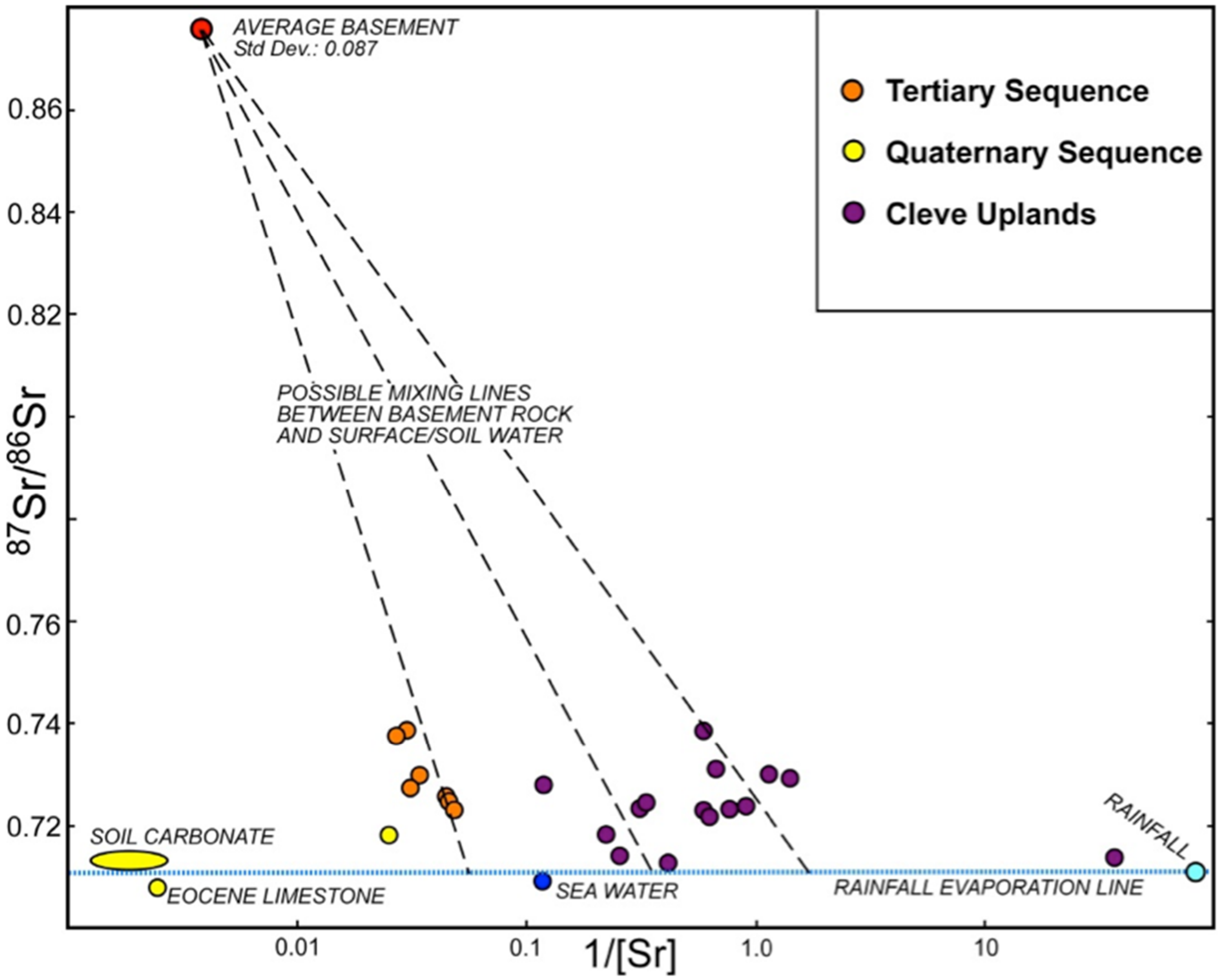

Figure 5.7 Strontium isotope ratio vs 1/Sr (L/mg) of groundwater, geology, seawater and rainfall

Table 5.2 Relative proportions of strontium contributed by rainfall and rock to the strontium isotope composition of groundwater for the Coastal Plain

GEOLOGICAL UNIT	SAMPLE ID	GRANITE-GNEISS ROCK	METEORIC WATER
Basement	63300566	0.216	0.784
	633100572	0.112	0.888
Tertiary	633100576	0.208	0.792
	633100575	0.127	0.873
	633100569	0.099	0.901
	MRH9C	0.208	0.792
	633100567	0.147	0.853

5.4 Stable isotopes

Cleve Hills

Groundwater samples from the Cleve Hills range in δ^2H from –100.8 to –21.1‰ and for $\delta^{18}O$ from –14.2 to –3.2‰ and are plotted against the Local Meteoric Water Line (LMWL) for Adelaide (Figure 5.8a). This meteoric water line may not be representative of the Eyre Peninsula. However, there is no closer location with sufficient temporal data. Temporal data for the LMWL was constructed using data available from the Global Network of Isotopes in Precipitation (GNIP) database (IAEA/WMO, 2014) and additional data published in Crosbie et al. (2012). For comparison to groundwater, the isotopic composition of rainfall from Uley South Basin near Port Lincoln as published in Swaffer et al.(2014) is presented, along with the calculated amount-weighted mean isotopic composition of different monthly rainfall (Figure 5.8).

Regardless of geology, all samples except for one plot parallel and to the right of the Adelaide Meteoric Water Line, suggesting varying degrees of evaporation during infiltration. A few groundwater samples from basement outcrop with thin overburden plot on or close to the meteoric line, suggesting an environment where infiltration to the watertable is more rapid. Based on patterns in stable isotopes in Adelaide rainfall, 40–60 mm of rainfall per month is required for recharge to occur in the Cleve Hills. The one extremely depleted groundwater sample (δ^2H = –100.8‰) suggest a significant episodic recharge from a localised high rainfall event. To exclude a potential analytical error, this sample was re-measured with different aliquots taken in the field and the result was reproducible.

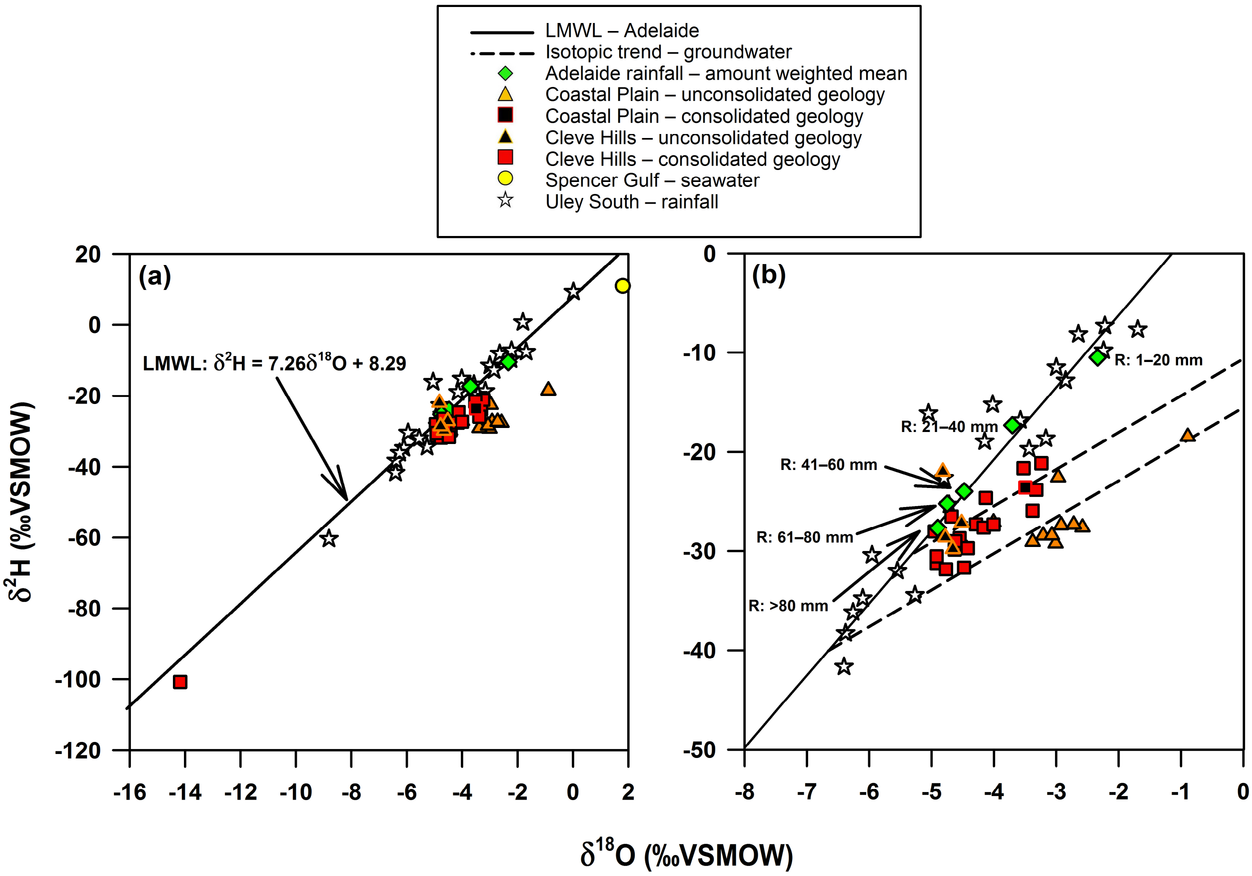

Figure 5.8 Isotopic composition of groundwater samples relative to (a) the Adelaide LMWL and rainfall from the Eyre Peninsula and (b) relative to the Adelaide amount weighted means for different monthly rainfall amounts

Coastal Plain

Groundwater samples from the Coastal Plain have a range in δ^2H from –29.2 to –18.5‰ and, for δ^{18}O, from –4.0 to –0.9‰ (Figure 5.8a). All samples have an evaporation signal and, relative to the Cleve Hills, this evaporation signal is stronger (Figure 5.8b). Based on Adelaide rainfall isotopic patterns, at least 80 mm of rainfall per month would be required for recharge in the Coastal Plain. According to historical rainfall data (Figure 2.1), this would be infrequent.

In addition to evaporation effects, stable isotope signatures have a clear elevation (or altitude) effect, with more depleted signatures for δ^{18}O at higher elevations (Figure 5.9a). The evaporation signal in the stable isotopes is also consistent with groundwater chloride concentrations, which are higher in samples with a more negative value for deuterium excess (Figure 5.9b).

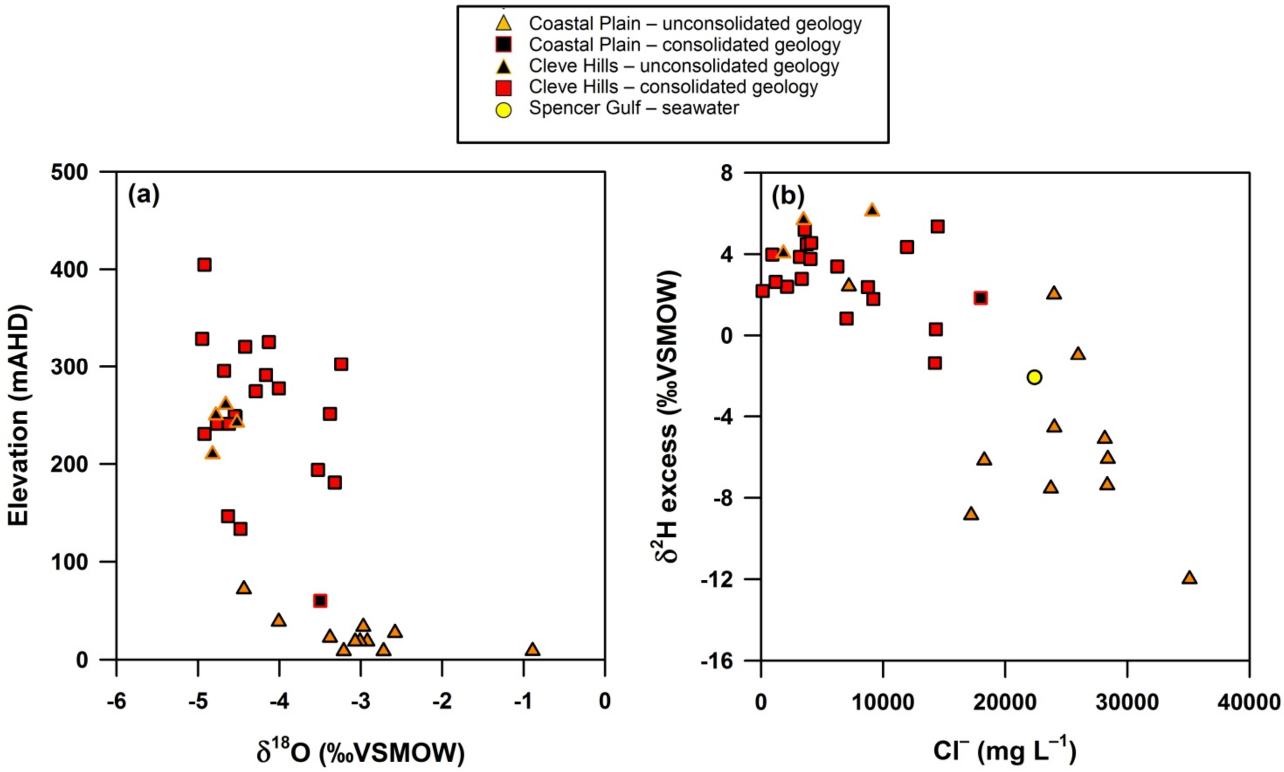

Figure 5.9 Plot (a) $\delta^{18}O$ versus elevation of the land surface and plot (b) $\delta^{2}H$ excess versus chloride

5.5 Anthropogenic gas tracers (CFCs and SF_6)

5.5.1 CFC-11 AND CFC-12

Eleven out of 27 wells were sampled for CFCs but the remaining 16 wells were unsuitable for this tracer because of low yields or a water level within 1 m of the screened interval. The range in CFC-11 in groundwater was 0.18–1.93 pmol/kg and, for CFC-12, 0.16–1.65 pmol/kg (Figure 5.10). As some samples have CFC concentrations above background, some of the groundwater was recharged within the last 50 years. The interpretation of the CFC data requires understanding the conditions at the time of recharge (temperature, salinity, elevation). This was evaluated using simple lumped parameter models (Figure 5.10).

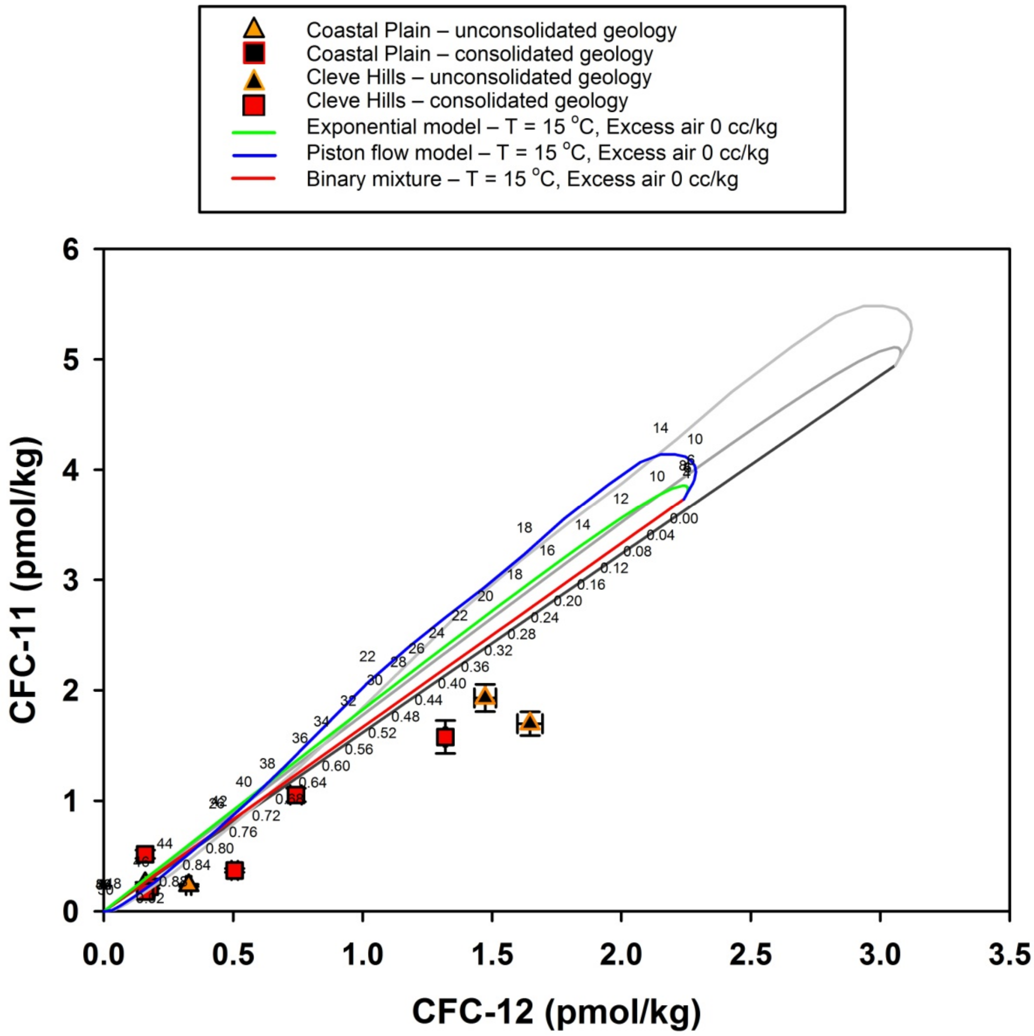

Figure 5.10 Concentrations of CFC-11 versus CFC-12 for groundwater in the study area

Because the temperature at the time of recharge is not known, the CFC data was interpreted in the lumped parameter models at two possible recharge temperatures: 15 °C (close to mean annual) and 10 °C (close to mean winter). Samples with CFCs concentrations above background all fall below model curves (Figure 5.10). This indicates that CFC degradation has occurred in the aquifer because CFC-11 degrades ten times faster than CFC-12 (Happell et al., 2003). The majority of samples with above background CFC concentrations were collected from the Cleve Hills with the exception of one from the Coastal Plain. For those samples with high concentrations, the MRT would ranges between >20 years for the exponential model and >15 years for the piston flow model (Figure 5.10).

Whereas the CFCs appear to be degraded, CFC-12 concentrations appear only slightly degraded and are still useful for the modelling of groundwater infiltration. Vertical infiltration velocities were estimated by plotting CFC-12 concentrations versus depth below the watertable (estimated using the measured hydraulic heads). Samples with high CFC concentrations were shallow (less than 20 m below the watertable) but many shallow groundwater samples had little or undetectable CFC-12. Thus, there is clearly a range in infiltration velocity across the study area. In addition, one of the samples with a high CFC concentration (623000844) was a well with a screen interval extending above the watertable, which is not suitable for CFC dating. Using different lumped parameter models, vertical infiltration velocities range from 50–1500 mm/year in the study area (Figure 5.11). Infiltration velocities are not the same as recharge rates. It is not possible to estimate recharge rates at present because aquifer porosities, in particular for the fractured rock aquifers, are not known.

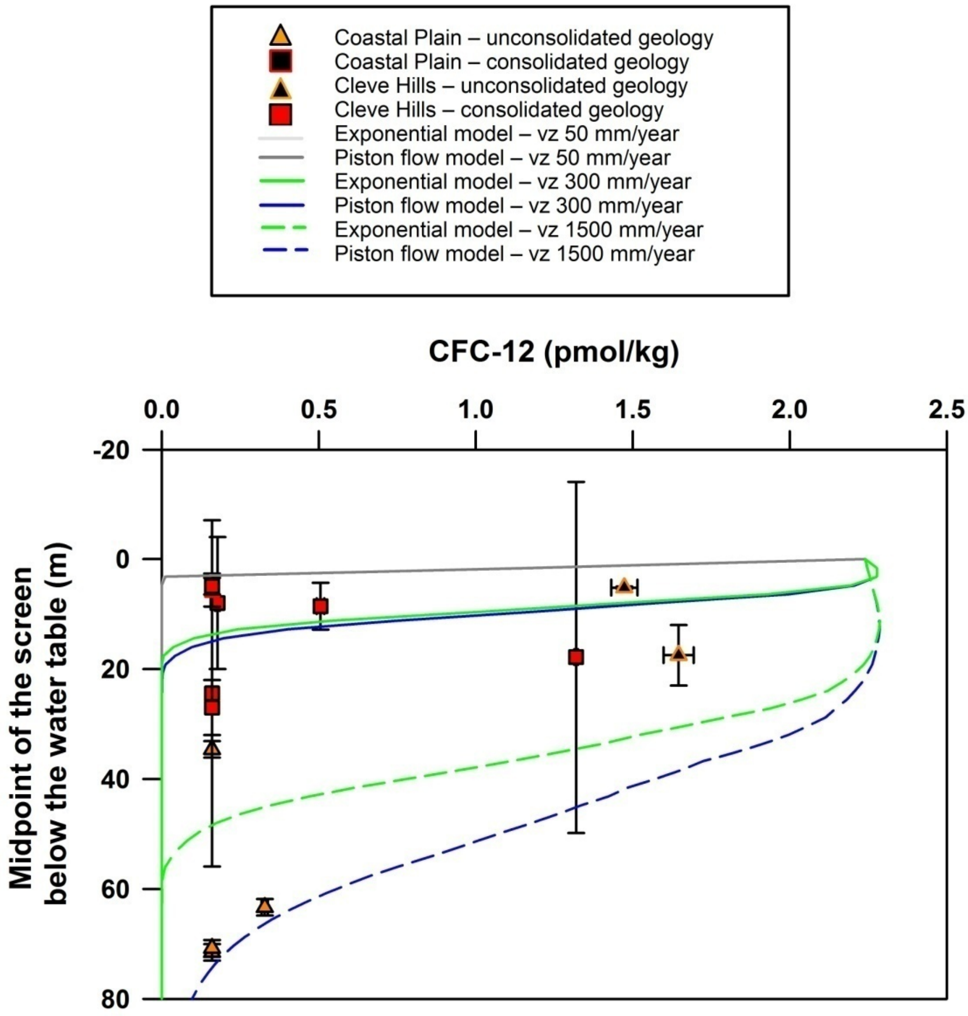

Figure 5.11 CFC-12 concentrations in groundwater versus depth below the watertable

5.5.2 SF_6

Groundwater SF_6 concentrations ranged from detection limit (0.2 fmol/kg) to <14 fmol/kg. This is beyond any reasonable range for air-water equilibrium with clean atmospheric air. As for CFCs, equilibrium groundwater SF_6 concentrations are influenced by conditions at the time of recharge. However, even when using extremes in recharge temperatures and excess air (air entrapped during localised recharge) concentrations above 6 fmol/kg are unlikely (Figure 5.12). Similar elevated SF_6 concentrations have been found elsewhere in Eyre Peninsula, (Risby and Harrington, 2014) the APY lands (Kretschmer and Wohling, 2014; Leaney et al., 2013) and internationally (Deeds et al., 2008; Friedrich et al., 2013; Koh et al., 2007; Rohden et al., 2010) and suggest that under some conditions, a geological source for SF_6 exists. Contamination during sampling is improbable because one well sampled in this study and the same well sampled by Risby and Harrington (2014) using different equipment had a very high SF_6 concentration. Until the mechanism for apparent underground production is understood and quantified, SF_6 is not a suitable tracer in this environment. There is also the possibility of the presence of CF_4 in groundwater, another gas with similar physical properties that cannot be separated by most current analytical equipment (Deeds et al., 2008; Harnisch et al., 1996; Harnisch and Eisenhauer, 1998; Harnisch et al., 2000; Mulder et al., 2013).

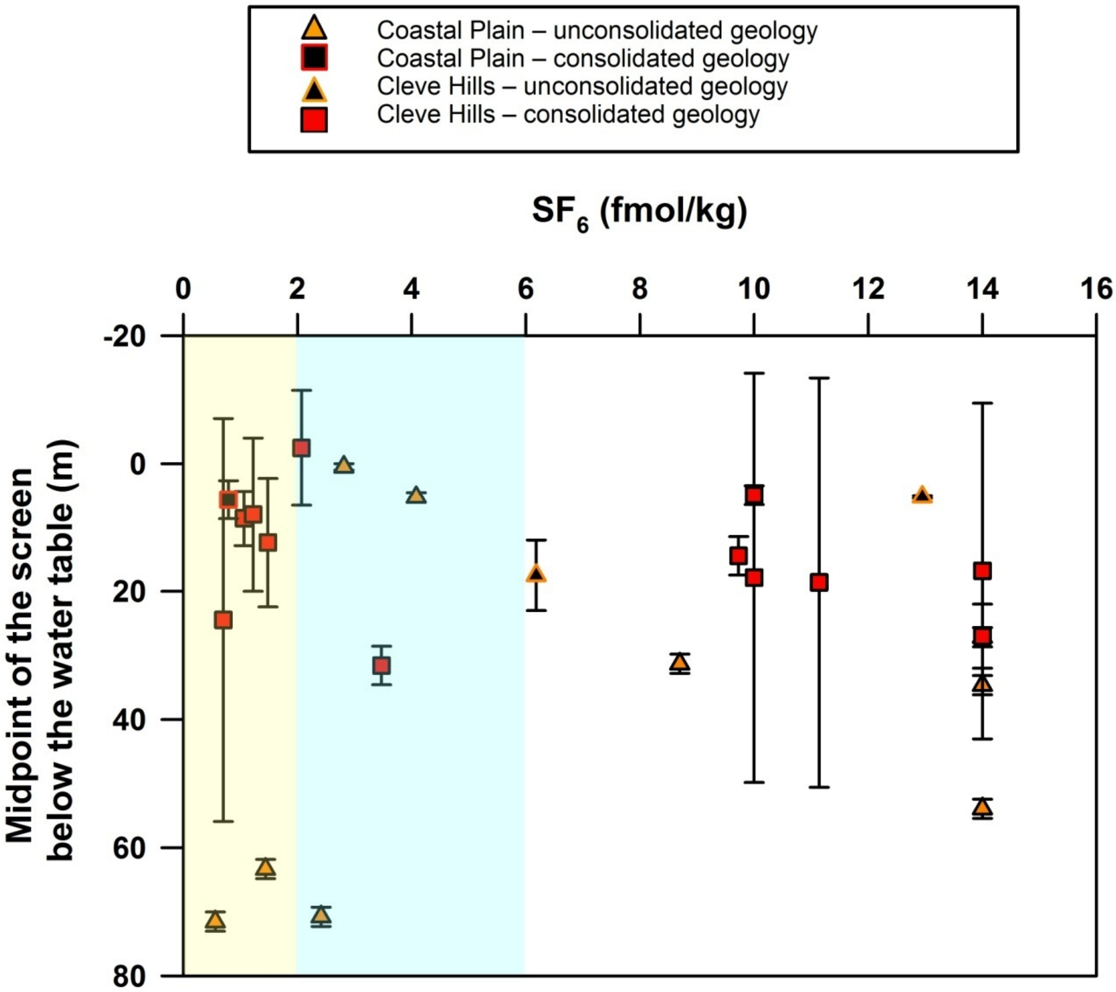

Figure 5.12 Concentrations of SF_6 in groundwater versus depth below the watertable; shaded areas represent the expected range in SF_6 concentration at air-water equilibrium under normal conditions (yellow) and with a large amount of excess air and a low recharge temperature (blue)

5.6 Radiocarbon

Carbon-14 activities in the samples ranged from 10–104 percent modern values (pMC). The lowest activities are in the Coastal Plain and the highest in the Cleve Hills. Carbon-14 is measured on total dissolved inorganic carbon (TDIC) and is influenced by water-rock interactions during infiltration and during groundwater flow. This process dilutes the original atmospheric ^{14}C ratio by introducing ^{14}C-free carbon from the rock matrix into TDIC. As a first approximation, the magnitude of this effect can be estimated by looking at the ^{14}C activities in young groundwater (as defined by groundwater containing CFC concentrations above background (Figure 5.13)). Using the best-fit lumped parameter model curves, a correction factor of 0.8 is required, corresponding to 80% of the carbon in TDIC originating from the atmosphere and the other 20% from the rock matrix. Due to the complexity of the geological environment in the study area, a unique correction factor for all ^{14}C values is a crude first approximation. However, the alternative (geochemical modelling of the TDIC cycle in each aquifer) is beyond the scope for this report.

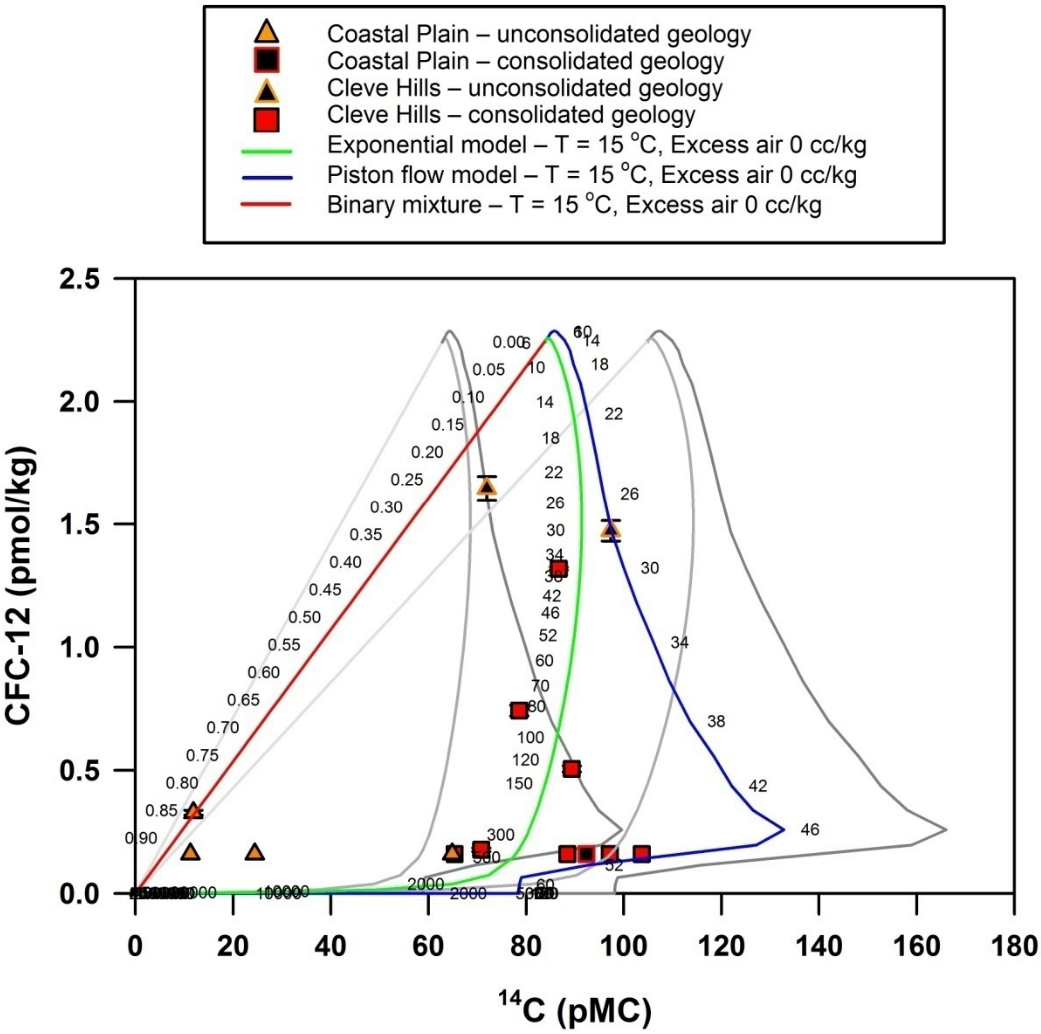

Figure 5.13 Concentrations of CFC-12 versus ^{14}C in groundwater including interpretation using a lumped parameter models

Using this assumption, ^{14}C shows evidence for different flow systems in the study area (that is, some samples are better when fitted with alternative lumped parameter models representative of simple and more complex flow systems). For example, some samples (Cleve Hills – unconsolidated) are better fitted with a piston flow model (blue line) which represents an idealised age without any mixing (Suckow, 2014). Other samples (Cleve Hills – consolidated) are better fitted with the exponential model (green line). This is not surprising because long well screens in thin aquifers will tend to collect samples from a variety of young and old groundwater flow paths. Two samples (Coastal – unconsolidated) appear to be a binary mixture of very young (<few years) and tracer-free very old water (red line). The majority of the samples seem to follow the exponential model, with a range of MRTs from a few decades to more than 10,000 years.

Similar to CFCs, ^{14}C was plotted versus depth below the watertable to estimate vertical infiltration velocities. A range of likely infiltration velocities was determined by comparing the same model curves as for the CFCs. The probable range of infiltration velocities from ^{14}C is from 10–300 mm/year. The case for an infiltration velocity of 1500 mm/year is possible with the CFCs, but can be excluded here because high ^{14}C concentrations at greater depth were not observed.

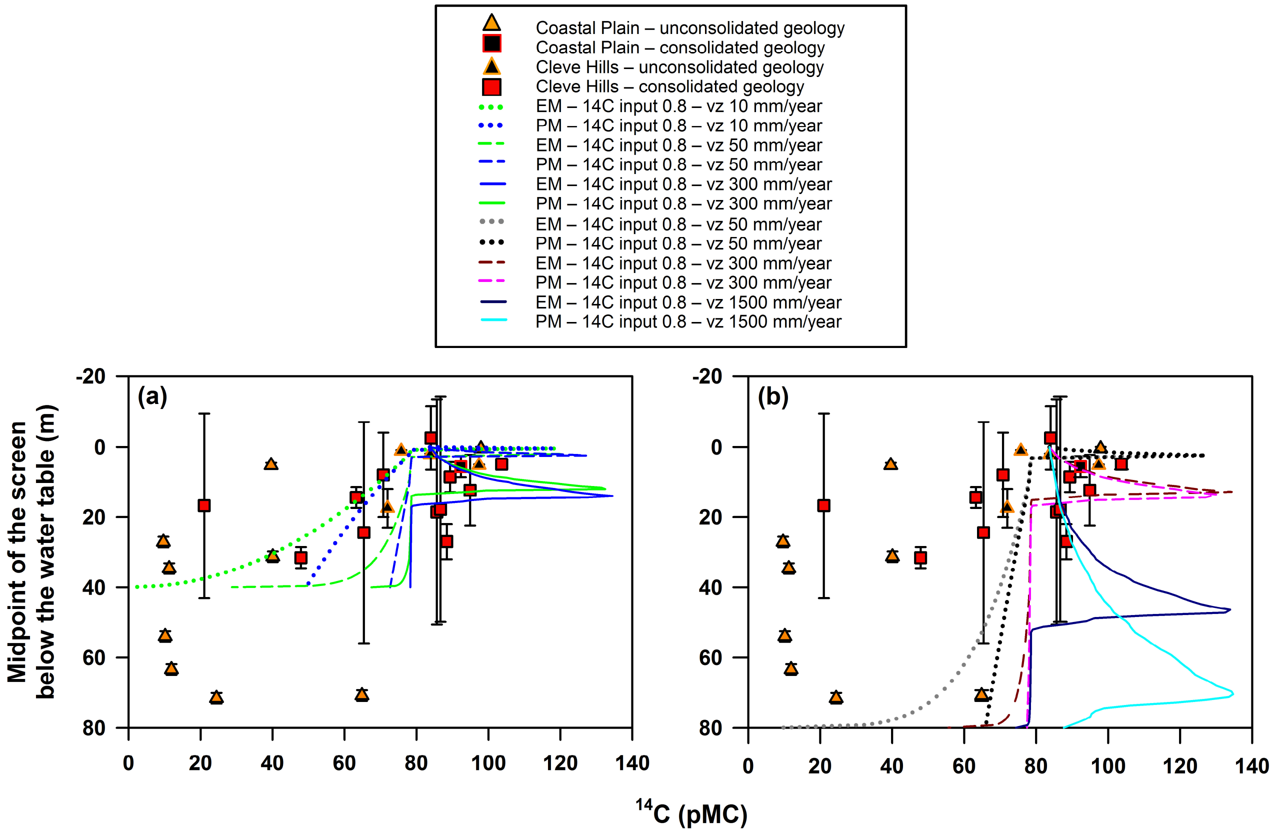

Figure 5.14 Concentrations of ^{14}C in groundwater versus depth below the watertable; including an interpretation of vertical infiltration velocities for two different aquifer depths (a) 40 m and (b) 80 m using lumped parameter models

5.7 Chemistry transects

In addition to the lumped parameter modelling, concentrations of dissolved solutes and environmental isotopes along the four previously described transects were analysed. This methodology is outlined in detail in Love et al. (1993) and is summarised briefly below.

This approach is based on the principle of gravity-induced groundwater flow occurring down a hydraulic gradient, superimposed by a sinusoidal watertable. Local flow systems are known to typically occur in regions with an undulating watertable, as significant variations therefore influence the hydraulic gradient (Love et al., 1993). In contrast, regional flow systems are more likely to occur in areas with flatter topography and little variation in the watertable. The changes in chemistry and environmental isotopes along the inferred flow direction (from the hydraulic gradient) can be analysed semi-quantitatively to observe which of the two flow systems (if not both) is likely to be occurring. If recharge from one point were the input for a discrete, regional flow path, it is likely that an evolutionary change in the concentration of environmental tracers would correspond to this conceptualisation. In contrast, if local flow systems are present with multiple recharge and discharge locations, an irregular and variable distribution of tracers is expected. Furthermore, the reader is referred to a comprehensive review of the distribution of the groundwater (age tracers) in Tóthian and Vogel groundwater flow domains (Suckow, 2013).

Cleve Hills

The changes in chemistry and environmental tracer concentrations in groundwater were examined along the three transects previously described (Figure 4.9). Water chemistry along each transect shows substantial variations and no evolutionary trend, and so does not provide any evidence for the presence of a regional, continuous flow path. Instead the trend is more indicative of local flow systems, with multiple recharge and discharge points in the landscape.

Chloride concentrations along the three transects show an irregular distribution (Figure 5.15). Other major ions (not shown here) including sodium, sulfate and magnesium, also exhibit a very similar trend to the chloride. This indicates that a mixing of groundwater with different chloride concentrations or mixing of different recharge inputs at different locations in the landscape may occur (Love et al., 1993). This irregularity indicates the presence of recharge and discharge zones that are apparent in local flow systems, correlating with the standing water levels for the three transects. Discharge zones may be inferred where chloride concentrations are the highest, and in the Western transect these also appear to correspond with steep hill slopes or topographic lows.

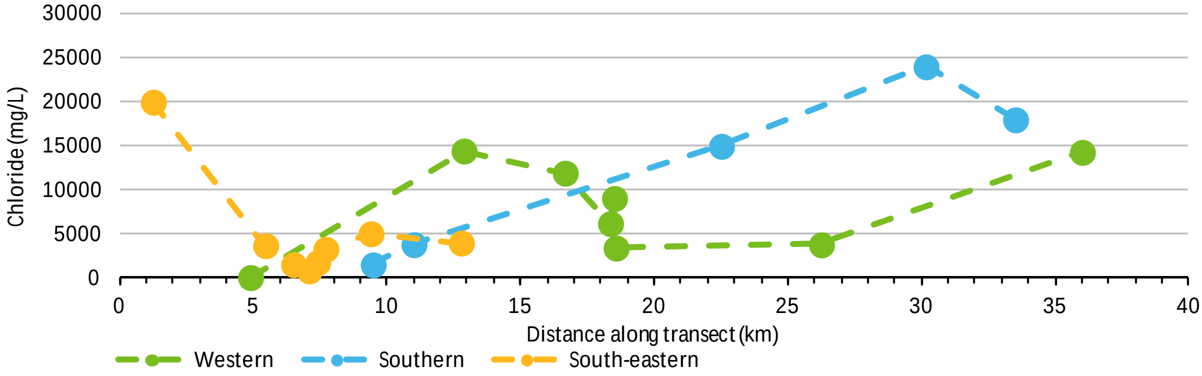

Figure 5.15 Chloride concentrations against distance along the three transects

There is no apparent trend in δ^2H and $\delta^{18}O$ composition with distance along the three transects (Figure 5.16). There is little variation in δ^2H; with values ranging from -30 to -22‰ for the Western transect; barring the outlier of Upland-1. In the Southern and South-eastern transect, a difference of only 2‰ for δ^2H was observed. The isotopic composition undulates most clearly on the Western transect. This further suggests that local recharge and discharge processes are dominant over regional flow.

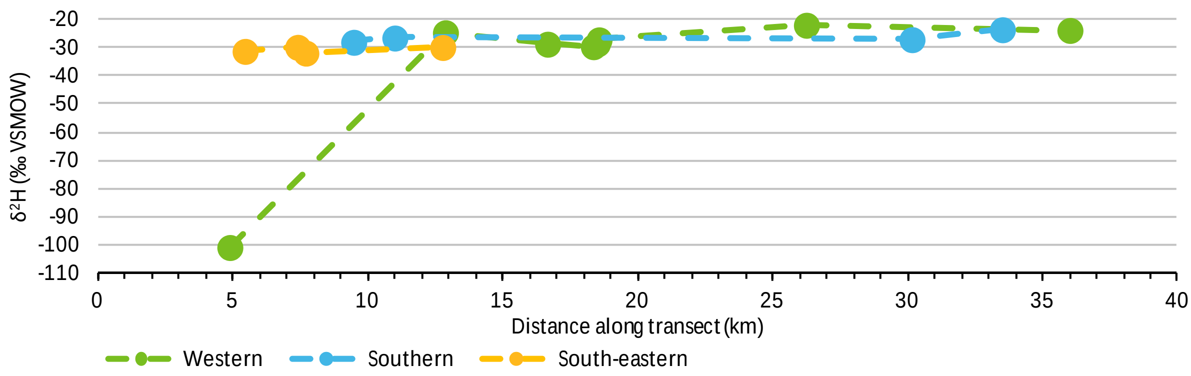

Figure 5.16 Deuterium composition versus distance along the three transects

Strontium isotopes also show variation and undulation along the transects, in particular the Western transect. If regional flow was occurring, a consistent increasing change in isotopic ratio with distance from recharge point would be expected.

The percentage of modern carbon from ^{14}C analysis exhibits significant variation (Figure 5.17). Values for the Cleve Hills are typically high, with some close to 100% pMC, further highlighting the degree of input of modern recharge to the system and the likely multiple recharge and discharge locations in the landscape.

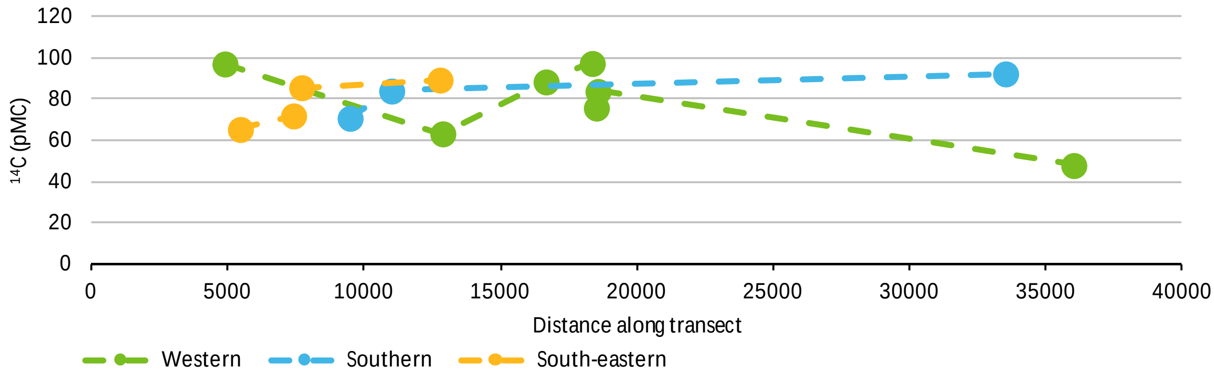

Figure 5.17 Radiocarbon concentration versus distance along the three transects

Coastal Plain

For the Coastal Plain setting near Whyalla there is no indication of local flow systems, as the watertable does not exhibit undulations. The hydraulic gradient is very small over the Uranium SA piezometer nest site (Figure 4.10), with standing water level only varying by 2.1 m over the 3.5 km transect, and this is not conducive to the establishment of local flow cells.

Chloride concentrations in the Tertiary aquifer vary by ~10,000 mg/L from 17,000 to 28,000 mg/L, without uniformly increasing with distance along the transect (Figure 5.18). Chloride concentrations in groundwater samples from the weathered basement have less variation ranging between 24,000 to 28,000 mg/L. The Quaternary aquifer has the highest groundwater chloride concentration at 35,100 mg/L, albeit from one sample location.

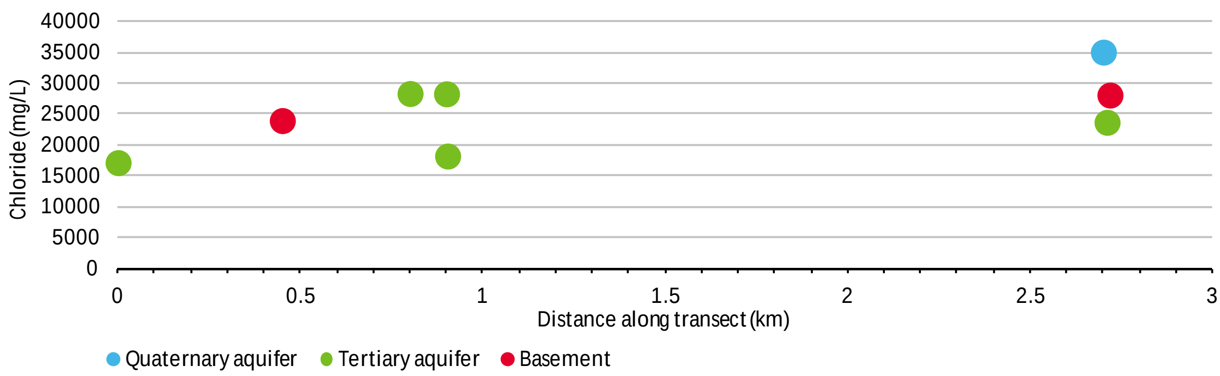

Figure 5.18 Chloride concentration with distance along the coastal transect

Strontium isotope ratios tend to increase with distance along the transect in the Tertiary and Basement aquifers although, there are only two samples from the Basement and for the Tertiary aquifer there is a lot of variation and no uniform increase in isotope ratio with distance (Figure 5.19). These results suggest varying degrees of water-rock interactions with the different aquifer materials of the Basement and Tertiary aquifers.

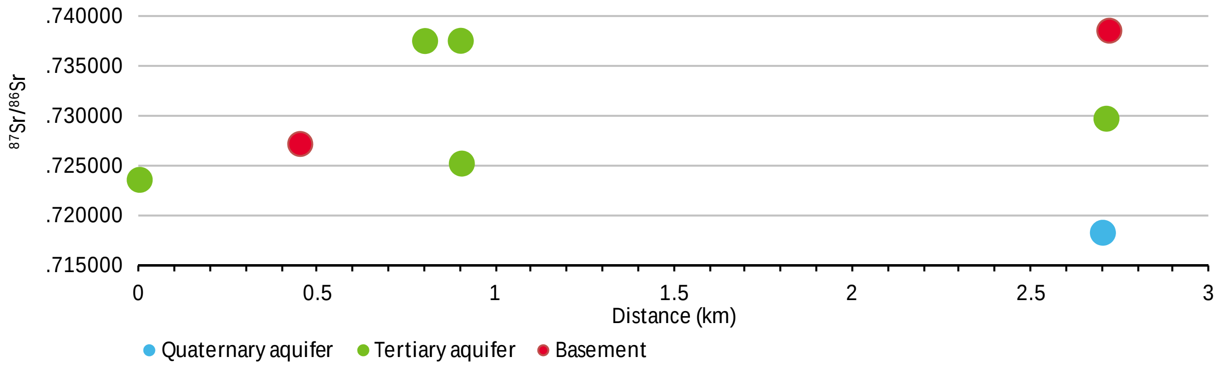

Figure 5.19 $^{87}Sr/^{86}Sr$ composition with distance along coastal transect

Values of ^{14}C for the Tertiary confined aquifer are variable and show a non-uniform increase with distance along the transect (Figure 5.20). This clearly highlights that the Tertiary aquifer is not behaving as a completely confined system, and that there are distinct inputs of younger water into the system. An increase in pMC is observed in the Tertiary confined aquifer at 0.8 km along the transect, and another significant increase is observed in the Tertiary and basement between the sample points at 0.8 and 2.8 km (Figure 5.20). This indicates an input of younger water into the confined system from downward leakage from the unconfined Quaternary aquifer through the confining clay and limestone units. These younger samples also correlate with high chloride concentrations (Figure 5.18) indicating that it is not fresh recharge that is entering the confined aquifer but saline water, most likely originating from the highly saline Quaternary system. The similarity in pMC between the unconfined and Tertiary confined samples closest to the coast further highlights the connectivity of the two systems at this location.

However, current hydraulic conditions indicate a potential for upward flow at this location, as the watertable in the Quaternary unconfined aquifer is below the potentiometric surface for the Tertiary confined aquifer (Figure 4.8). Therefore this inter-aquifer mixing has not occurred recently, and must have occurred during a time period when the watertable was higher and recharge was greater, than at present. Alternatively, the Coastal Plain transect is very short and there could be recharge occurring upgradient of the transect, further inland. This would have most likely occurred when climatic conditions in Australia were less arid, with the transition to upward flow a recent phenomenon. The presence of downward flow through the confining layers is in disagreement with previous studies which suggested that these confining units had very low permeability, and that the Tertiary confined aquifer was expected to behave as a completely confined system (Jeuken, 2011).

The input of modern water at this location could also indicate seawater intrusion, as also observed by the high conductivity region along the coast from geophysics (Figure 6.9).

This approach of interpretation is limited by the presence of only one sample for the Quaternary unconfined aquifer in contrast to five data points for the Tertiary aquifer. Multiple data points from additional piezometers on this transect that are screened into the Quaternary unit would be required for a comprehensive assessment of inter-aquifer leakage. However, from a preliminary interpretation it can be concluded that there is a component of horizontal flow in the Coastal Plain setting, with significant vertical inter-aquifer leakage.

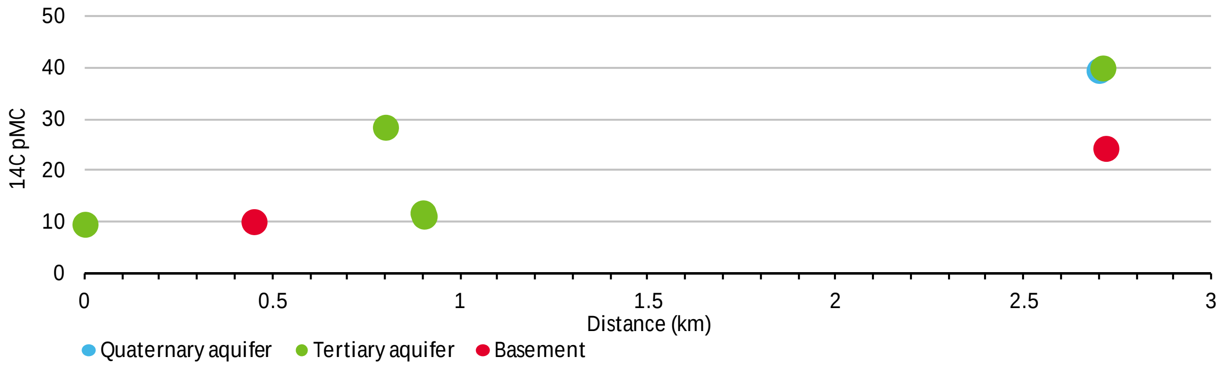

Figure 5.20 Trends in ^{14}C with distance along coastal transect

5.8 Discussion

The patterns in environmental tracers are more consistent with local flow systems rather than regional ones in North-eastern Eyre Peninsula. For example, the stable isotopes of water had a clearly visible altitude effect of 0.5‰ $\delta^{18}O$ per 100 m. If there was one regional flow system, this altitude effect would not be so pronounced because groundwater recharge at higher elevations would be found in discharge areas. Similarly, ^{14}C activity above background was found across the study area. This suggests that a significant fraction of groundwater is recharged locally. Otherwise, because of low recharge rates, little ^{14}C would be found in discharge areas.

Preliminary estimates of vertical infiltration velocities range from 50–1500 mm/year with CFCs and 10–500 mm/year with ^{14}C. It is not surprising that the two tracers give a different range in infiltration velocity because they integrate infiltration over different timescales. For example, CFC-based infiltration velocities can easily be higher because of the influence of recent and rare episodic recharge events which are less apparent in the radiocarbon record because they average over time. Combining the two tracers together, the most appropriate range in vertical infiltration velocities for the study area is 50–300 mm/year.

As stated above, vertical infiltration velocities are not the same as recharge rates. Recharge rates are obtained by multiplying infiltration velocities by the effective porosity of the aquifer. Typical values for porosity in sedimentary aquifers are about 30% but are typically lower and more variable in fractured bedrock aquifers. In the case of the Cleve Hills, porosity would tend to vary significantly with depth as the vertical profiles shift from unconsolidated sediments to saprolite and then to fractured bedrock. The porosity of the different porous media in the study area is not known. Because the bulk of the aquifer appears to be in fractured bedrock, recharge rates are probably much lower than vertical infiltration velocities. For example, if the vertical infiltration velocity is 300 mm/year this would correspond to a vertical recharge rate of 3 mm/year if the fractured bedrock aquifer has a porosity of 1%.

At the time of writing this report results for tritium and noble gas data were not available yet. Tritium would provide a complimentary estimate to CFC-based estimates of vertical infiltration velocity as it estimates the age in groundwater over a similar timescale. In addition, unlike CFCs and SF_6, tritium may be more robust because it is not prone to degradation (CFCs) or to be influenced by an apparent underground source or an inability to separate from similar gases (SF_6). Noble gases will be useful to better learn about the recharge environment, such as past recharge temperatures. Thus, the variations in noble gas concentrations could help understand the influence of rare episodic recharge events on the water balance. Finally, helium-4 which is useful for dating old groundwater would help to verify that many of our samples contain an apparent mixture of old and young groundwater. The noble gas and ^{3}H data collected can be found in Appendix B .

6 Airborne electromagnetics

By adopting a consistent approach, the project was able to generate comparable conductivity models across the northern Eyre Peninsula. It was important to take account of the different AEM system characteristics in order to achieve high levels of consistency across the study area. Higher conductivities are noted to largely coincide with low parts of the contemporary landscape. This clearly shows the valleys that contain a conductive fill in the Cleve Hills, but on the Coastal Plain of the east coast, the sediment package over basement is conductive and more so as you approach the coast. This is likely to be resulting from salt water intrusion. In the Cleve Hills area, the AEM coverage reveals strong north-south grain in the conductivity, reflecting the orientation of the basement geology, showing the spatial extent of a conductive valley fill (pink/red areas in Figure 6.1). In parts of the Eyre Peninsula, valley fill has the potential to host groundwater resources. Dark blue areas represent sub-cropping and out-cropping of basement rock.

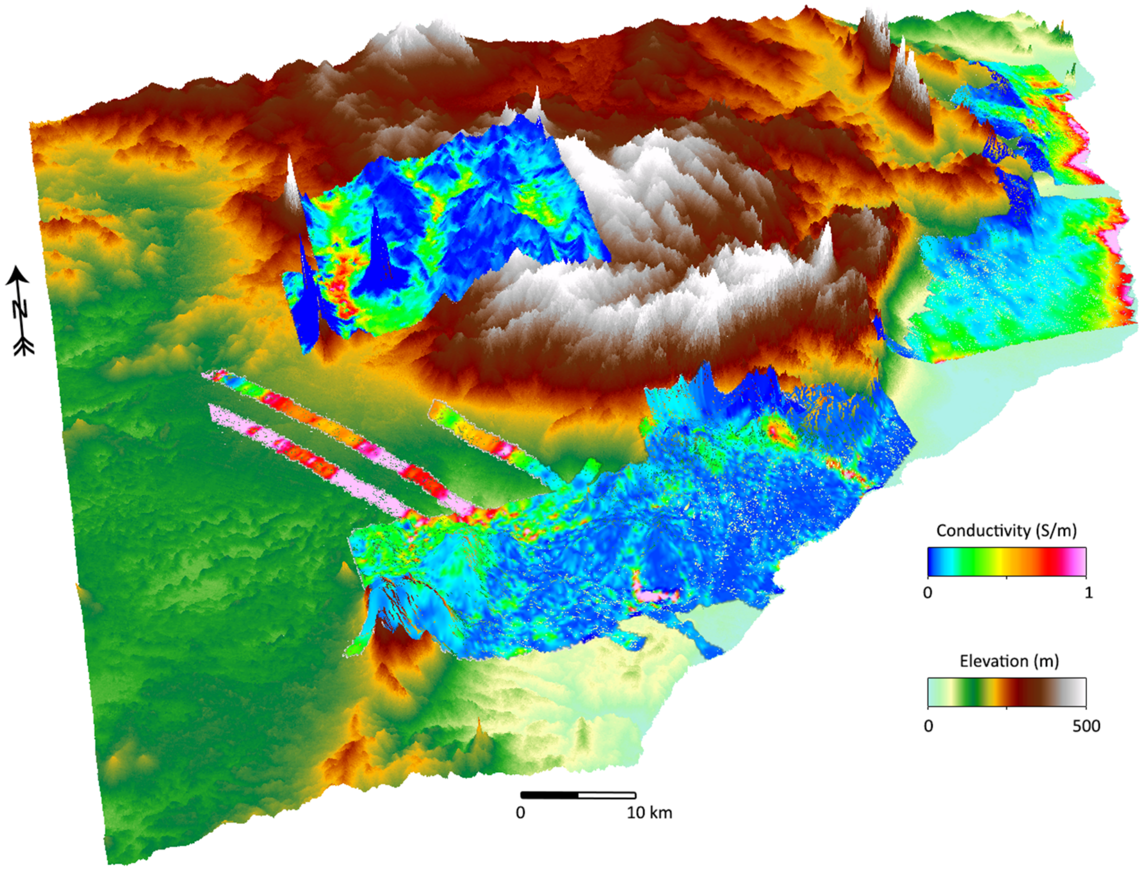

Figure 6.1 Depth slice (at 20m below ground surface) of areas of inverted AEM in the Cleve Hills case study area (approximately the same area as Figure 6.6 and Figure 6.9) overlying the land surface topography

Comparison of the AEM with contemporary topography indicates the general coincidence of thick conductance sequences and contemporary valley systems. As previously mentioned, MrVBF (Gallant and Dowling, 2003) analysis of surface topography, provides a tool to map the spatial continuity of low/flat regions in the landscape, and the potential association of these regions with palaeovalley networks. In comparison to Figure 4.12, the topographic index for the study area has been further classified to provide clearer evidence of surface drainage lines. Figure 6.1 shows how AEM data identifies pre-Pliocene valley systems that are coincident with contemporary valleys as outlined using MrVBF (Figure 6.2). This allows our knowledge to be potentially up-scaled beyond the localised AEM survey areas, and across the broader northern Eyre Peninsula.

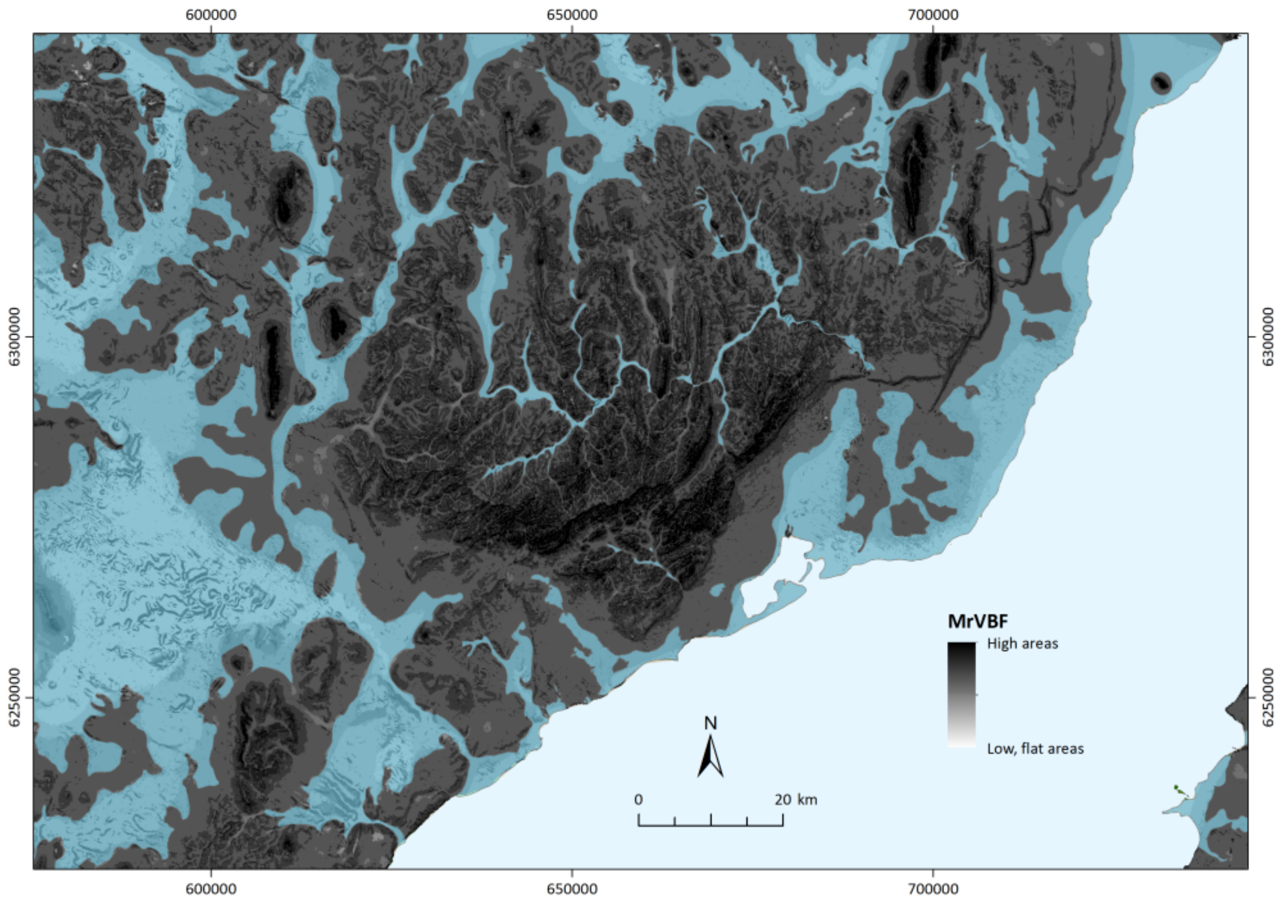

Figure 6.2 Using MrVBF analysis of surface topography to highlight contiguous surface drainage lines in the south-eastern part of the case study area (Cleve Hills) of the northern Eyre Peninsula. The paler areas are the low/flat parts of the landscape

6.1 Cleve Hills AEM

A study of the AEM interval conductivity slices derived from the fully inverted data over the Cleve Hills area indicates that the region is characterised by a complex conductivity structure varying with depth. Figure 6.3 and Figure 6.4 show a conductivity structure influenced by litho-structural variations in the metamorphosed Palaeoproterozoic Hutchison Group rocks (a sequence of complexly folded and faulted metasediments), and a regolith comprising in situ weathered clastic and chemical sediments and transported Palaeogene materials that infill valleys dissecting the higher parts of the landscape. These valleys, developed in the early Palaeogene, are over 100 m deep in places.

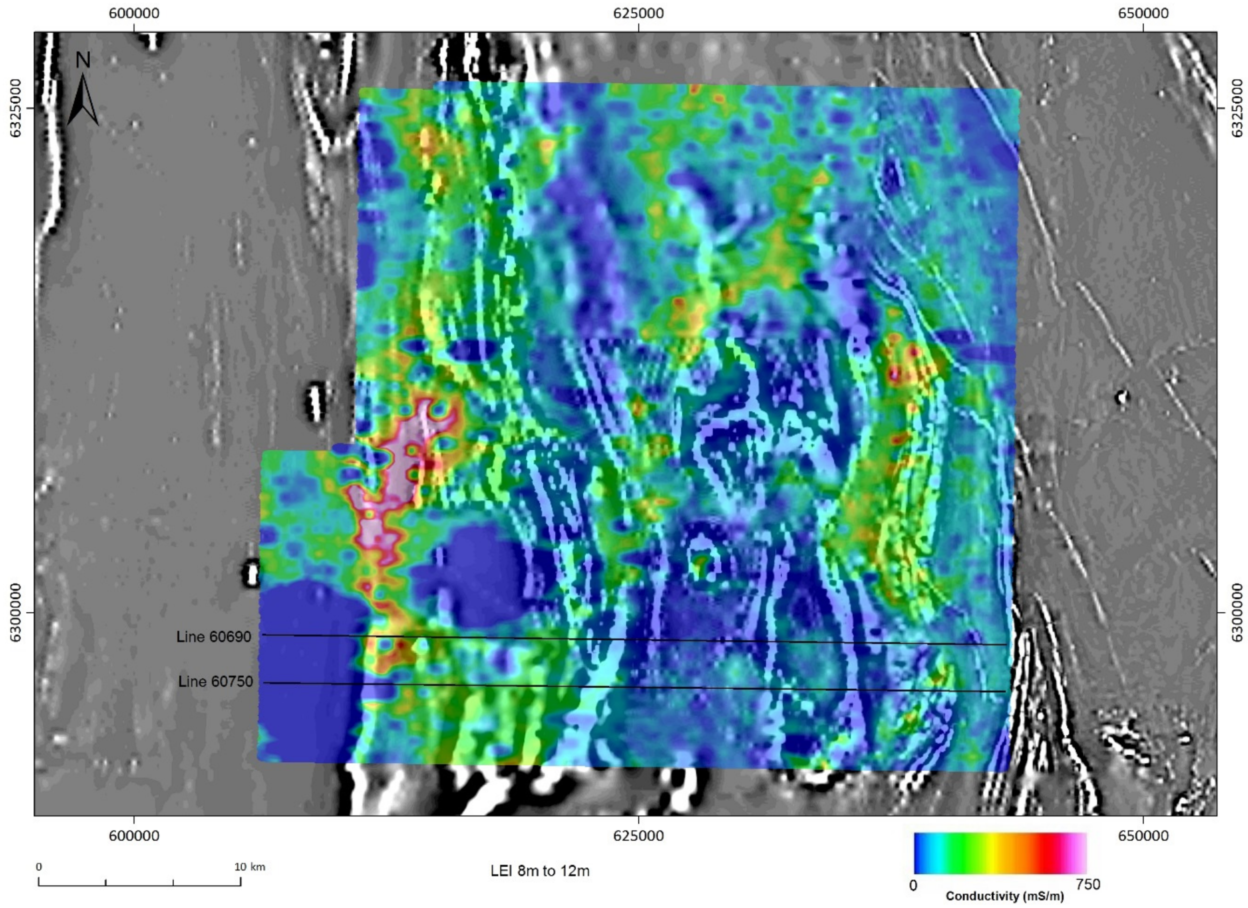

Figure 6.3 Pseudo-coloured Interval conductivity (8-12 m) below the ground surface from a layered earth inversion of TEMPEST AEM data, acquired over the Cleve Hills in Eastern Eyre Peninsula. The image is overlain on 1stVD magnetics (grayscale image) highlighting the complex folded metasediments of the region. Flight lines 60690 and 60750 are also shown.

The more conductive areas in the near surface depth interval (Figure 6.3) are spatially associated with valley fill sediments, and in-situ weathered rocks (saprolite). Figure 6.4 shows the conductivity structure for a region between 17 and 23 m below the surface. The conductive valley-fill sediment packages are more apparent in this depth slice, and the spatial continuity of the buried valleys better represented. The litho-structural control in determining the orientation of these old valley systems is also better defined. The conductive zones are aligned between magnetic lithologies but also cross cut magnetic sequences where faults occur (Figure 6.4). A drape of the 17-23 m conductivity-depth slice over the 1sec shuttle DEM (Figure 6.5) clearly depicts the coincidence of conductive areas with contemporary lows and valleys in the landscape.

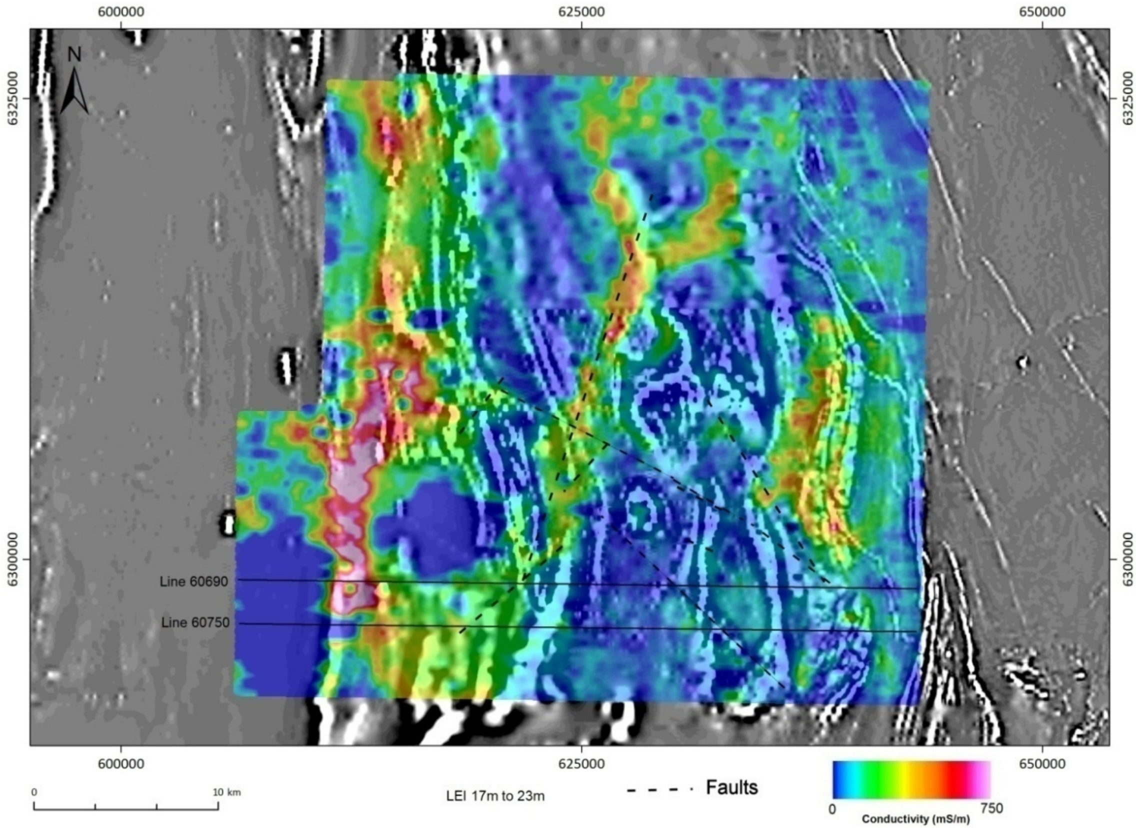

Figure 6.4 Pseudo-coloured Interval conductivity (17-23 m) below the ground surface from a layered earth inversion of TEMPEST AEM data, acquired over the Cleve Hills in Eastern Eyre Peninsula. The image is overlain on 1stVD magnetics (grayscale image) highlighting the complex folded metasediments of the region. Flight lines 60690 and 60750 are also shown.

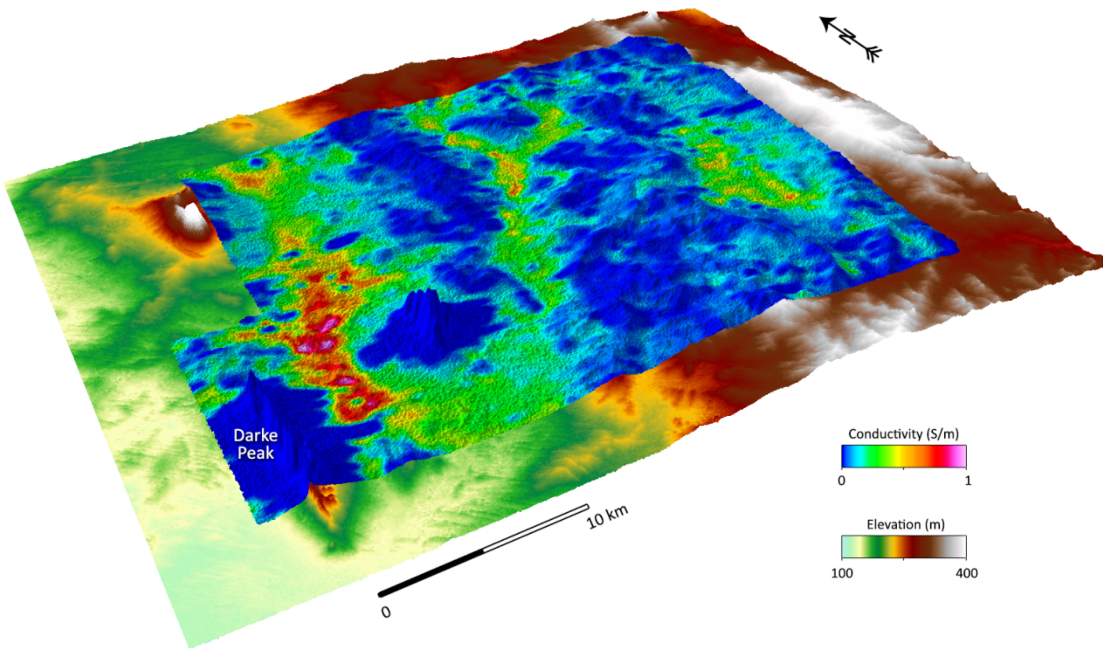

Figure 6.5 Pseudo-coloured Interval conductivity (17–23 m) draped on a perspective view of the Cleve Hills region Red and green colours indicate a more conductive part of the landscape. Blues are resistive areas often associated with fresh rock or sub-crop.

Analysis of a conductivity-depth section for an east-west oriented flight-line 60750 (Figure 6.6) provides further insight into the relationship between contemporary topography and the observed conductivity structure of the Cleve Hills region. The section extends from Darke Peak in the west, and to a region just south of Mt Bosanquet in the east. The most conductive parts of the section are associated with the regolith in a broad valley east of Darke Peak. We interpret the regolith of this valley to comprise a combination of in-situ saprolite overlying steeply dipping graphite-bearing metasediments. The AEM data suggest weathering may extend to depth along fractures and bedding planes. These materials are in turn overlain by transported valley fill sediments. This observation is supported, in part, by exploration reports filed by graphite explorers with DSD. The valley fill and in-situ regolith are relatively conductive, and available well data suggest the watertable is close to the surface, indicating that much of the regolith profile will be saturated with relatively saline groundwater (Figure 6.8). Differentiation of the in-situ regolith from the transported cover using the AEM is, in this instance, not readily achieved in the inverted data, supporting the observation that the aquifers are part of a complex unconfined system exceeding 100 m thick in places, overlying a fractured rock aquifer.

Small, relatively confined conductive zones in the near surface are apparent in the higher parts of the landscape in the eastern side of the section (Figure 6.6). These are attributed to small highly localised groundwater flow systems developed in a regolith comprising in-situ saprolite overlain by alluvial and colluvial transported materials. The localised near surface conductors extending from surface to depth (tens of metres) suggest these systems are also unconfined. A similar pattern is observed for line 60690 located further north (Figure 6.7).

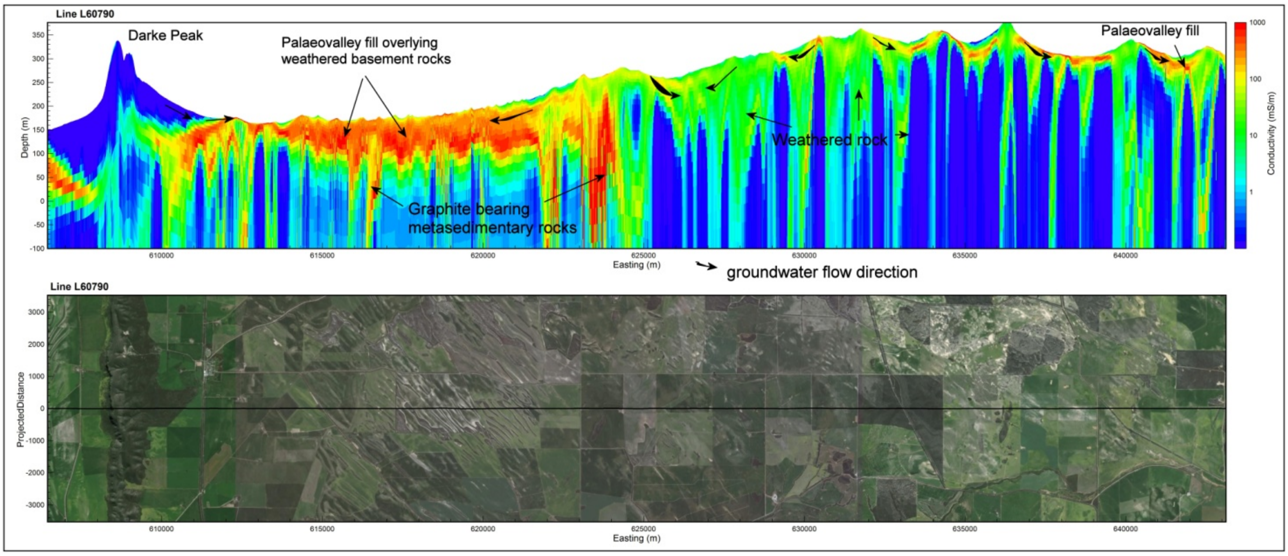

Figure 6.6 Conductivity-depth section (1D Layered Earth Inversion (top) for flight line 60790. The flight line is overlain on a Landsat true colour composite image (bottom panel). See Figure 6.3 and 6.4 for flight line locations.

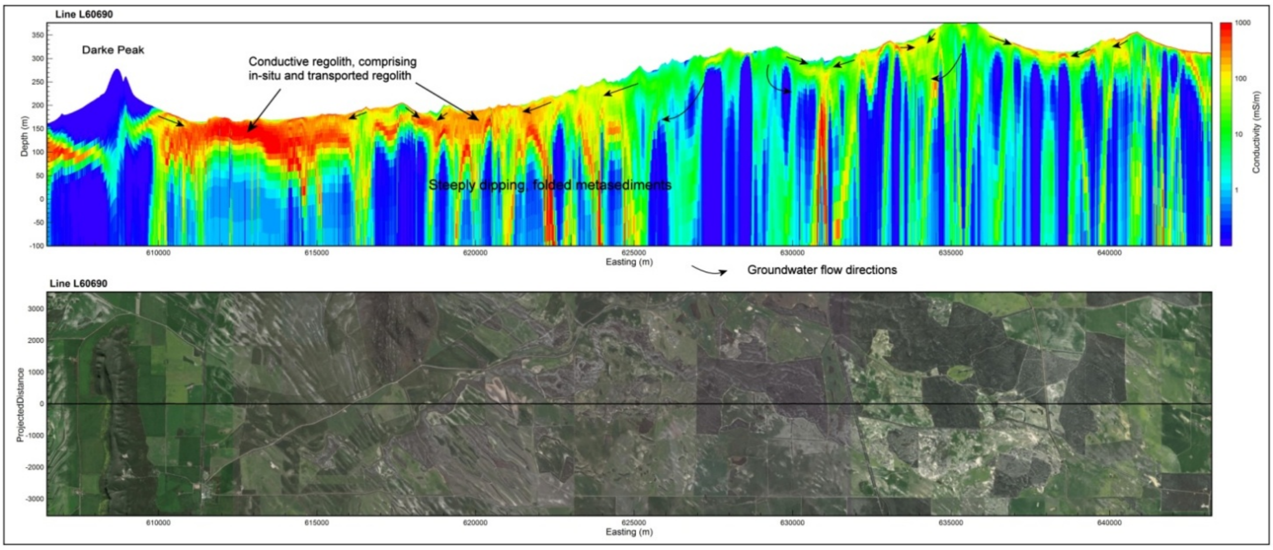

Figure 6.7 Conductivity-depth section (1D Layered Earth Inversion (top) for flight line 60690. The flight line is overlain on a Landsat true colour composite image (bottom panel). See Figure 6.3 and 6.4 for flight line locations.

Consideration of the observed ground conductivity structure against available well TDS indicates a good correlation between the measured groundwater salinity and the indicated conductivity (Figure 6.8). In general, higher TDS is associated with elevated ground conductivity, lending support to suggestion that the AEM data is mapping the spatial distribution of groundwater quality across the landscape. In places the modelled conductivity from the AEM doesn't match that defined from the wells, but this could be attributed to several factors, including that the AEM data are a gridded representation of ground conductivity and it may not be resolving finer scaled variations in groundwater conductivity identified at the resolution of the well data.

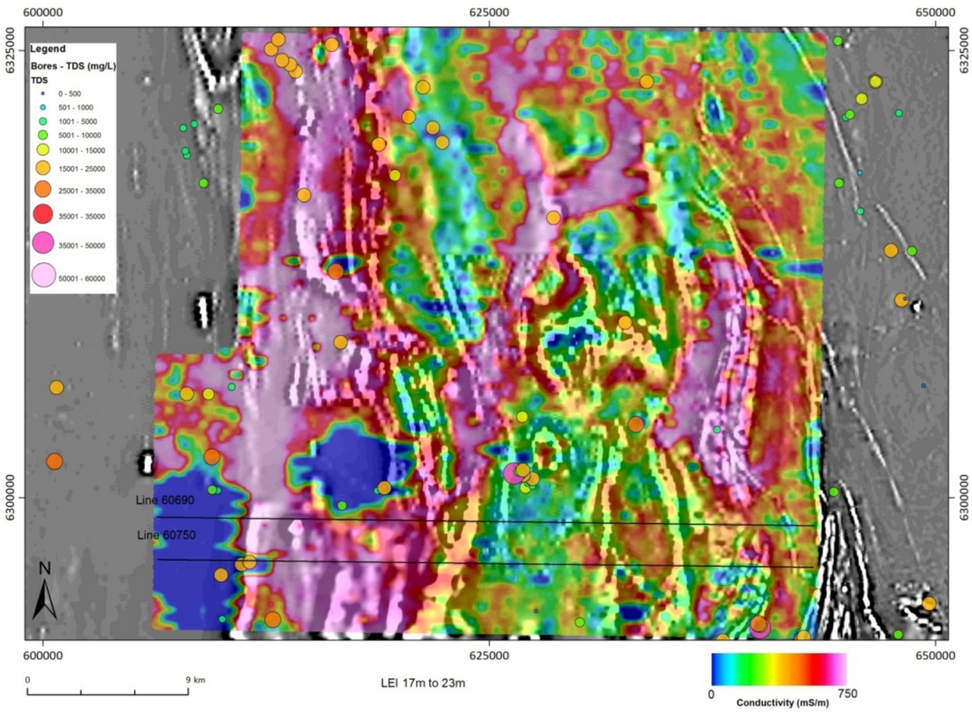

Figure 6.8 Pseudo-coloured Interval conductivity (17–23 m) below the ground surface from a layered earth inversion of TEMPEST AEM data, acquired over the Cleve Hills in Eastern Eyre Peninsula. The image is overlain on 1stVD magnetics (grayscale image) highlighting the complex folded metasediments of the region. Also overlain on the image are well water quality data indicative of groundwater salinities. Higher salinities are more commonly associated with lower more conductive parts of the landscape.

6.2 Coastal Plain AEM

The inversion for the coastal transect (Figure 4.9) is presented in Figure 6.9. At piezometer 633100566 (two high-conductivity wedges at ~1000 mS/m are present at depths of 0 to -20 m to and -40 to -80 m and could indicate seawater intrusion. Between these high-conductivity wedges there is a slightly lower conductivity layer of ~>500 mS/m, which roughly corresponds to the low permeability layer of the bioclastic Melton Limestone. The basement granite at this location is not easily distinguishable from the overlying monomict sands, possibly due to the conflating signature of the very highly saline groundwater at this location.

Lithologies at piezometer locations 633100569 and 633100572 do not appear to be accurately reflected in the conductivity values, with the clay exhibiting a range of conductivities and the limestone and polymict sands appearing of similar conductivity. The transition between clay, limestone, sand and basement appears to be best highlighted at the locations MRH9C and 633100575.

Variations in hydraulic conductivities of the various geological units, such as the low-conductivity consolidated granitic rock compared to the high-conductivity unconsolidated Tertiary sands, can result in the apparent electrical conductivity of the unit being influenced by the water content of the lithological medium. Also, the electrical conductivity signature may be a reflection of a combination of the lithology type and water salinity. For example, a granitic rock bearing saline water may produce a signature of medium conductivity. A geological unit may also express variations of electrical conductivity as a result of weathering, such as basement granite weathered in-situ to kaolinitic clay in the lower Tertiary aquifer of the Coastal Plain. Overall, AEM appears to have limited usefulness for differentiating the salinity of the aquifer water, but may be useful for interpreting major lithological zones and depth to basement.

6.3 Discussion

AEM typically has a coarser lateral resolution than ground-based methods and as such not be able to accurately resolve small, localized features. AEM systems must be configured to the desired depth, and as such cannot simultaneously map shallow and deep features. The latter is not of great importance for this investigation, as the watertable and inferred bottom of the aquifer is shallow relative to the lateral extent.

AEM shows promise to map and delineate subsurface features and groundwater systems over large areas at a level of detail unobtainable by using lithology from wells alone. It has been used in central Australia to map the extent of palaeovalleys (Magee, 2009). By extension, AEM may be used to provide an indication of groundwater salinity over large areas, if sufficient knowledge of the underlying geology exists to be able to make sound interpretations of the data. Additionally, conductivity data from AEM needs to be compared with measured groundwater salinity data to assess the accuracy and reliability of this method. In summary, inversion of AEM data does not provide a unique solution, the derived models are the result of the search for the simplest model that fit surface observations. However, it is useful for identifying areas for further consideration and investigation. By ground-truthing interesting features identified using AEM, targeted drilling will provide lithology, water level and water quality data to validate the interpretation of potential aquifers identified.

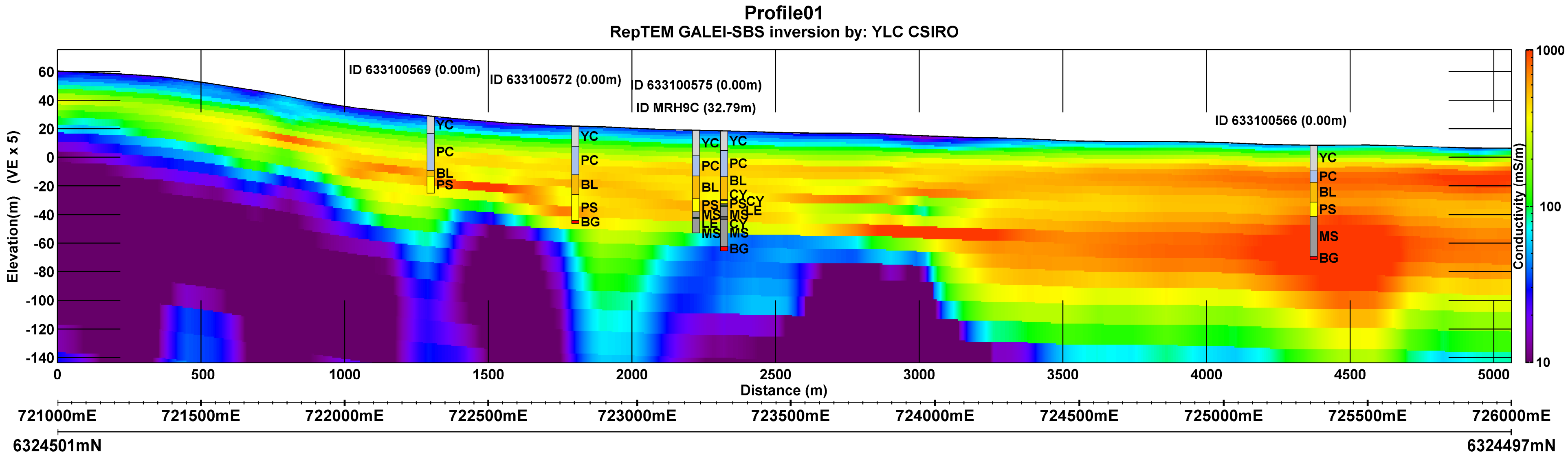

Figure 6.9 AEM inversion for the Coastal Plain transect

7 Conclusions and Recommendations

7.1 Conclusions

The case study locations in the North-eastern Eyre Peninsula are geologically complex and data-poor. The characterisation of hydrogeological systems in this complex environment is challenging, however the multi-disciplinary approach used here enabled to provide a first evaluation of the region's available groundwater resources.

Lithology, remote sensing, environmental tracers and hydrogeological modelling all indicated that hydrogeological systems in the North-eastern Eyre Peninsula are primarily local rather than regional in nature. This implies that the development of groundwater resources, if it occurs, will have to focus at the level of the local flow systems. Most of the smaller valley fills are a few tens of meters deep and only a few km wide, so they do not represent a large potential groundwater resource ('shallow younger fill' indicated in Figure 7.1). Valley fill groundwater is also usually quite saline.

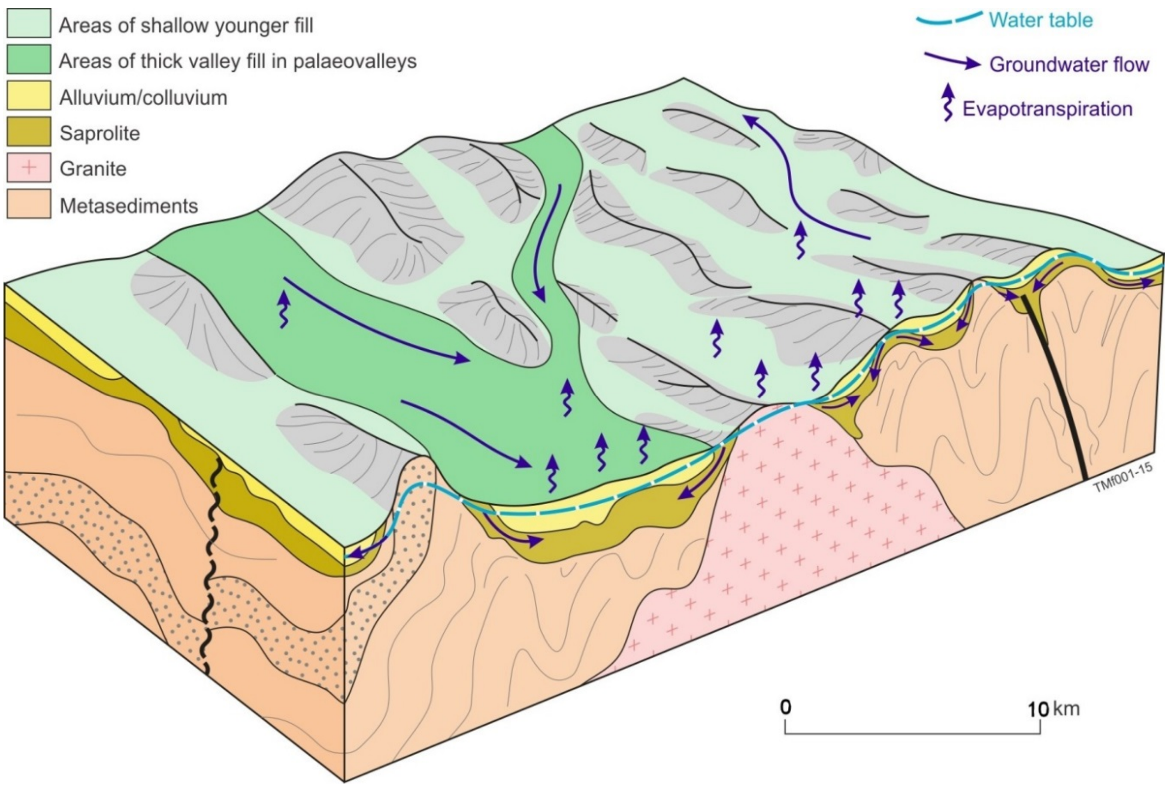

Figure 7.1 Hydrogeological conceptual model for the Cleve Hills (same area as figures in Chapter 6.1)

A key finding of the study was the presence of significant areas with deeply weathered or fractured bedrock across the region, with some of the weathering profiles extending to more than 100 m into the bedrock. Weathered and fractured bedrock aquifers, especially in recharge areas, probably offer the greatest potential to host relatively fresh groundwater resources. However, as the different weathered or fractured bedrock units do not appear well connected, this would represent local rather than a regional resource.

Aquifers have potential to occur in the form of fractured bedrock, weathered bedrock and different types of valley fills, including some potentially significant palaeovalley deposits on the west side (dark green 'thick valley fill' indicated in Figure 7.1). In terms of volume, this represents the largest potential groundwater resource identified, in these larger palaeovalley deposits. AEM shows a large conductance zone, which suggests a significant saline groundwater resource in the palaeovalley, although there are no wells to allow this to be investigated at this stage. More typical sedimentary aquifers are found along the coast, but due to high groundwater salinities and low recharge rates, offer limited scope for economic development as a water resource. Irrespective of the size of the potential aquifers, low recharge rates across the region imply that sustainable extraction rates will likely be low.

7.2 Recommendations

This assessment was greatly complicated by the scarcity of groundwater monitoring infrastructure in north-eastern Eyre Peninsula, in particular the absence of a nested piezometer network in easily accessible areas. There was also very limited infrastructure on the parts of the landscape (bedrock outcrops and palaeovalley deposits) most likely to offer suitable groundwater resources in terms of volume or low salinity. Piezometer nests would also be much better tools (relative to the wells with wide screens presently available) to evaluate recharge rates using environmental tracers, especially if efforts are made to also characterise aquifer porosity for the geological formation they are located in. Thus, the recommendations from this study are to:

- Plan further assessments of the region's groundwater resources at the scale of the hydrostratigraphic units most likely to fill a water resource need, such as palaeovalley for the volume of groundwater or bedrock outcrops in recharge areas for low-salinity groundwater.
- Install a piezometer nest network in the key hydrostratigraphic units identified during the study to better characterise and, eventually, manage the resource. This would be especially useful to help calibrate remote sending information obtained by airborne electromagnetics or other techniques.
- Initiate rainfall sampling across the elevation gradient in the Cleve Hills region to determine the local meteoric water line for the stable isotopes of water. Stable isotopes are a relatively inexpensive tracer and provide useful information about recharge mechanisms along elevation gradients.
- Proceed cautiously with the exploitation of groundwater resources in north-eastern Eyre Peninsula because the aquifers are small and recharge rates probably low.

References

Auken E, Christiansen AV, Kirkegaard C, Fiandaca G, Schamper C, Behroozmand AA, Binley A, Nielsen E, Effersø F, Christensen NB, Sørensen K, Foged N and Vignoli G (2014) An overview of a highly versatile forward and stable inverse algorithm for airborne, ground-based and borehole electromagnetic and electric data. *Exploration Geophysics*. Online early. http://dx.doi.org/10.1071/EG13097. Exploration Gephysics.

Berens V, Alcoe DW and Watt EL (2011) *Non-prescribed groundwater resources assessment – Eyre Peninsula Natural Resources Management Region. Phase 1 - Literature and Data Review,* DFW Technical Report 2011/16, Government of South Australia, through Department for Water, Adelaide.

BOM (2013) The National Groundwater Information System. Data viewed, February 2014, www.bom.gov.au/water/groundwater/ngis.

BOM (2014) Climate statistics for Australian locations, Bureau of Meteorology, Climate Data Online (CDO) database. Viewed February 2014, <http://www.bom.gov.au/climate/data/.

Boyd JP (2001) Chebyshev and Fourier Spectral Methods. Dover Publishers.

Bresciani E, Ordens CM, Werner AD, Batelaan O, Guan H and Post VEA (2014) Spatial variability of chloride deposition in a vegetated coastal area: implications for groundwater recharge estimation, Journal of Hydrology, 519, pp. 1177-1191.

Brodie R and Richardson M (2015) Open Source Software for 1D Airborne Electromagnetic Inversion. *ASEG Extended Abstracts 2015*, 1–3. http://dx.doi.org/10.1071/ASEG2015ab197.

Bullen TD and Kendall C (1998) Tracing of Weathering Reactions and Water Flowpaths: A Multi-Isotope Approach. Isotope Tracers in Catchment Hydrology, Elsevier, 611-646.

Busenberg E and Plummer N (1992) Use of Chlorofluorocarbons (CCl_3F and CCl_2F_2) as Hydrologic Tracers and Age-Dating Tools: The Alluvium and Terrace System of Central Oklahoma. Water Resources Research 28(9), 2257–2283.

Capo RC, Stewart BW and Chadwick OA (1998) Strontium isotopes as tracers of ecosystem processes: theory and methods. Geoderma 82, 197-225.

Charles SP and Fu G (2015) Statistically Downscaled Projections for South Australia, Goyder Institute for Water Research Technical Report Series No. 15/1, Adelaide, South Australia.

Cook PG (2003) A guide to regional groundwater flow in fractured rock aquifers. CSIRO Land and Water, Glen Osmond, South Australia.

Cook PG and Böhlke J-K (2000) Determining timescales for groundwater flow and solute transport, in Environmental tracers in subsurface hydrology, edited by P G Cook and A L Herczeg. Kluwer Academic Publishers, Norwell, Massachusetts, USA.

Crosbie RS, Morrow D, Cresswell RG, Leaney FW, Lamontagne S and Lefournour M (2012) New insights into the chemical and isotopic composition of rainfall across Australia. CSIRO Water for a Healthy Country Flagship, Australia.

Dart RC, Barovich KM and Chittleborough D (2005) Pedogenic carbonates, strontium isotopes and their relationship with Australian Dust Processes. CRC LEME, School of Earth and Environmental Sciences, University of Adelaide, SA, 5005.

Davies P and Crosbie R (2014) Australian chloride deposition rate. v1. CSIRO. Data Collection. 10.4225/08/545BEE54CD4FC.

Deeds DA, Vollmer MK, Kulongoski JT, Miller BR, Muhle J, Harth CM, Izbicki KA, Hilton DR and Weiss RF (2008) Evidence for crustal degassing of CF4 of SF6 and in Mojave Desert groundwater. Geochimica et Cosmochimica Acta 74(4), 999–1013. DOI: 10.1016/j.gca.2007.11.027.

Department for Water (2011) Eyre Peninsula Demand and Supply Statement. Government of South Australia, Department for Water.

DEWNR (2014) WaterConnect Groundwater Data, available through the Government of South Australia's water information portal, Department of Environment Water and Natural Resources. Viewed February 2014, https://www.waterconnect.sa.gov.au/Systems/GD/Pages/default.aspx#Unit Number.

Dogramaci SS and Herczeg AL (2002) Strontium and carbon isotope constraints on carbonate–solution interactions and inter-aquifer mixing in groundwaters of the semi-arid Murray Basin, Australia. Journal of Hydrology 262, 50-67.

Drexel JF and Preiss WV (1995) The geology of South Australia. Vol 2, The Phanerozoic, South Australia Geological Survey, Bulletin 54, Adelaide.

Drexel JF, Preiss WV and Parker AJ (1993) The geology of South Australia. Vol 1, The Precambrian, South Australia Geological Survey, Bulletin 54, Adelaide.

DSD (2014) South Australian Resources Information Geoserver (SARIG) a secure online map based web application that delivers state wide geological and geospatial data. Available through the Department of State Development, https://sarig.pir.sa.gov.au/Map.

Elderfield H (1986) Strontium isotope stratigraphy. Palaeogeography, Palaeoclimatology, Palaeoecology 57(1), 71-90.

Erickson E and Khunakasem V (1969) Chlroide concentration in groundwater, recharge rate and rate of deposition of chloride in the Israel Coastal Plain. Journal of Hydrology 7, 178-197.

Eyre Peninsula Natural Resources Management Board (2009) State of Our Resources, Recognising the state of natural resources of the Eyre Peninsula. Government of South Australia, Eyre Peninsula Natural Resources Management Board.

Fallon SJ, Fifield LK and Chappell JM (2010) The next chapter in radiocarbon dating at the Australian National University: Status report on the single AMS. Nuclear Instruments & Methods in Physics Research Section B 268, 898-908.

Fornberg B (1996) *Practical Guide to Pseudo Spectral Methods*, Cambridge University Press, Cambridge.

Fox L and Parker IB (1968) *Chebyshev Polynomials in Numerical Analysis.* Oxford University Press, Oxford.

Friedrich R, Vero G, von Rohden C, Lessmann B, Kipfer R and Aeschbach-Hertig W (2013) Factors controlling terrigenic SF6 in young groundwater of the Odenwald region (Germany). Applied Geochemistry 33, 318-329. DOI: http://dx.doi.org/10.1016/j.apgeochem.2013.03.002.

Gallant JC and Dowling TI (2003) A multiresolutional index of valley bottom flatness for mapping depositional areas. Water Resources Research 39(12), 1347.

Gilfedder M and Munday T (2013) *Facilitating Long-term Outback Water Solutions (G-FLOWS Stage-1) Final Report*. Goyder Institute for Water Research Technical Report Series No. 13/13.

Golder Associates (2014) Hydrogeological desktop baseline assessment, Prepared for Archer Exploration Limited – Campoona Graphite Project.

Green G, Banks E, Wilson T and Love A (2007) Knowledge and Information Division – Department of Water, Land and Biodiversity Conservation – *GROUNWATER RECHARGE AND FLOW INVESTIGATIONS IN THE WESTERN MOUNT LOFTY RANGES, SOUTH AUSTRALIA* – Department of Water, Land and Biodiversity Conservation Report 2007/29 – September 2007.

Green G, Bestland EA and Walker GS (2004) Distinguishing sources of base cations in irrigated and natural soils: evidence from strontium isotopes. Biogeochemistry 68, 199-225.

Happell JD, Price RM, Top Z and Swart PK (2003) Evidence for the removal of CFC-11, CFC-12, and CFC-113 at the groundwater–surface water interface in the Everglades. Journal of Hydrology 279, 94–105.

Harding A, Henschke C, Ciganovic P and Dooley T (2002) Eastern Cleve Hills Salinity Management Plan. Rural Solutions SA, Government of South Australia.

Harnisch J, Borchers R, Fabian P, Gaeggeler HW and Schotterer U (1996) Effects of natural tetrafluormethane. Nature 384.

Harnisch J and Eisenhauer A (1998) Natural CF4 and SF6 on Earth. Geophyscal Research Letters 25, 2401-2406. DOI: 10.1029/98GL01779.

Harnisch J, Frische M, Borchers R, Eisenhauer A and Jordan A (2000) Natural fluorinated organics in fluorite and rocks. Geophysical Research Letters 27, 1883-1886. DOI: 10.1029/2000gl008488.

Hem JD (1989) Study and Interpretation of the Chemical Characteristics of Natural Water. United States Geological Survey Water-Supply Paper 2254.

Henschke C, Dooley T and Ciganovic P (2001) Dryland salinity management in the Driver River basin, PIRSA, Rural Solutions South Australia.

Henschke CJ, McCarthy DG and Branford T (1994) Investigation and management of dryland salinity in a catchment near Darke Peak on Upper Eyre Peninsula. PIRSA Technical Paper Number 37. June 1994.

IAEA/WMO (2014) Global Network of Isotopes in Precipitation. The GNIP Database. Accessible at: http://www.iaea.org/water.

Jessel M, Boamah K, Agyei Duodu J and Ley-Cooper Y (2015) Geophysical evidence for a major palaeochannel within the Obosum Group of the Volta Basin, Northern Region, Gahana. Journal of African Earth Science. DOI: http://dx.doi.org/10.1016/j.jafrearsci.2015.04.007.

Jeuken B (2011) Mullaquana Project Hydrogeological setting, Australian Groundwater Technologies Pty Ltd, Mecrus Group, pages 4 – 15.

Koh D-C, Plummer LN, Busenberg E and Kim Y (2007) Evidence for terrigenic SF6 in groundwater from basaltic aquifers, Jeju Island, Korea: Implications for groundwater dating. Journal of Hydrology 339, 93-104.

Kretschmer P and Wohling D (2014) Groundwater recharge in the Anangu Pitjantjatjara Yankunytjatjara Lands, South Australia, DEWNR Technical Report 2014/06, Government of South Australia, through the Department of Environment, Water and Natural Resources, Adeliade.

Leaney FW, Taylor AR, Jolly ID and Davies PJ (2013) Facilitating Long Term Out-Back Water Solutions (G-FLOWS) Task 6: Groundwater recharge characteristics across key priority areas. Goyder Institute for Water Research Technical Report Series No. 13/6, Adelaide, South Australia. <http://www.goyderinstitute.org/uploads/13_6%20Leaney%20et%20al%20GFLOWS%20-%20COMPRESSED.pdf>.

Ley-Cooper AY, Annetts D and Munday T (2015) Reprocessing multiple datasets of legacy airborne electromagnetic data in the northern Eyre Peninsula, South Australia. Goyder Institute for Water Research Technical Report Series No. XX/x, Adelaide.

Ley-Cooper AY and Munday TJ (2013) *Groundwater Assessment and Aquifer Characterization in the Musgrave Province, South Australia: Interpretation of SPECTREM Airborne Electromagnetic Data*. Goyder Institute for Water Research Technical Report Series No. 13/7, Adelaide, South Australia.

Love AJ, Cook PG, Harrington GA and Simmons CT (2002) Groundwater Flow in the Clare Valley, Dept. for Water Resources Final Report, DWR02.03.0002.

Love AJ, Herczeg AL, Armstron D, Stadter F and Mazor E (1993) Groundwater flow regime within the Gambier Embayment of the Otway Basin, Australia: evidence from hydraulics and hydrochemistry. Journal of Hydrology 143, 297-338.

Love AJ, Smith PC, Dodds S and Dennis K (1994) Musgrave proclaimed wells area groundwater assessment, South Australian Department for Mines and Energy, Report Book 94/27.

Magee JW (2009) Palaeovalley Groundwater Resources in Arid and Semi-Arid Australia – A Literature Review. Geoscience Australia Record 2009/03. 224 pp.

Małoszewski P and Zuber A (1996) Lumped parameter models for interpretation of environmental tracer data. Manual on mathematical models in isotope hydrogeology, IAEA-TECDOC-910. IAEA, Vienna, Austria, pp 9–58.

Mulder I, Huber SG, Krause T, Zetzsch C, Kotte S, Dultz S and Schöler HF (2013) A new purge and trap headspace technique to analyze low volatile compounds from fluid inclusions of rocks and minerals. Chemical Geology 358, 148-155. DOI: http://dx.doi.org/10.1016/j.chemgeo.2013.09.003.

Munday T, Abdat T, Ley-Cooper Y and Gilfedder M (2013) *Facilitating Long-term Outback Water Solutions (G-FLOWS Stage-1: Hydrogeological Framework*. Goyder Institute for Water Research Technical Report Series No. 13/12.

Ordens CM, Werner AD, Post VEA, Hutson JL, Simmons CT and Irvine BM (2011) Groundwater recharge to a sedimentary aquifer in the topographically closed Uley South Basin, South Australia, Hydrogeology Journal, 20, pp. 61-72.

Orszag SA and Patterson GS (1972) Numerical simulation of three-dimensional homogeneous isotropic turbulence. Physical Review Letters 28(2), 76–79.

Parker AJ, Fanning CM and Flint RB (1984) Geology of Eyre Peninsula: Geological survey, Department of Mines and Energy, Adelaide, 1984.

Parsons Brinckerhoff (2011) 2011 Resources and Energy Infrastructure Demand Study. Government of South Australia, Department of State Development (http://www.pir.sa.gov.au/minerals/home/resic).

Post V, Kooi H and Simmons C (2007) Using Hydraulic Head Measurements in Variable-Density Ground Water Flow Analyses. Groundwater 45(6), 664–671.

Raiber M, Webb JA and Bennetts DA (2009) Strontium isotopes as tracers to delineate aquifer interactions and the influence of rainfall in the basalt plains of southeastern Australia. Journal of Hydrology 367, 188-199.

Risby L and Harrington G (2014) Non-prescribed groundwater resources assessment – Eyre Peninsula Natural Resources Management Region, Phase 2 – Hydrogeochemistry, DEWNR Technical Report 2014/10, Government of South Australia, through Department of Environment, Water and Natural Resources, Adelaide.

Robinson NI and Love AJ (2013) Hidden channels of groundwater flow in Tóthian drainage basins. Advances in Water Resources 62, 71–78.

Rohden Cv, Kreuzer A, Chen Z and Aeschbach-Hertig W (2010) Accumulation of natural SF6 in the sedimentary aquifers of the North China Plain as a restriction on groundwater dating. Isotopes in Environmental and Health Studies 46, 279-290. DOI: 10.1080/10256016.2010.494771.

Shand P, Darbyshire DPF, Love AJ and Edmunds WM (2009) Sr isotopes in natural waters: Applications to source characterisation and water-rock interaction in contrasting landscapes. Applied Geochemistry 24, 574-586.

Sheard MJ and Primary Industries and Resources SA CSIRO Division of Exploration and Mining and CRC LEME Australia (2008) *Regolith benchmark atlas, Gawler Craton, South Australia / compiled by M.J. Sheard* CRC LEME Bentley, W.A <http://crcleme.org.au/Pubs/OFRSindex.html>.

Suckow A (2013) Analyses Using Multitracer Approaches`, in Isotope Methods of Dating Old Groundwater, IAEA.

Suckow A (2014) The age of groundwater - Definitions, models and why we do not need this term. Applied Geochemistry 50, 222–230. DOI: http://dx.doi.org/10.1016/j.apgeochem.2014.04.016.

Swaffer BA, Holland KL, Doody TM, Li C and Hutson J (2014) Water use strategies of two co-occurring tree species in a semi-arid karst environment. Hydrological Processes 28, 2003–2017. DOI: 10.1002/hyp.9739.

Thompson JE (2014) Hydrogeological characterisation of sedimentary and fractured rock groundwater in the eastern Eyre Peninsula, South Australia. Honours thesis, Flinders University, South Australia.

Twidale CR, Tyler MJ and Davies M (1985) History of Eyre Peninsula. Royal Society of South Australia Inc.

Tóth J (1963) A theoretical analysis of groundwater flow in small drainage basins. Journal of Geophysical Research 68(16), 4795–4812.

Tóth J (2009) Gravitational Systems of Groudwater Flow: Theory, Evaluation, Utilization, Cambridge University Press, United Kingdom.

Webb AW, Thomson BP, Blissett AH, Daley SJ, Flint RB and Parker AJ (1982) Geochronology of the Gawler Craton, South Australia. Department of Mines and Energy South Australia.

Weiss RF (1968) Piggyback sampler for dissolved gas studies on sealed water samples. Deep-sea Research 15, 695–699.

Appendix A Groundwater flow systems

Hydraulic, environmental tracer and geophysical data have provided useful insights into the groundwater flow systems in the study area. However, there is still some ambiguity in this when examining flow systems in the Cleve Hills region. This is due to an overall lack of data, and also the position in the landscape of the available data. For example, there is a paucity of data beneath the most elevated regions and steepest terrain, as these regions are not usually feasible for landholders to drill water wells due to the high drilling expenses. A detailed understanding of the watertable is paramount for distinguishing between local, intermediate and regional systems.

The major question investigated, is whether or not subsurface water flow can move over distances of 30–40 km along the previously described transects (Figure 4.4; Figure 4.5; Figure 4.6), based on the hydrogeological information available. Unfortunately the current information is limited, consisting of sparse hydraulic head measurements and the knowledge of the existence of a few springs. In addition, the depth of essentially impermeable rocks is not known. In order to make an assessment, a model is proposed based on gravity driven basin (Tóth, 1963; 2009) The main assumptions are that watertables are static, groundwater flows parallel to the chosen two dimensional cross-section, the hydrogeology has constant and uniform porous properties and that no-flow boundaries exist at the bottom and sides of the model domain. Based on these assumptions, calculations are made.

A.1 Hydrological modelling calculations

The initial step is to create potential watertable curves from field data of surface topography and well data along transects. This is then followed by assuming that the positions of watertables are constant with time and that a two-dimensional flow model applies as a Tóthian, gravity driven drainage basin of an isotropic and homogeneous porous medium (Tóth, 1963; 2009). The analysis of this model first maps a geometrical cross-section onto a square as indicated in Apx Figure A 1, then uses a two-dimensional series of Chebyshev polynomials in a collocation procedure (Boyd, 2001) (Fornberg, 1996).

A.1.1 SMOOTHED CONTOURS

Apx Figure A 2, Apx Figure A 3 and Apx Figure A 4 correspond to respective, Western (W), South East (SE) and Southern (S) transects, show the existing topographic surface curves and discrete well data as well as their smoothed contours.

Smoothing was done using a least squares fit to topographic and well data with a polynomial of the form

$$h(X) = \sum_{k=0}^{K} b_k X^k \qquad \text{(A.1)}$$

$h(X)$ and horizontal coordinate X are shown on Apx Figure A 1 and b_k are determined by the fitting process. The polynomial order, K, was kept to a minimum sufficient to represent the essential features of the data but not too large where excessive rippling occurs. The values of K obtained are as follows: for topography K = [18, 21, 16] : [W, SE, S] and for wells K = [8, 13, 8] : [W, SE, S].

For wells, it was necessary to add fictitious data, indicated in Apx Figure A 2, Apx Figure A 3 and Apx Figure A 4 in order to overcome the sparsity of data near both ends $X = 0$ and $X = S$, but roughly maintaining the form of the overlying surface topography.

Because of the sparsity of well data and the existence of springs, indicating that the watertable is near surface, it was deemed prudent to take not only the smooth curve fitting well data as one likely watertable but also to consider the smoothed topographic surface as another and a third averaging these two curves. Although there is some small error in taking the watertable coincident with the surface and not as a subsurface replica of it, the difference in shape of the topographic curve and the watertable curve is the matter of importance.

A.1.2 MATHEMATICAL MODEL

With coordinates X and Z as shown in Apx Figure A 1, the defining partial differential equation for Φ is the Laplace equation

$$\nabla^2\Phi = \frac{\partial^2\Phi}{\partial X^2} + \frac{\partial^2\Phi}{\partial Z^2} = 0 \tag{A.2}$$

with boundary conditions

vertical sides: $$\frac{\partial\Phi}{\partial X} = 0 \,, \qquad X = 0 \text{ and } X = S \tag{A.3}$$

base: $$\frac{\partial\Phi}{\partial Z} = 0 \,, \qquad Z = 0 \tag{A.4}$$

top surface: $$\Phi = Z = H(X) = Z_0 + h(X) \tag{A.5}$$

where Z_0 is the depth below sea level ($h(X)$ being defined above sea level).

Although the problem is specified in terms of Φ, it is essential that flow lines are determined orthogonal to Φ. This can be done numerically by path tracking using velocity components $\partial\Phi/\partial X$ and $\partial\Phi/\partial Z$. However, a more efficient way (available for the solution method to follow) is to determine the flow lines as stream lines defined by constant values of a stream function, Ψ, and determined analytically from either or both of the Cauchy-Riemann conditions

$$\frac{\partial\Psi}{\partial X} = -\frac{\partial\Phi}{\partial Z} \,, \quad \frac{\partial\Psi}{\partial Z} = \frac{\partial\Phi}{\partial X} \tag{A.6}$$

Ψ is set to zero on the base $Z = 0$, although and arbitrary constant can be added to Ψ if needed.

The original domain is now mapped to the square (Orszag and Patterson, 1972) as shown in Apx Figure A 1 with new variables, $-1 \le \xi \le 1, \quad -1 \le \varsigma \le 1$, with the connections

$$X = C_{1X} + C_{2X}\,\xi, \qquad C_{1X} = C_{2X} = \frac{S}{2}$$

$$Z = C_{1Z} + C_{2Z}\,\varsigma, \qquad C_{1Z} = C_{2Z} = \frac{H(X)}{2}$$

The partial derivatives of Φ become

$$\frac{\partial\phi}{\partial X} = \frac{1}{C_{2X}}\frac{\partial\phi}{\partial\xi}, \qquad \frac{\partial^2\Phi}{\partial X^2} = \frac{1}{C_{2X}^2}\frac{\partial^2\Phi}{\partial\xi^2}$$

$$\frac{\partial\phi}{\partial Z} = \frac{1}{C_{2Z}}\frac{\partial\phi}{\partial\varsigma}, \qquad \frac{\partial^2\Phi}{\partial Z^2} = \frac{1}{C_{2Z}^2}\frac{\partial^2\Phi}{\partial\varsigma^2} \tag{A.7}$$

The Laplace equation becomes

$$\frac{1}{C_{2X}^2}\frac{\partial^2\Phi}{\partial\xi^2} + \frac{1}{C_{2Z}^2}\frac{\partial^2\Phi}{\partial\varsigma^2} = 0 \tag{A.8}$$

and boundary conditions become

$$\frac{\partial \Phi}{\partial \xi} = 0, \quad \xi = \pm 1; \qquad \frac{\partial \Phi}{\partial \varsigma} = 0, \quad \varsigma = -1 \tag{A.9}$$

and on the top surface

$$\Phi = H(X), \quad \varsigma = 1 \tag{A.10}$$

To solved the problem in the mapped domain, set

$$\Phi = \sum_{m=0}^{M+1} \sum_{n=0}^{N+1} a_{mn} T_m(\xi) T_n(\varsigma) \tag{A.11}$$

where $T_k(u)$ is a Chebyshev polynomial of the first kind and of order k, for $-1 \le u \le 1$, with particular properties of interest (Boyd, 2001; Fox and Parker, 1968) $T_k(u) = \cos(k\theta), \quad \theta = \cos^{-1} u$

$$\frac{dT_k(u)}{du} = \frac{k \sin k\theta}{\sin \theta}, \qquad \frac{d^2 T_k(u)}{du^2} = \left(k \cos\theta \sin k\theta - k^2 \sin\theta \cos k\theta\right) / \sin^3 \theta \tag{A.12}$$

$$\int T_0(u)\,du = T_1(u), \qquad \int T_1(u)\,du = \frac{1}{4}\left[T_0(u) + T_2(u)\right]$$

$$\int T_k(u)\,du = \frac{1}{2}\left[\frac{T_{k+1}(u)}{k+1} - \frac{T_{k-1}(u)}{k-1}\right] \tag{A.13}$$

From the second of the Cauchy-Rieman conditions,

$$\Psi = \int_0^Z \frac{\partial \Phi}{\partial X} dZ = \frac{C_{2z}}{C_{2X}} \int_{-1}^{\varsigma} \frac{\partial \Phi}{\partial \xi} d\varsigma \tag{A.14}$$

and in double series form

$$\Psi = \frac{C_{2X}}{C_{2Z}} \sum_{m=0}^{M+1} \sum_{n=0}^{N+1} a_{mn} \frac{\partial T_m(\xi)}{\partial \xi} \int_{-1}^{\varsigma} T_n(\varsigma)\, d\varsigma \tag{A.15}$$

and use of the integration expressions of (A.12).

The alternative definition of Ψ:

$$\Psi = -\int_0^X \frac{\partial \Phi}{\partial Z} dX = \int_{-1}^{\xi} \frac{C_{2x}}{C_{2z}} \frac{\partial \Phi}{\partial \varsigma} d\xi \tag{A.16}$$

is not used because $C_{2z} = H(X)/2$ is variable along the ξ path and numerical integration is required.

The coefficients, a_{mn}, are determined by satisfaction of a linear set of equations from Laplace's equation and boundary conditions at collocation points:

$$\xi_m = \cos\left(\frac{(2m+1)\pi}{2(M+1)}\right), \qquad m = 0,1,2,\ldots,M$$

$$\varsigma_n = \cos\left(\frac{(2n+1)\pi}{2(N+1)}\right), \qquad n = 0,1,2,\ldots,N \tag{A.17}$$

and also at the four corner points $(-1,-1)$, $(-1,1)$, $(1,-1)$, $(1,1)$. This produces MN points inside the square, $2M + 2N$ points on the sides and 4 at the corner points with a total of $MN + 2M + 2N + 4 = (M+2)(N+2)$. This corresponds to the $0 - M+1$, T_m terms and $0 - N+1$, T_n terms. As M and N increase, the accuracy of the series representation (A.11) of Φ

improves. In practice M, 25-50 and N, 25-50 suffice to give accuracies better than 0.1%. The measure of accuracy is by comparison with arbitrary positions along the boundary and also by comparison with the solutions given by (Tóth, 1963) with flat top surface and linear plus sinusoidal head distribution in analytical form and polynomial fitted form (A.1).

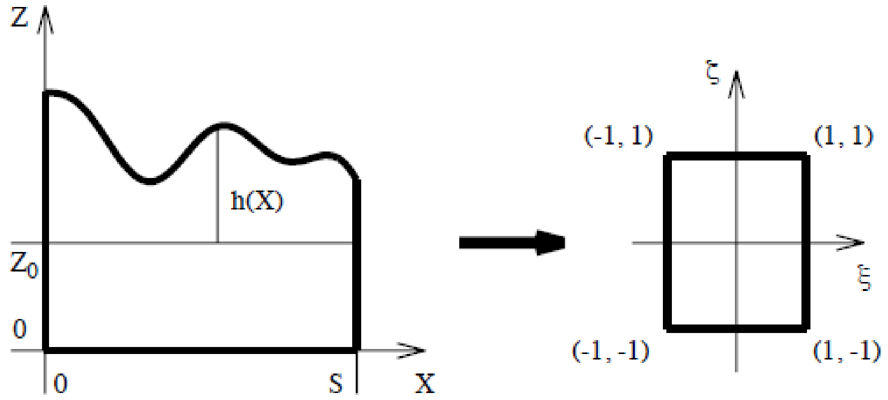

Apx Figure A 1 Original and mapped transects

A.2 Results

When considering the most interesting results of the modelling, although the basic solution is in terms of Φ, the real interest is in the stream function, Ψ, and constant values of it along streamlines creating flow patterns. Consequently, no results are given for Φ.

In a series of figures, Apx Figure A 2 to Apx Figure A 24, flow patterns are shown for each of the three transects and their three potential watertable smoothed curves: surface topography, well data and their arithmetic average. The value z_0 = 100 m is constant throughout. All flow patterns are drawn for equal increments of Ψ, but not necessarily the same increments from one pattern to another. Each incremental choice included Ψ = 0 with streamlines along the base, sides and in particular in the appearance of interior vertical lines connecting base to top surface. The values Ψ = 0 also appear on curves of surface stream function in figures accompanying each flow pattern. The cells formed between vertical lines are isolated from each other. This provides the important conclusion that in none of the transects with a base depth of 100 m can there be lateral subsurface flow from highest elevations near X = 0 right through to lowest elevations near $X = S$ if the initial assumptions of the modelling prevail: two-dimensional steady state flow in gravity driven Tóthian basins of isotropic and homogeneous porous media.

What should be the effect of having different basal depths z_0? From Tóth's original work of 1963 (Tóth, 1963; 2009) it can be concluded that as z_0 increases, the possibility exists to have regional flow from one side of the basin to the other without the appearance of separating cells. This is found to be true here, and critical values of z_0 indicating the onset of regional flow are found in the range 1300–6000 m. Probably such basal depths do not occur on the Eyre Peninsula.

The way these critical depths were determined was by examining the presence or otherwise of stagnation points along the base line. These occur where the vertical flow lines of Ψ = 0 in the flow patterns intersect the base with the conditions $\partial\Phi/\partial X = 0$ and the given $\partial\Phi/\partial Z = 0$. Some idea of the progression from baseline values of $\partial\Phi/\partial X$ at z_0 = 100–5000 m can be seen from Apx Figure A 23 and for the Western transect. It is interesting to note that the top surface curves of Ψ in the Western transect curves of Apx Figure A 6, Apx Figure A 8 and Apx Figure A 10 have the same form as the $\partial\Phi/\partial X$ curves at z_0 = 100 m. This means that top surface Ψ curves could also be used to detect regional flow. However, as seen from one of Tóth's cases (Robinson and Love, 2013; Tóth, 1963) stagnation points may lie on the vertical sides, with Ψ = 0 lines connecting the sides to the top surface, suggesting that the baseline $\partial\Phi/\partial X$ = 0 approach is more reliable.

In summary, the main conclusion is that at reasonable depths to an impermeable basement of the order of a 100 m, the subsurface water flow cannot proceed along the entire transect. Typical flow patterns that would be produced for a watertable defined by the surface topography are shown in the three transects (Apx Figure A 5; Apx Figure A 11 and Apx Figure A 17). Flow along transects can occur if it assumed that impermeable basement depths exist ranging from 1300–6000 m. However, based upon the geological understanding, it is unlikely that such depths prevail on the Eyre Peninsula. A final point of practical importance is that the regions of discharge in the flow patterns would indicate the presence of springs and seeps. A more detailed field investigation along these hydrogeological transects may provide confirmation of the model adopted.

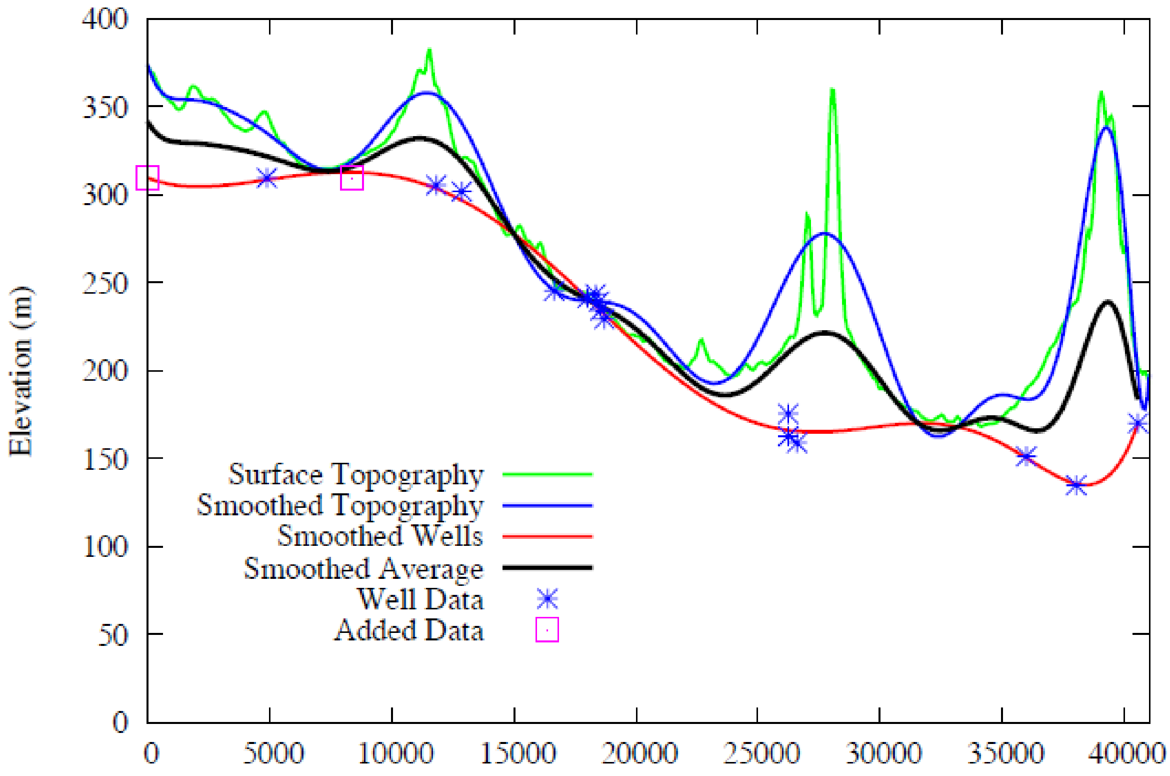

Apx Figure A 2 Western transect. Surface and well data, smoothed and average

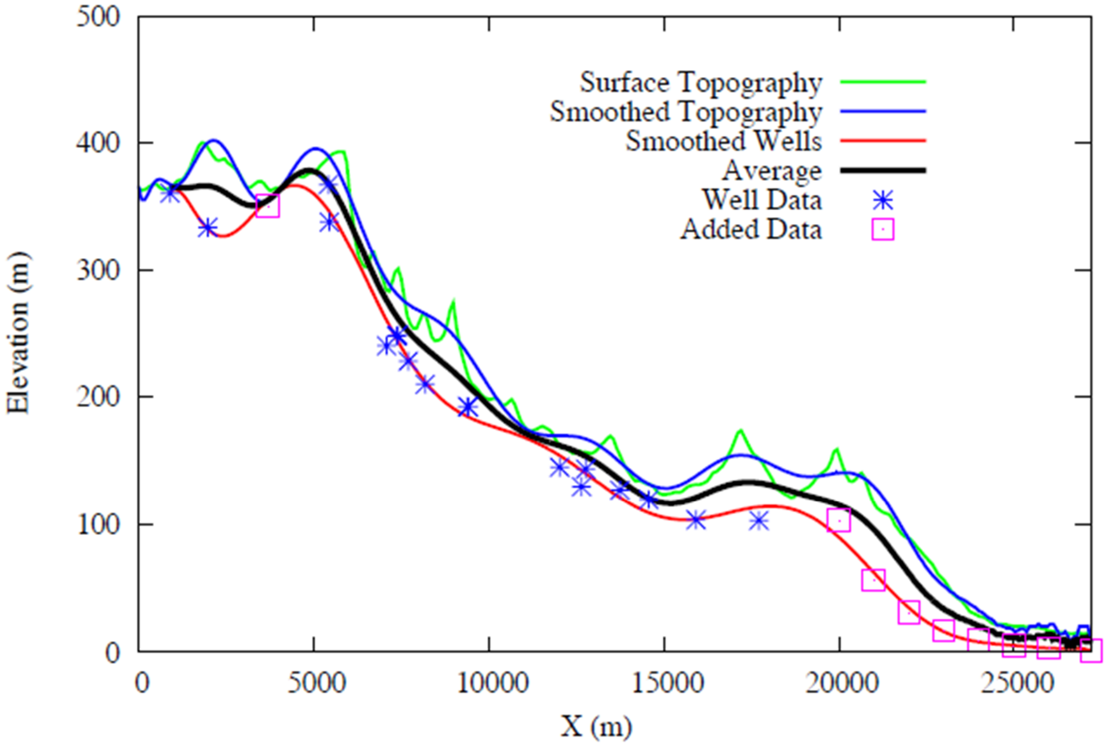

Apx Figure A 3 South-eastern transect. Surface and well data, smoothed and averaged

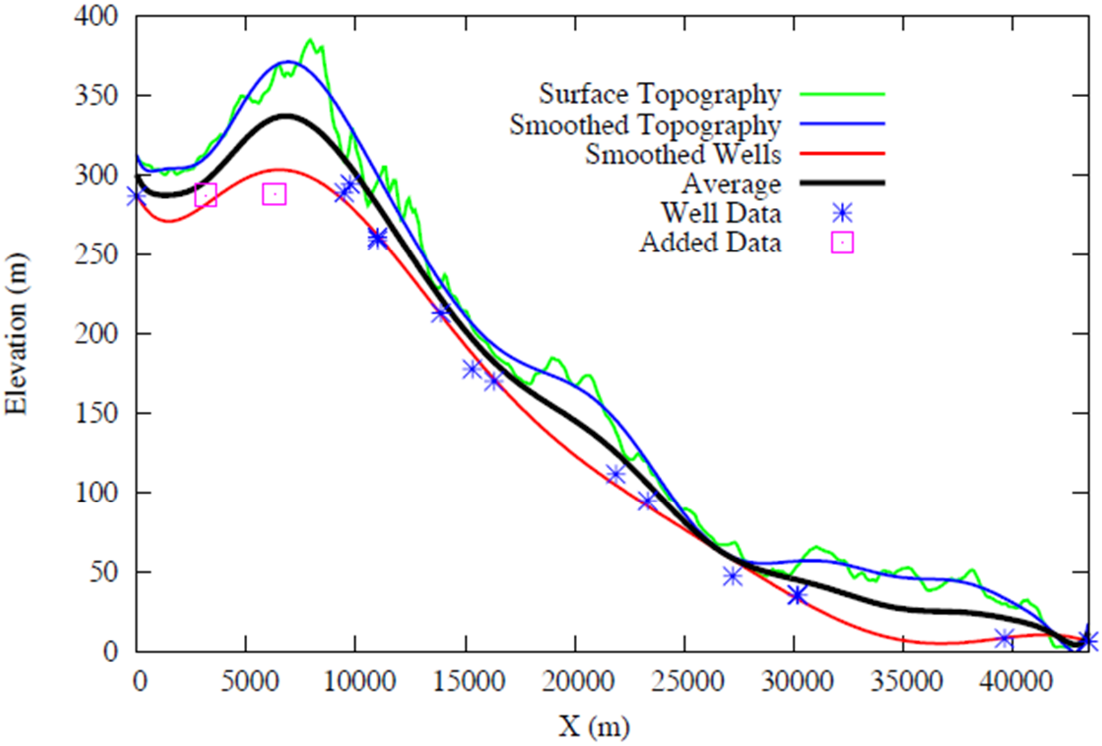

Apx Figure A 4 Southern transect. Surface and well data, smoothed and average

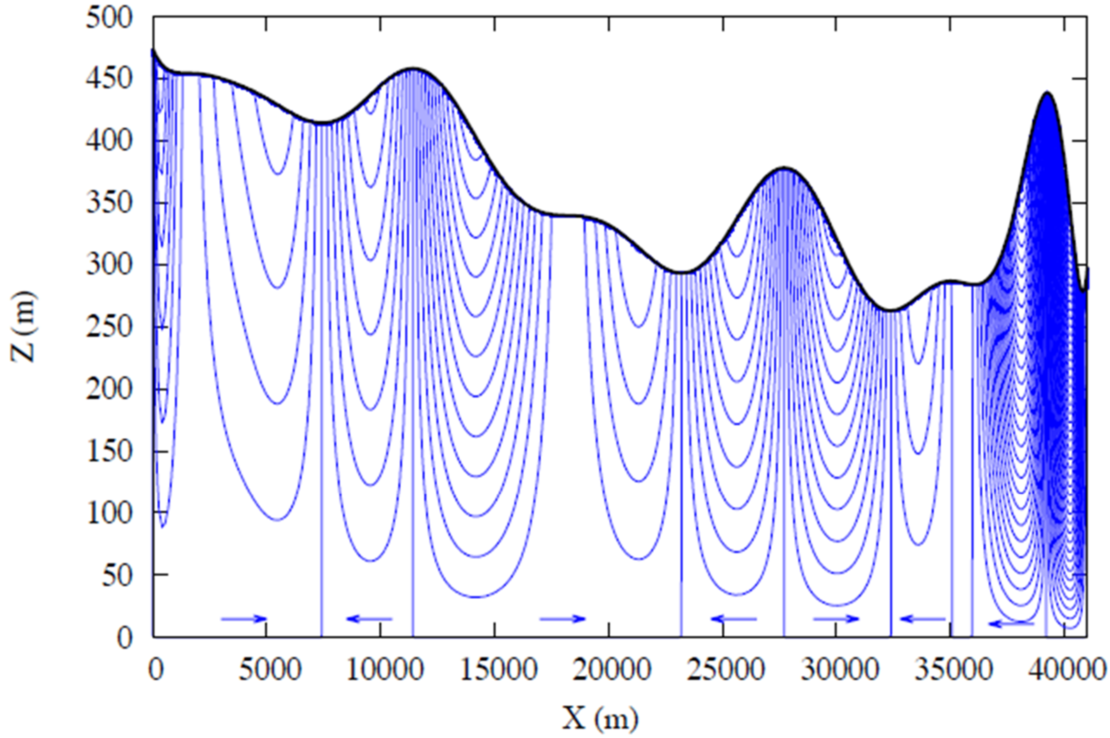

Apx Figure A 5 Western transect topography flow contours

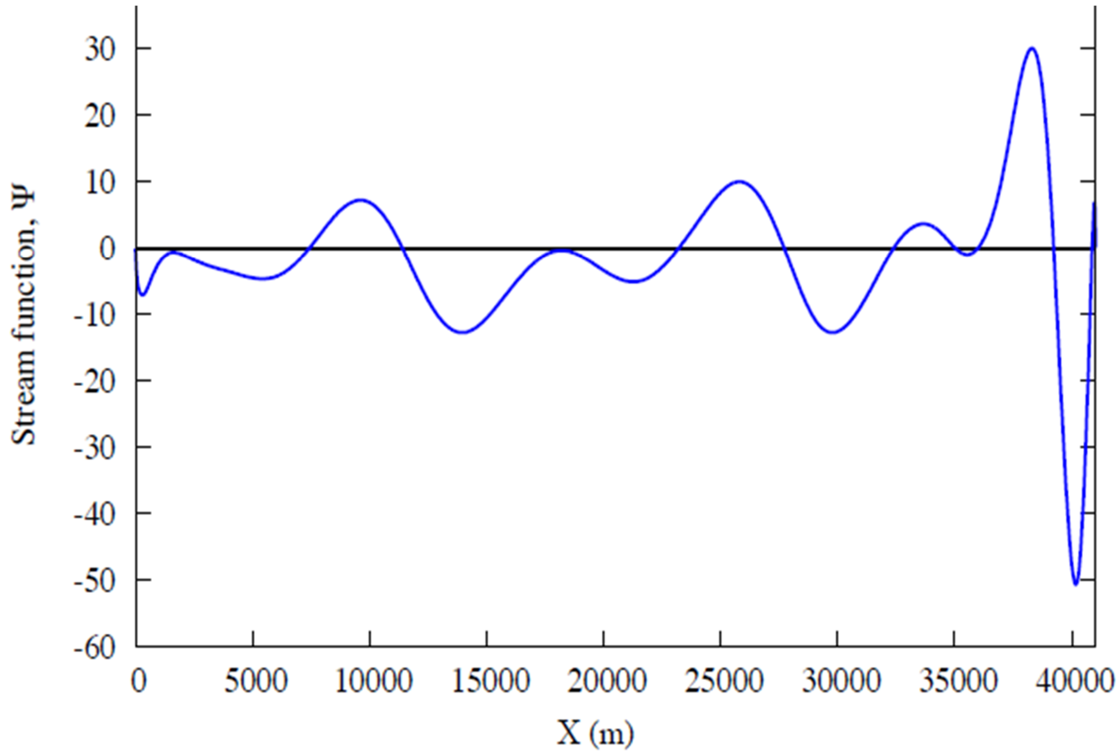

Apx Figure A 6 Western transect topography surface stream function, Ψ

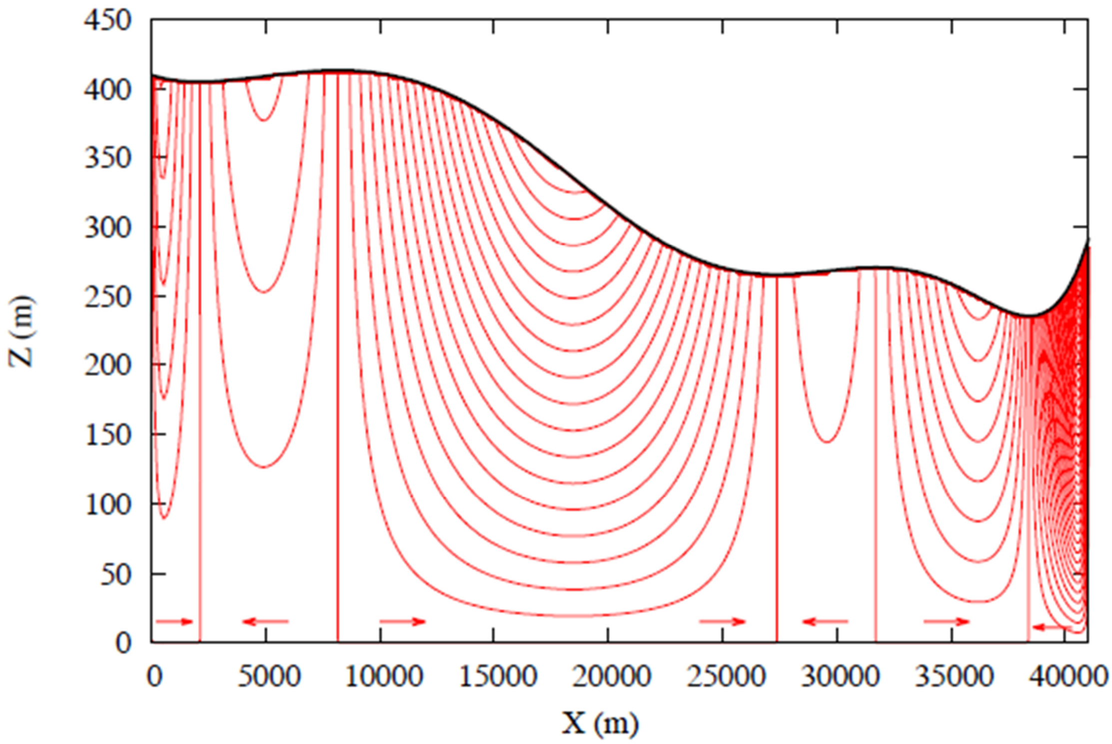

Apx Figure A 7 Western transect well flow contours

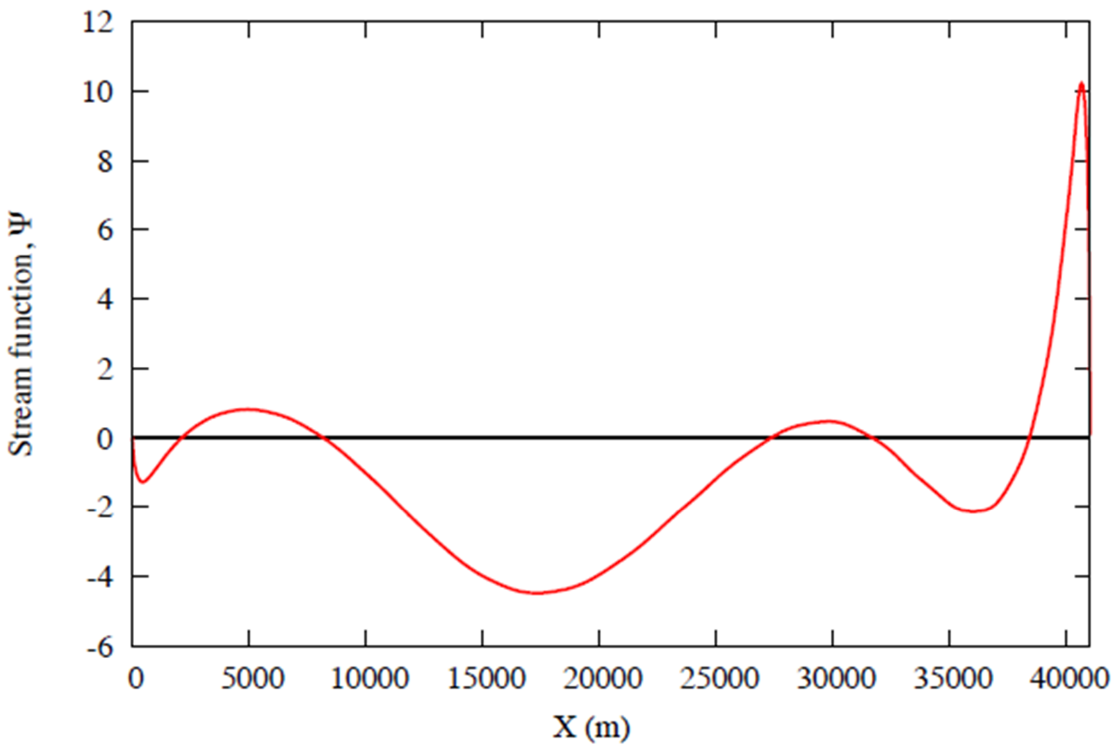

Apx Figure A 8 Western transect well surface stream function, Ψ

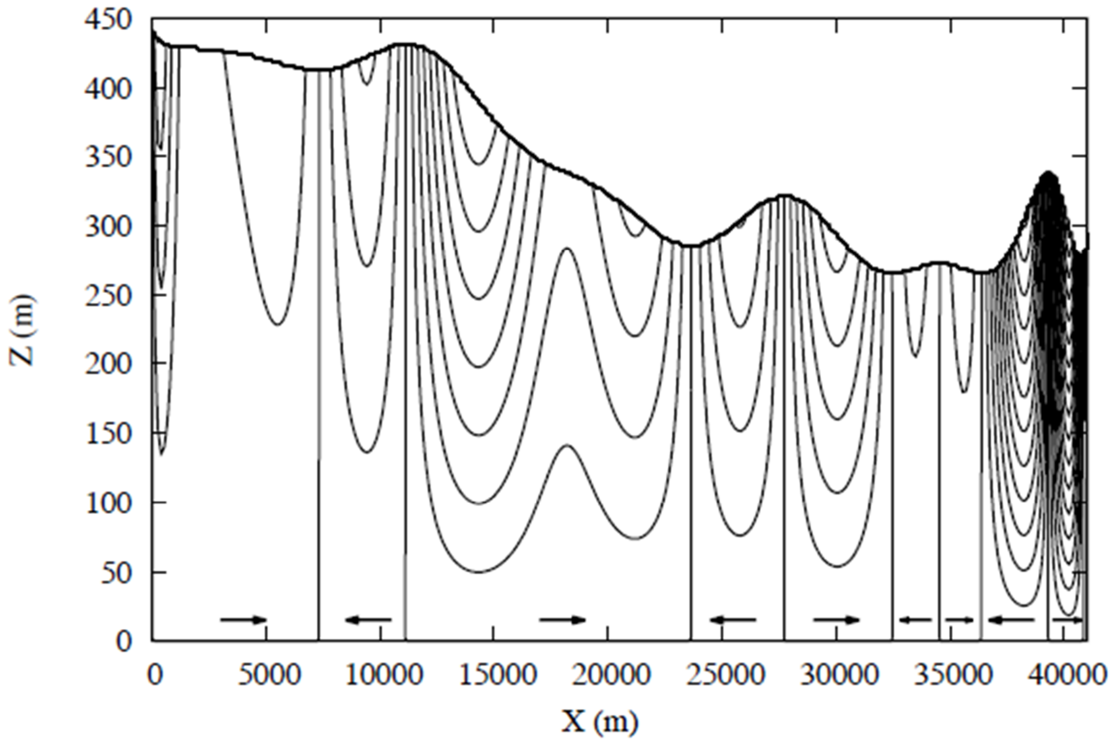

Apx Figure A 9 Western transect average flow contours

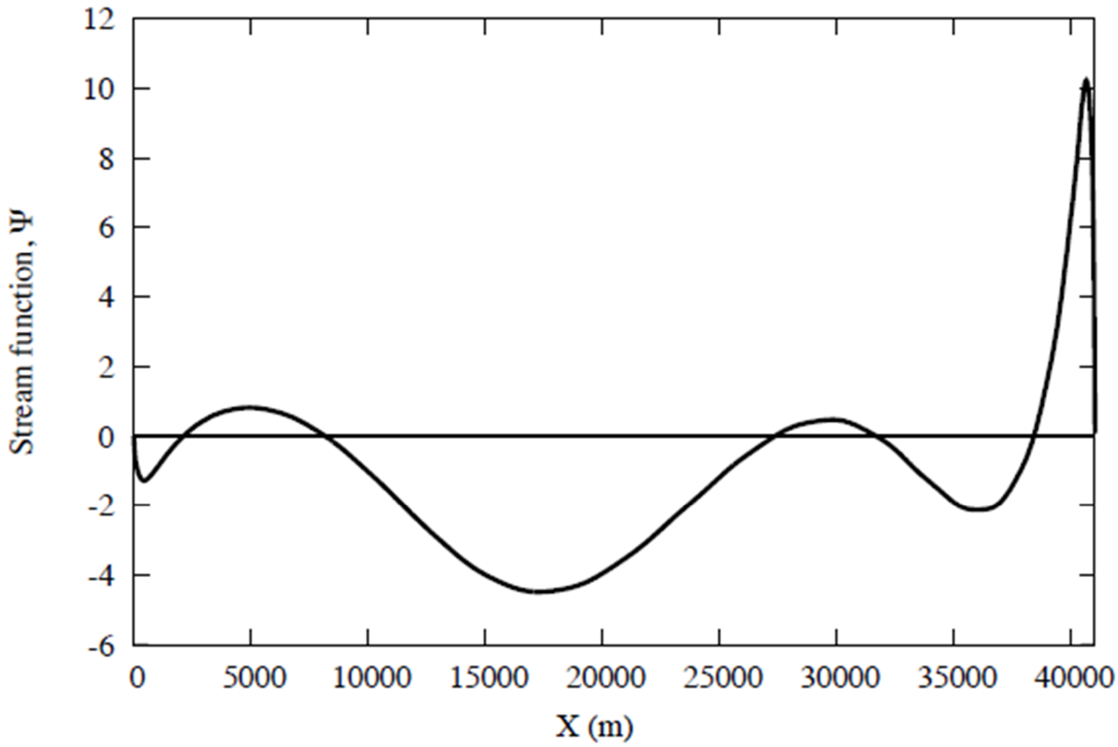

Apx Figure A 10 Western transect average surface stream function,

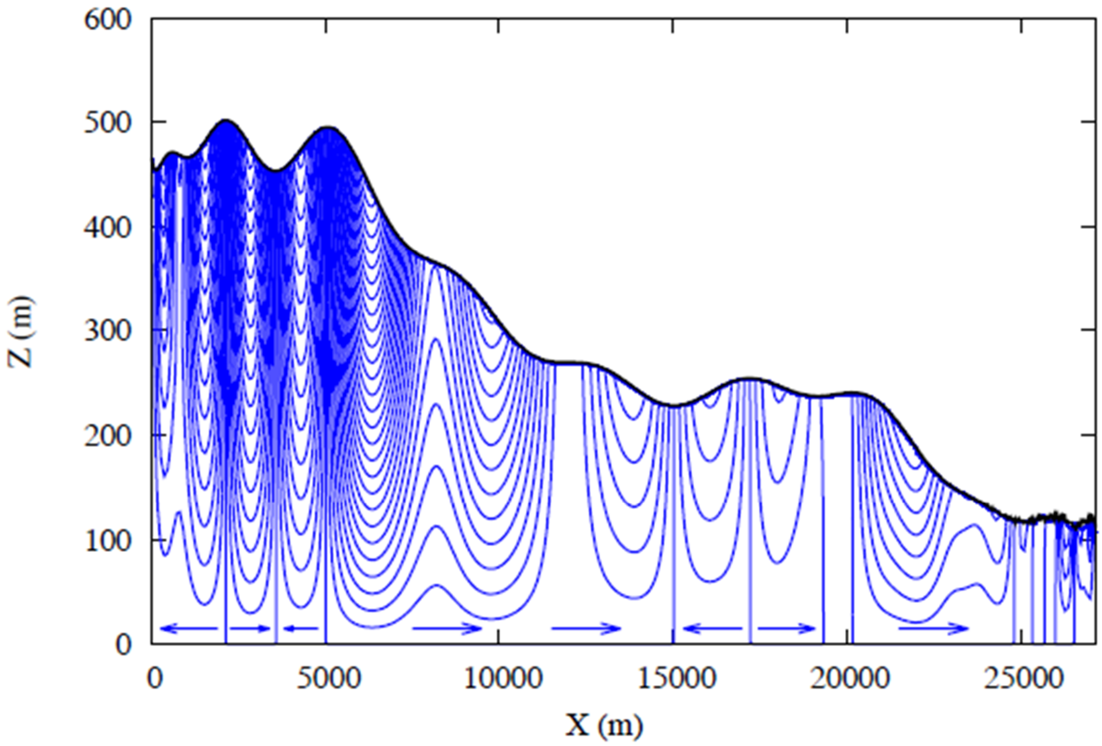

Apx Figure A 11 South-eastern transect topography flow contours

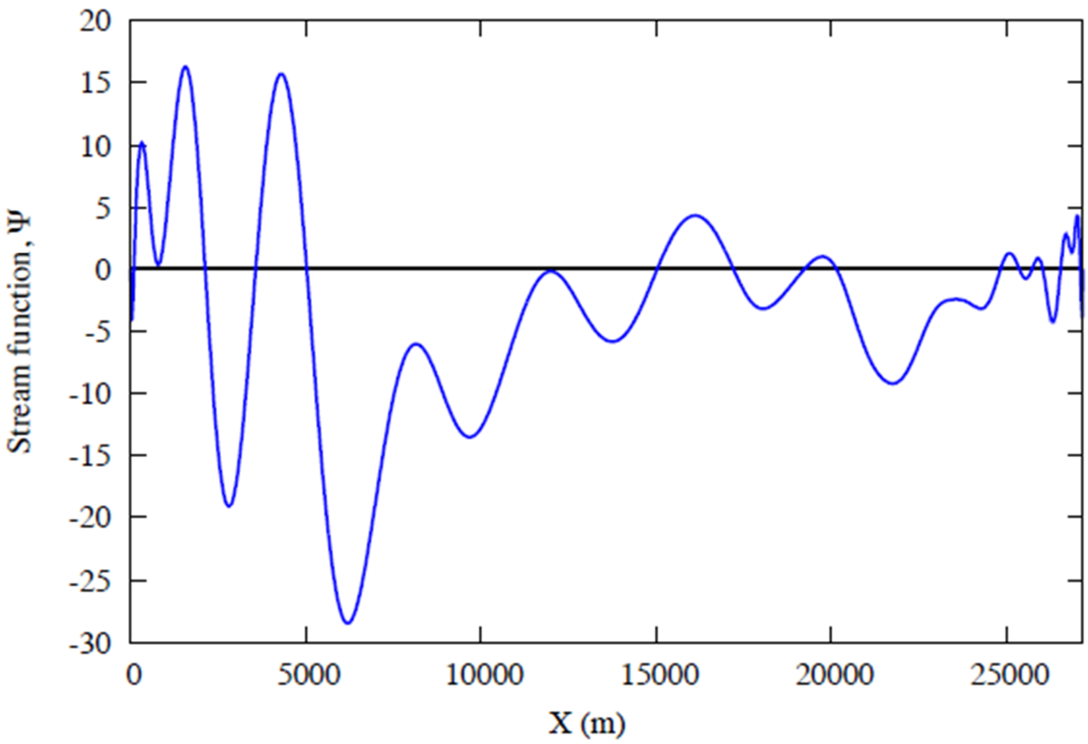

Apx Figure A 12 South-eastern transect topography surface stream function, Ψ

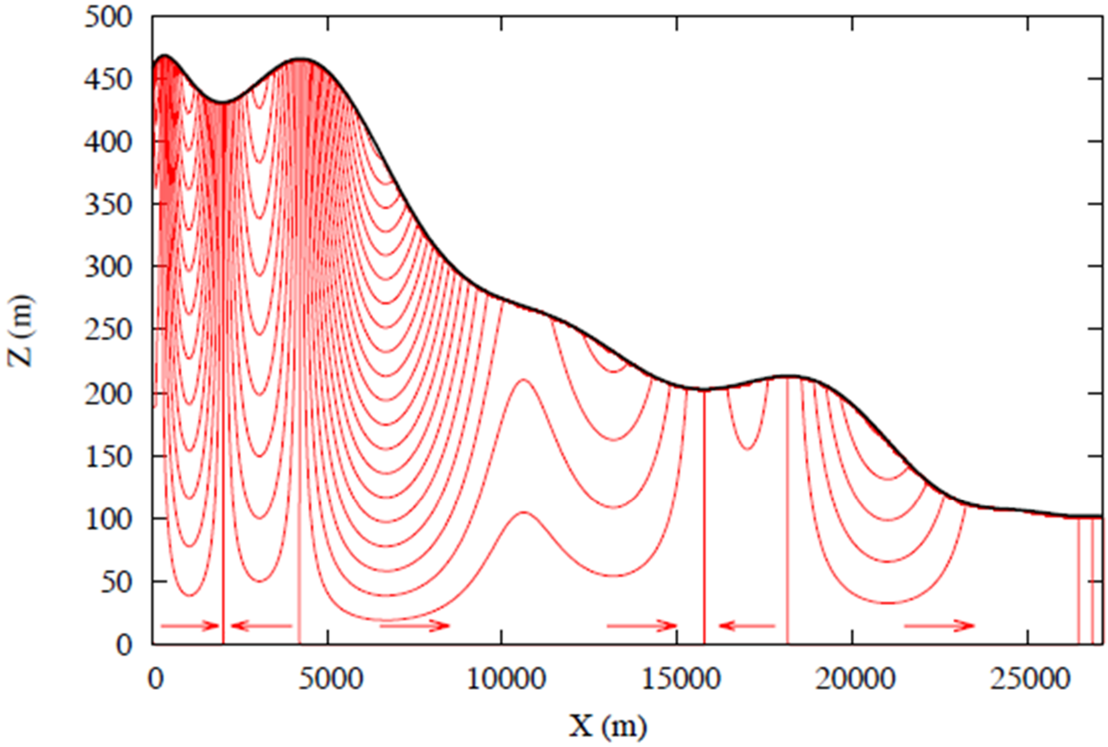

Apx Figure A 13 South-eastern transect well flow contours

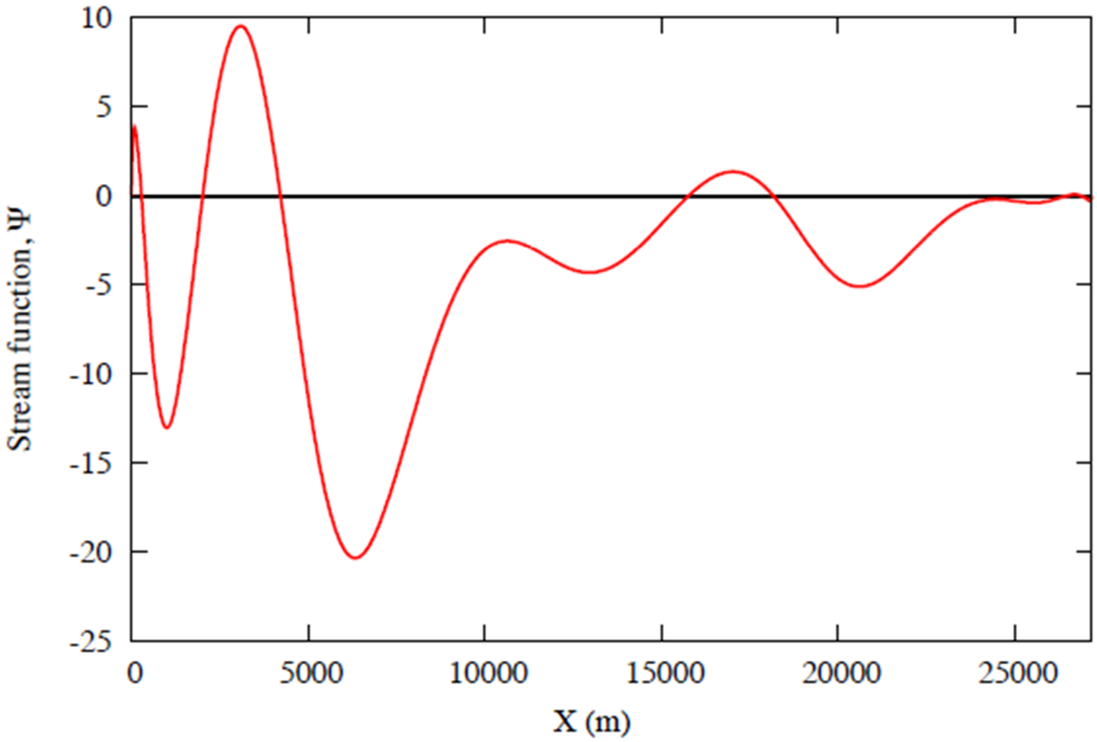

Apx Figure A 14 South-eastern transect well surface stream function, Ψ

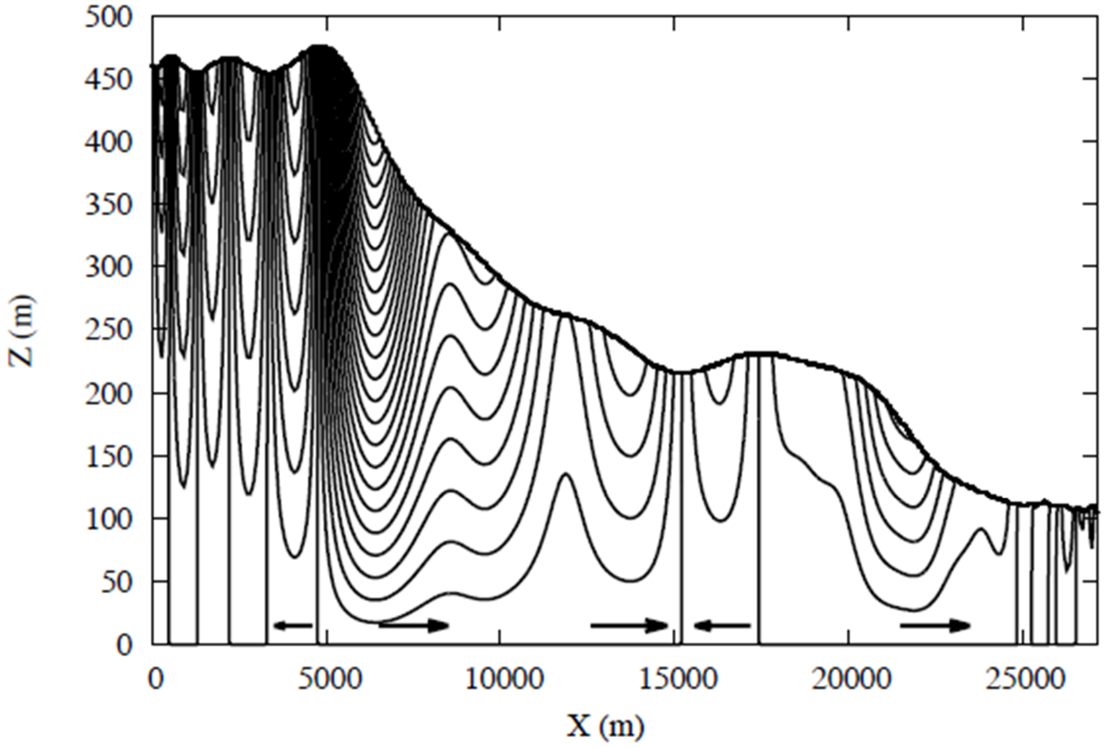

Apx Figure A 15 South-eastern transect average flow contours

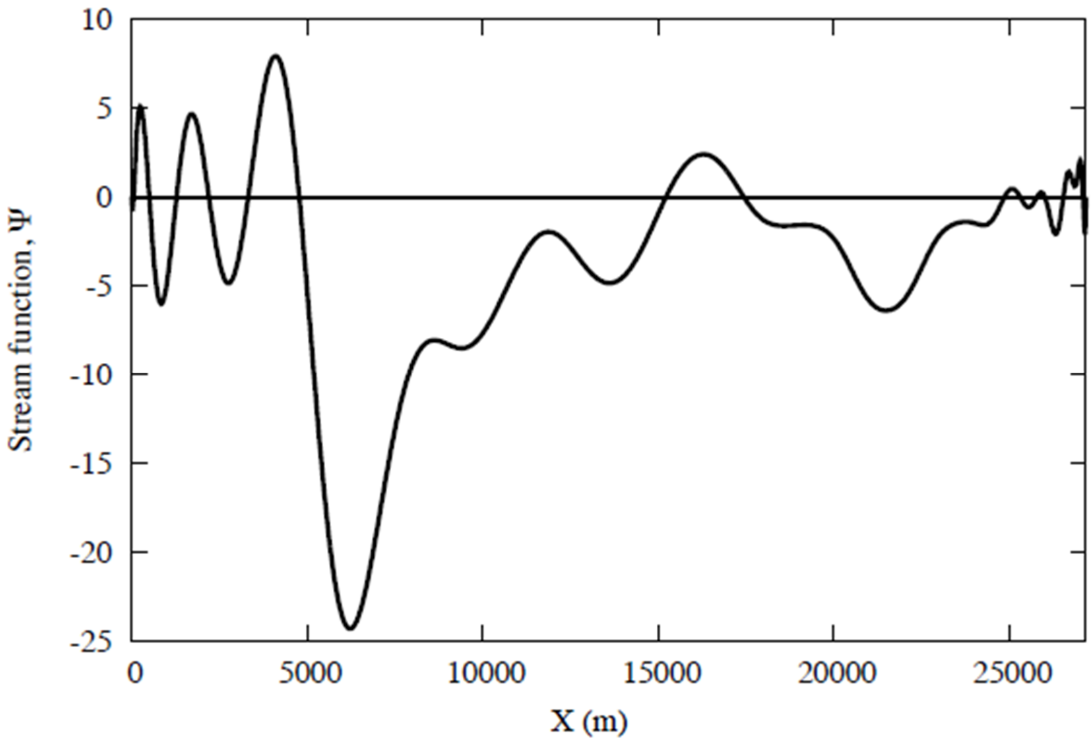

Apx Figure A 16 South-eastern transect average surface stream function, Ψ

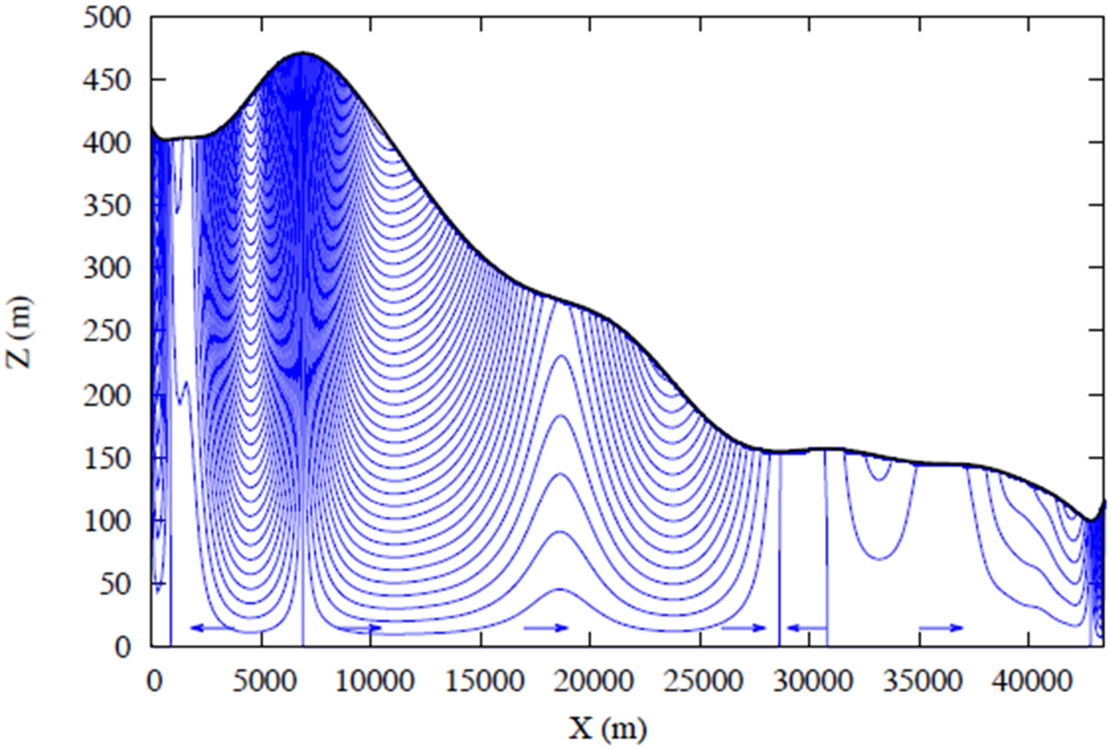

Apx Figure A 17 Southern transect topography contours

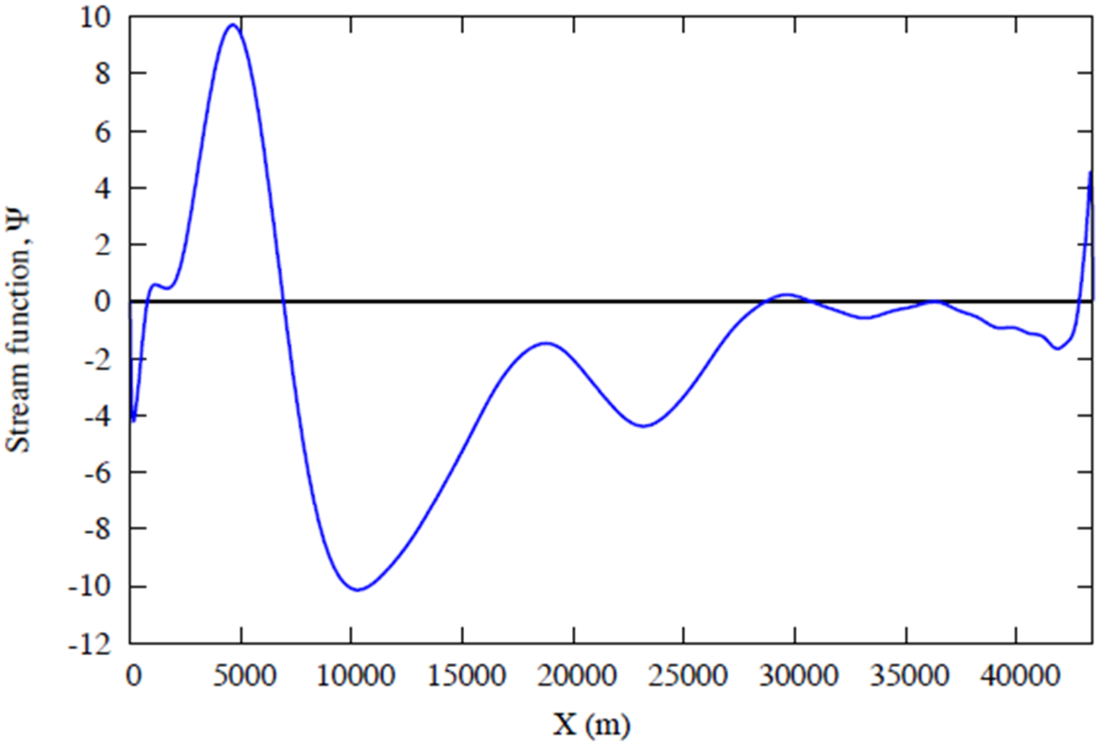

Apx Figure A 18 Southern transect topography surface stream function, Ψ

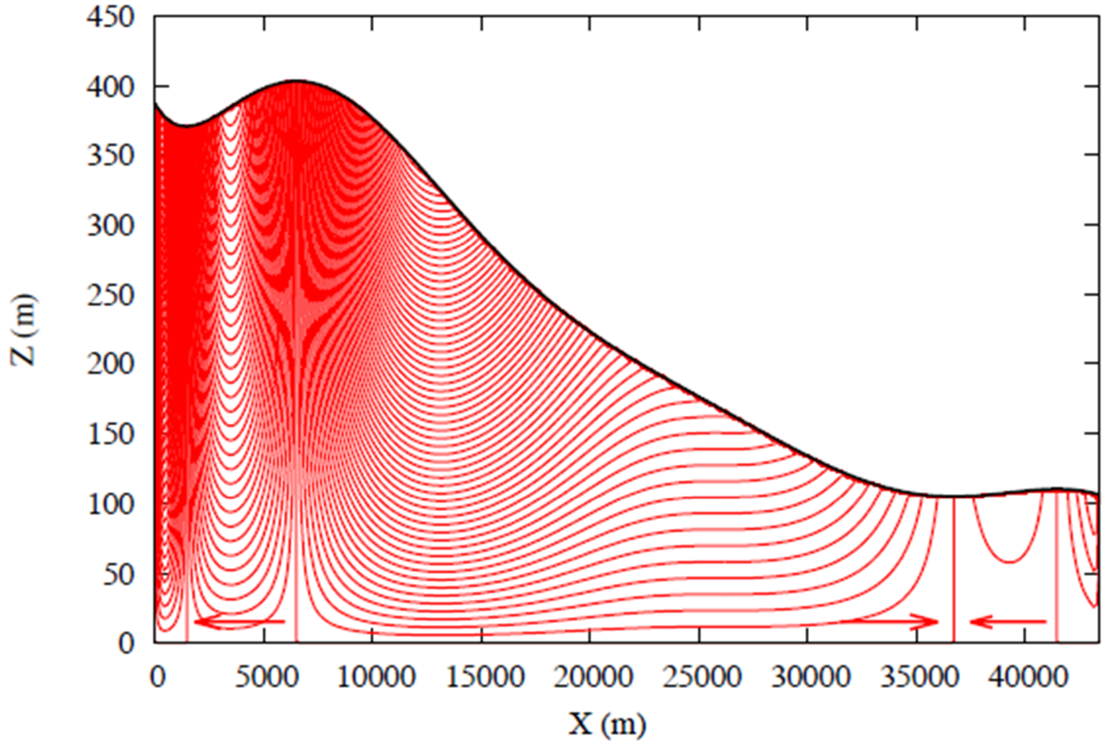

Apx Figure A 19 Southern transect well flow contours

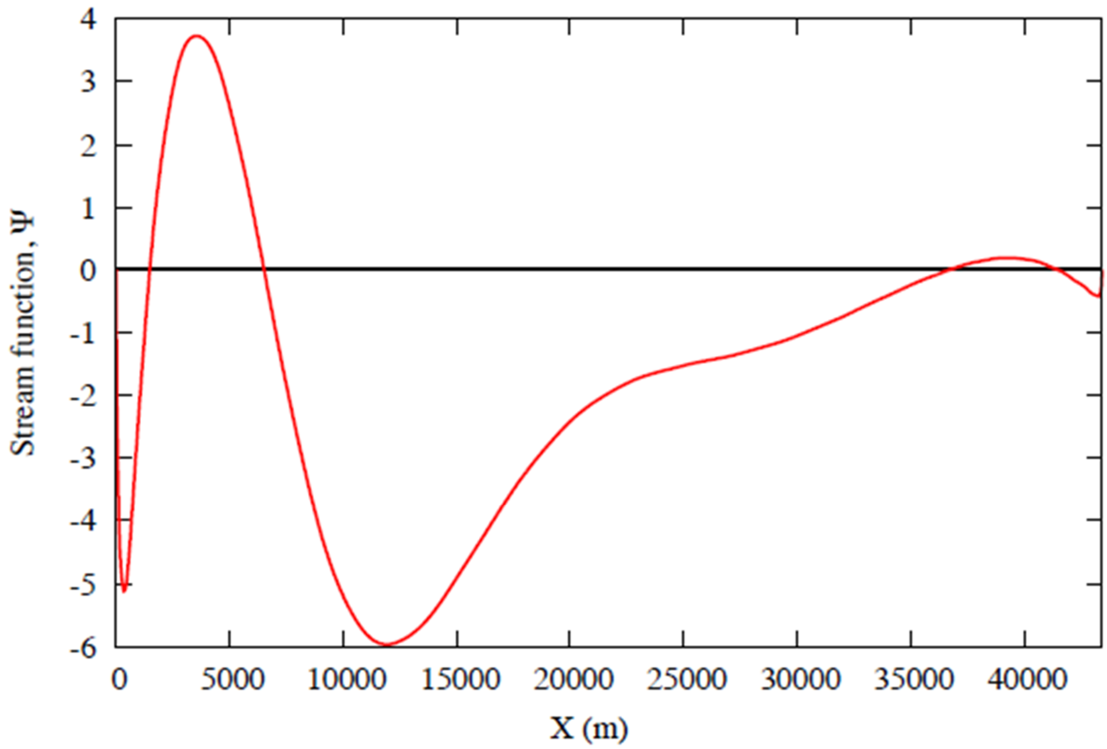

Apx Figure A 20 Southern transect well surface stream function, Ψ

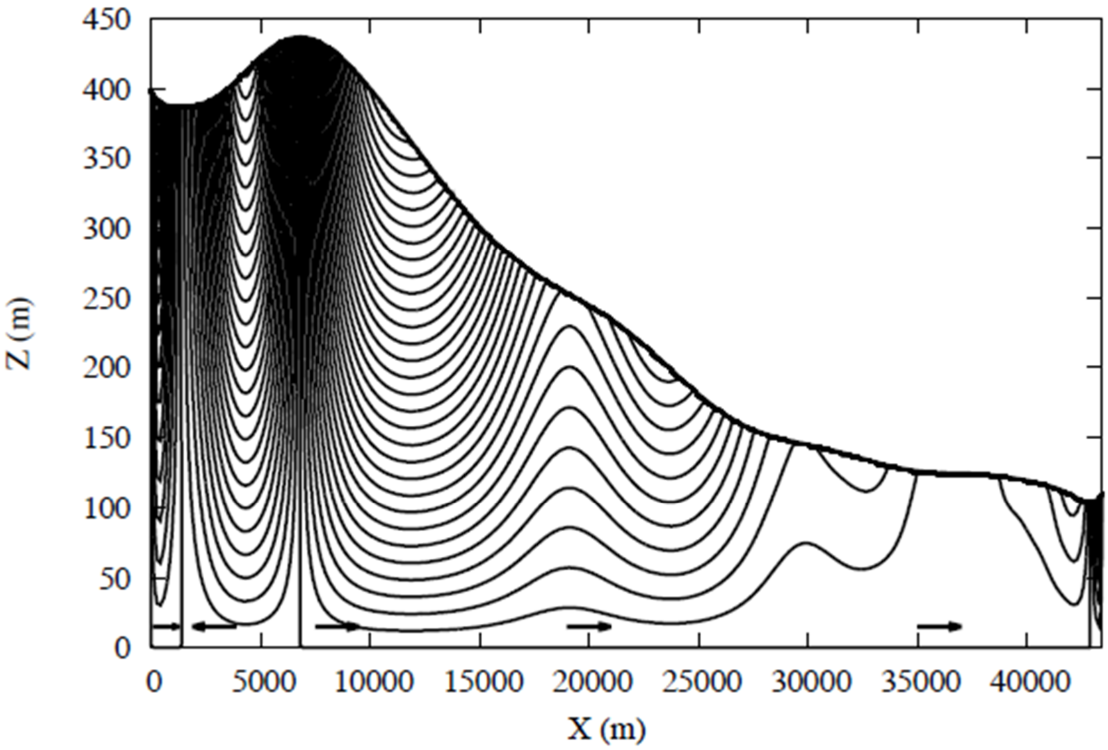

Apx Figure 21 Southern transect average flow contours

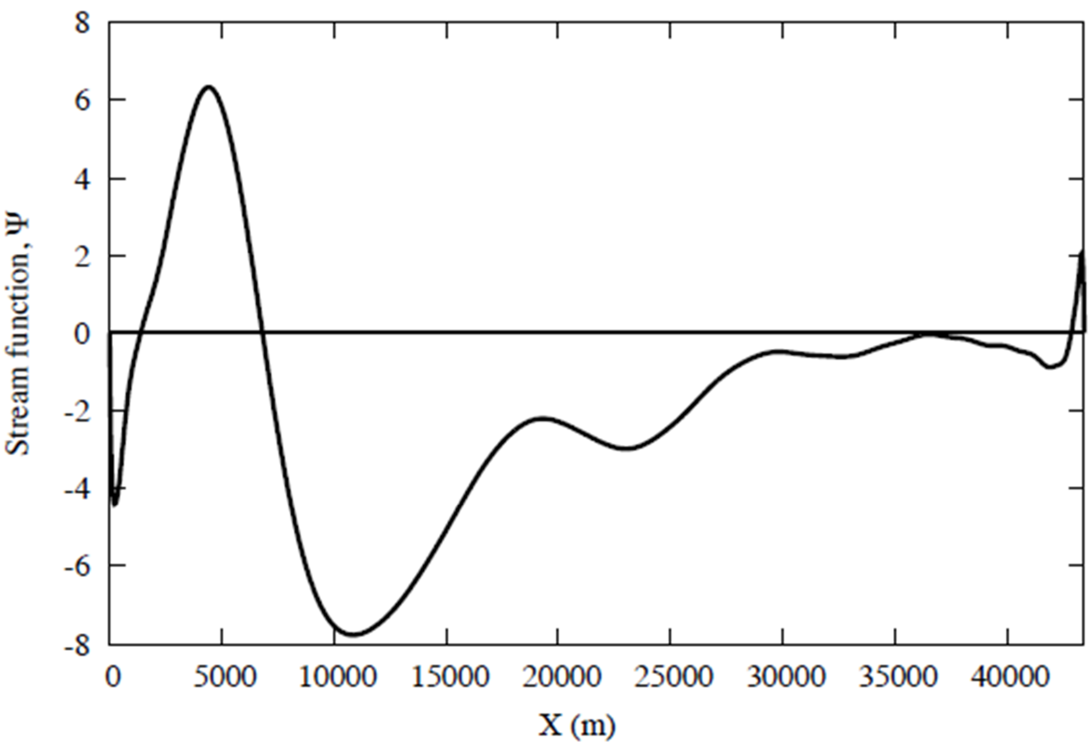

Apx Figure A 22 Southern transect average surface stream function, Ψ

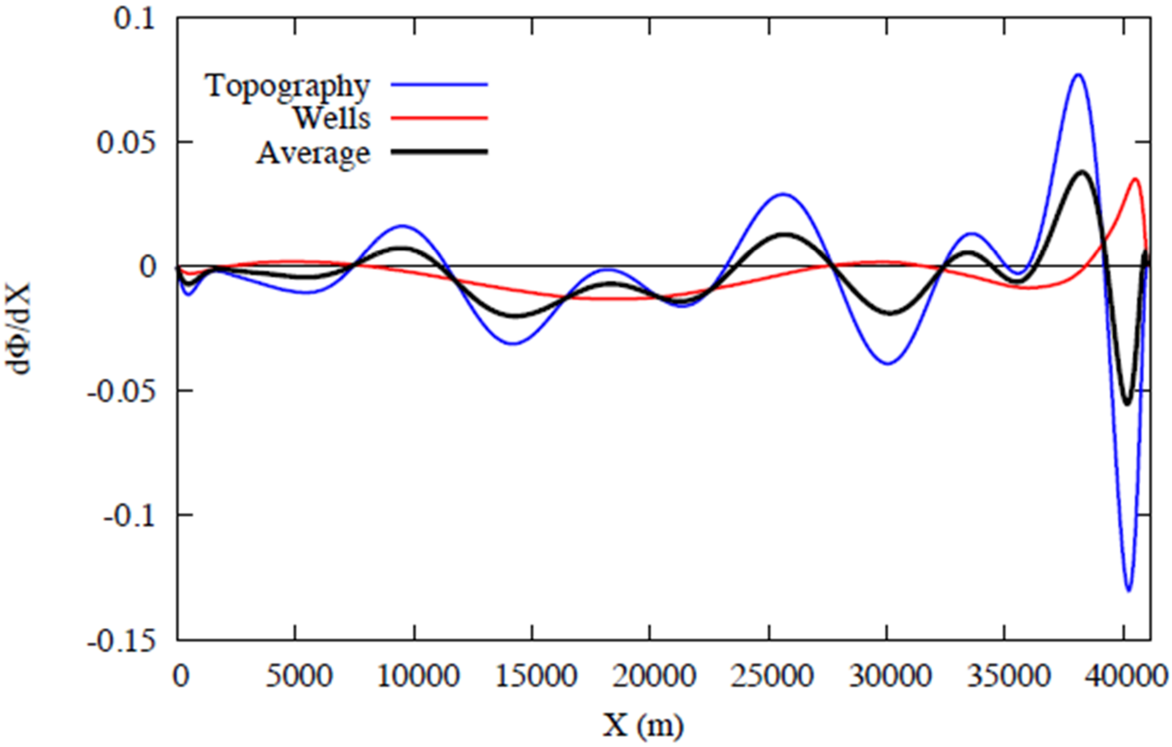

Apx Figure A 23 Western transect. Z_0 = 100 m. Baseline gradients, dΦ/dX. Curves for surface topography, wells and their average

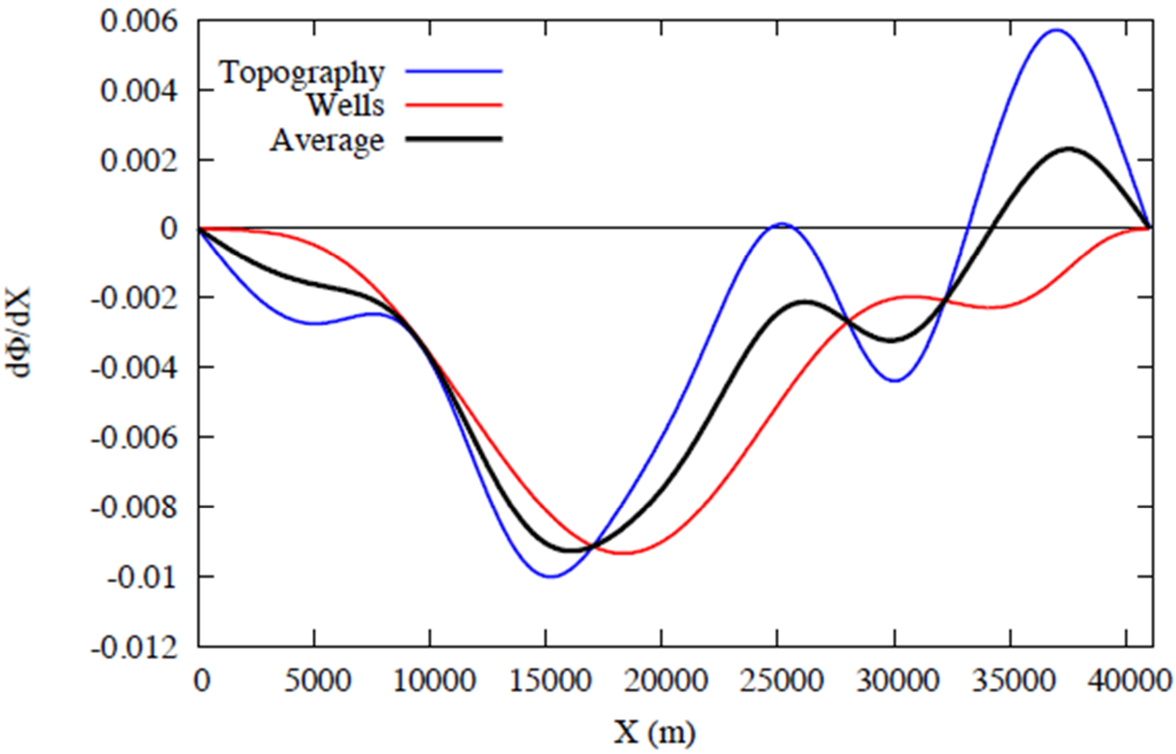

Apx Figure A 24 Western transect. Z_0 = 5000 m. Baseline gradients, dΦ/dX. Curves for surface topography, wells and their average

Appendix B Field sampling data

Apx Table B.1: Sampled well details

SAMPLE ID	LATITUDE (°)	LONGITUDE (°)	TOP OF SCREEN (m)	BOTTOM OF SCREEN (m)	TOTAL DEPTH (m)	SWL (m)	ELEVATION (mAHD)	LITHOLOGY AT SCREEN INTERVAL
613000955	-33.8895011	136.3847396	2	3	4.21	2.01	29.99	Surficial Sediments
613100052	-33.427697	136.281502	-	-	50.29	47.65	210.59	Saprolite
613100132	-33.419724	136.363277	5.31	5.85	5.85	3.92	243.29	Surficial Sediments
613100133	-33.418563	136.362333	4.51	5	5	2.11	236.69	Surficial Sediments
613100489	-33.4179518	136.3647012	8.73	9.13	9.13	3.24	246.79	Igneous
613100791	-33.38628	136.41406	36	42	84	24.07	326	Metamorphic
613100863	-33.4671771	136.1960968	59	65	70	29.43	180.97	Metamorphic
613100872	-33.405667	136.377417	25	35	109	3	241	Metamorphic
613201459	-32.996268	136.2499945	15	67.5	67.5	24.46	202.54	Metamorphic
623000298	-33.6850268	136.7503285	7.32	15.85	15.85	3	146.53	Metamorphic
623000439	-33.6509693	136.5174364	36	60	60	40	328.77	Igneous
623000663	-33.6508668	136.6868267	24	35	93	12	260.66	Metamorphic
623000682	-33.6620319	136.501614	24	42	42	34.83	295.50	Metamorphic
623000716	-33.6318564	136.6855503	30	93	35	37.06	404.65	Metamorphic
623000844	-33.6676461	136.6419772	0	64	50	13.04	241.29	Metamorphic
623100060	-33.3396886	136.7332442	4.6	24.7	12	2.29	302.51	Saprolite
633100565	-33.1949782	137.4168044	11	12.5	13.77	6.47	8.09	Surficial Sediments
633100566	-33.1949834	137.4169975	76	79	80.5	6.15	8.64	Surficial Sediments
633100567	-33.1949581	137.4169111	36	39	41.89	6.21	8.11	Tertiary
633100569	-33.1955443	137.3846672	50	53	52.19	24.36	27.32	Surficial Sediments
633100572	-33.1954757	137.3901242	71	74	77.5	18.56	22.32	Surficial Sediments
633100575	-33.1972539	137.3951811	77	80	82.29	15.15	18.58	Surficial Sediments
633100576	-33.1971812	137.3952113	48	51	82	14.87	18.58	Tertiary
613100955 - surface water	-33.8895011	136.3847396	-	-	-	-	-	-
Cowleds Landing - seawater	137.449025	-33.157425	-	-	-	-	-	-
Harradine	-33.311798	136.322323	-	-	12.94	3.13	274.52	Surficial Sediments
MRH9C	-33.1971768	137.3940315	-	-	80.61	15.98	18.47	Saprolite
Traeger	136.496422	-33.687786	-	-	27.15	13.43	-	-
Upland-1	-33.41542441	136.5109427	-	-	80	37.65	248.35	Igneous

Apx Table B.2: General chemistry and major ions

Sample ID	pH	EC (dS/m)	Total Alkalinity (meq/L)	Acidity (meq/L)	F^- (mg/L)	Cl^- (mg/L)	Br^- (mg/L)	NO_3^- (mg/L)	$SO_4^{=}$ (mg/L)	Ca (mg/L)	K (mg/L)	Mg (mg/L)	Na (mg/L)	S (mg/L)
613000955	3.8	62		11	<2	25970	79	12	3410	497	290	1650	13800	1050
613100052	3.6	11		69	0.2	3850	11	0.15	6.3	301	30	40	458	<2.5
613100132	7.5	26	21		<1	9100	31	<1	1560	302	137	668	5090	484
613100133	8.2	12	18		<1	3480	12	1.1	690	70.2	54	159	2430	213
613100489	7.5	19	8.8		<1	6250	22	139	990	167	145	368	3530	305
613100791	7.1	38	6.9		<2	14470	41	<2	1920	481	109	1080	7460	597
613100863	6.4	38	1.7		<2	14320	47	1.5	2640	169	160	916	8260	826
613100872	7.0	33	7.7		<2	11960	37	<2	2160	388	108	1100	6050	677
613201459	6.5	38	1.4		<2	14240	47	<2	2990	554	165	1030	8010	953
623000298	7.9	13	12		0.7	4050	13	1.3	590	101	75	212	2360	177
623000439	7.5	5.5	10		<0.5	1580	4.8	15	250	100	26	159	900	76
623000663	7.8	6.5	11		<0.5	1840	5.4	25	290	97	40	185	1020	88
623000682	7.3	12	6.4		<0.5	3870	12	0.5	670	190	63	319	1960	200
623000716	7.0	11	9.1		<0.5	3750	12	1.0	420	112	87	389	1730	126
623000844	8.2	11	15		0.7	3340	11	24	620	139	57	278	1910	186
623100060	7.5	7.7	16		<0.5	2130	7.2	<0.5	360	94	48	176	1340	112
633100565	6.7	81	1.6		0.2	35100	87	0.9	3950	2030	97	2100	18100	1240
633100566	7.2	65	2.7		<2	28150	62	4.3	2970	2640	148	1670	13000	933
633100567	7.2	59	2.8		0.7	23740	54	1.5	3290	1990	119	1560	11300	1040
633100569	7.4	45	3.1		<2	17210	41	9.1	3800	1410	82	1310	8900	1220
633100572	7.4	58	2.8		<2	24020	55	2.0	3370	2230	112	1800	11200	1080
633100575	7.3	66	2.9		<2	28350	61	2.3	2870	2810	135	1780	13100	910
633100576	7.7	46	3.6		<2	18280	43	2.3	3740	1510	87	1400	8890	1170
613100955 - surface water	3.9	71		6.3	<2	29230	86	4.5	4230	668	321	1740	16300	1330
Cowleds Landing - seawater	8.1	57	2.7		0.4	22410	72	1.1	3240	472	449	1440	12400	1020
Harradine	7.6	11	17		<0.5	3190	9.3	<0.5	660	182	60	172	2090	197
MRH9C	7.1	67	2.9		0.4	28400	60	1.2	2870	2700	149	1730	13100	903
Traeger	7.6	12	10		<0.5	3580	11	3.8	641	273	49	316	1820	197
Upland-1	6.0	0.5	0.11		<0.05	145	0.48	<0.05	7.7	2.8	2.5	2.1	43	2.3

Apx Table 3 Environmental tracers

SAMPLE ID	$\delta^{18}O$ (‰)	$\delta^{2}H$ (‰)	CFC-11 (pmol/kg)	CFC-12 (pmol/kg)	SF_6 (fmol/L)	$\delta^{13}C$ (‰VPDB)	^{14}C (pMC)	$^{87}Sr/^{86}Sr$	^{4}He cc STP/g	^{3}H (TU)
613000955	-2.97	-22.54	–	–	2.81	-14.78	97.93	0.7248844	4.84E-07	0.29
613100052	-4.82	-21.96	–	–	–	–	–	0.714525	–	1.00
613100132	-4.78	-28.6	–	–	–	-9.12	75.76	0.7181715	–	0.79
613100133	-4.52	-27.14	–	–	–	-11.40	83.80	0.723198	–	1.28
613100489	-4.54	-29.57	1.93	1.47	12.95	-11.21	97.38	0.7244816	7.90E-08	1.60
613100791	-4.13	-24.62	–	–	9.73	-12.39	63.25	0.7321636	5.47E-06	0.14
613100863	-3.32	-23.8	–	–	3.47	-4.59	47.87	0.7141777	1.31E-07	0.06
613100872	-4.55	-28.68	<0.18	<0.16	>14	-10.79	88.43	0.7216013	3.16E-07	0.43
613201459	-3.38	-25.91	–	–	>14	-6.90	21.00	0.7233697	1.39E-05	0.03
623000298	-4.63	-29.85	0.37	0.51	1.06	-10.84	89.33	0.7219094	6.67E-07	0.70
623000439	-4.95	-28.01	0.22	0.18	1.22	-11.03	70.80	0.7293146	1.12E-07	0.17
623000663	-4.66	-29.8	1.70	1.65	6.18	-10.78	71.94	0.7302236	1.16E-07	0.63
623000682	-4.68	-26.5	–	–	2.07	-9.78	84.01	0.7229057	8.77E-08	0.02
623000716	-4.92	-31.23	0.52	0.16	0.7	-10.14	65.37	0.7386336	1.78E-07	0.08
623000844	-4.77	-31.85	–	–	11.14	-9.82	85.64	0.7312083	6.11E-08	0.49
623100060	-3.24	-21.13	–	–	1.48	-10.73	94.91	0.7236721	–	1.61
633100565	-0.89	-18.46	–	–	4.08	-4.83	39.58	0.7183843	–	–
633100566	-3.21	-28.41	<0.18	<0.16	0.56	-7.90	24.42	0.7386587	3.48E-04	0.01
633100567	-2.72	-27.3	–	–	8.7	-7.64	40.05	0.7298263	–	–
633100569	-2.58	-27.59	–	–	>14	-6.35	9.66	0.7236905	2.04E-05	0.07
633100572	-3.38	-29.08	–	–	>14	-6.36	10.17	0.7272919	2.29E-04	0.04
633100575	-3.01	-29.24	0.23	0.33	1.44	-7.17	11.88	0.7376444	3.91E-04	0.06
633100576	-2.92	-27.37	0.25	<0.16	>14	-7.16	11.24	0.7253234	1.01E-04	0.04
Cowleds Landing - seawater	1.8	10.98	–	–	1.66	–	–	0.7092125	–	–
Harradine	-4.29	-27.28	1.05	0.74	12.09	-11.06	78.57	0.7126911	1.06E-07	1.00
MRH9C	-3.07	-28.38	–	–	0.9	-7.85	28.53	0.737621	–	–
Traeger	-4.92	-30.53	–	–	13.59	-11.49	64.32	0.7230359	1.13EE-07	0.11
Upland-1	-14.18	-100.76	<0.18	<0.16	1.93	-5.04	97.15	0.7139378	1.44E-07	1.48

The Goyder Institute for Water Research is a partnership between the South Australian Government through the Department of Environment, Water and Natural Resources, CSIRO, Flinders University, the University of Adelaide and the University of South Australia.